# Thermal Comfort in Indoor Sports Facilities and the Adequacy of Demand-controlled Ventilation

Si Nguyen-Ky

**School of Engineering**

Thesis submitted for examination for the degree of
Master of Science in Technology.

Leppäkoski 21.12.2022

**Supervisor**

Prof. Heidi Salonen

**Advisors**

Adj. Prof. Jarek Kurnitski

DSc. Camilla Vornanen-Winqvist

Aalto University
School of Engineering

Aalto University
School of Engineering

Aalto University, P.O. BOX 11000, 00076 AALTO
www.aalto.fi
Abstract of the master's thesis

**Author** Si Nguyen-Ky

**Title** Thermal Comfort in Indoor Sports Facilities and the Adequacy of Demand-controlled Ventilation

**Degree programme** Building Technology

**Major** Indoor Environment Technology **Code of major** ENG27

**Supervisor** Prof. Heidi Salonen

**Advisors** Adj. Prof. Jarek Kurnitski, DSc. Camilla Vornanen-Winqvist

**Date** 21.12.2022 **Number of pages** 74+20 **Language** English

**Abstract**

In sports environments, the unstable occupancy density together with the increased heat and moisture emissions from the sports players imposes an extra duty on the ventilation system. This thesis studies the human thermal response and the adequacy of demand-controlled ventilation in indoor sports facilities as part of the LIIKU project, which investigates the indoor air environment therein and the possible effects on the well-being and health of the occupants.

Several approaches to assess and predict the thermal sensation of sports players were reviewed, including the Fanger's predicted mean vote model. Amongst those, thermo-physiological comfort models were shown to have strong potential to be applied in sports environments where the human activity level is high and constantly changing. Dynamic thermal sensation (DTS) vote from the IESD-FIALA model was proved to be more reliable and superior to the predicted mean vote in sports-related situations.

Ventilation requirements and common practices in indoor sports facilities were investigated, along with the use of demand-controlled ventilation solutions (DCV). The pros and cons of DCV were discussed, particularly the operational challenges. The Latorkartano sports hall in Helsinki was chosen to be studied more closely with an indoor climate and energy simulation in IDA ICE software. In order to predict the thermal sensation of the occupants, the FIALA-IESD model was applied and the DTS was calculated. It was found that reducing the temperature setpoint by 1 to 2℃ compared to the current Finnish regulation, which is at 17 to 16℃, could save from 13 to 18% in heating energy of this sports hall without affecting the thermal comfort of the sports players.

**Keywords** Indoor Sports Facilities, Demand-controlled Ventilation, Thermal Comfort, Indoor Air Conditions, IDA ICE

# Acknowledgements

I would like to express my deepest gratitude to Professor Heidi Salonen for giving me the opportunity to work as part of the LIIKU project, and for her guidance and support since the beginning of this work. I would like to send my warmest thanks to my thesis instructors Professor Jarek Kurnitski and DSc. Camilla Vornanen-Winqvist for their continued presence, encouragement, helpful advice, and constructive feedback. I kindly thank Mohammad Elwan from the City of Helsinki for providing me with practical support and technical documentation on the site visits. I acknowledge the Finnish Work Environment Fund for realising this project through their funding. I am very much indebted to my work supervisor at Vahvacon Insinööritoimisto Oy Ilkka Råman for your firm and generous support towards my study as well as your arrangement for my study leave so that I could finish my courses and thesis work. To me, you are more than a work supervisor, but a teacher – an inspiring and influential one – what more could one ask for. It is truly a blessing that I have you, Nhung and Max, as my good friends and colleagues. I really appreciate your supportive opinions, sharing, and advice in our professional fields.

This endeavour would not have been possible without Meeri for her deep-seated belief and encouragement that she gave me, lifted me up, brought me hopes through the most difficult and darkest time to date of mine which I could have not overcome without her. She guided me through, helped me to gradually resolve and heal my inner child, to eventually find back my motivation to study, and most importantly, to finish this work. I cannot thank my closest friend Junnu enough for your reassurance and care, the unforgettable fishing and mushroom-picking trips, and the joyful moments with your siblings and family. I admit that I have failed to show my heartfelt appreciation to all my friends, whether in Finland, Vietnam or somewhere around the globe. I will not promise to tell you those cheesy but hearty words anytime soon but please do not forget that those have always been in my mind. You are always there for me through my ups and downs, sharing with me the most incredible energy, the cherished time we spent together or through our hour-long calls, the best laughter and tears, adding myriads of colours to my life.

Last but not least, I am forever in debt to my parents, my big brother, and my dearest relatives for your unwavering support for me in every way, for your respect and faith in any life path I chose. No words could ever express my gratefulness for having you beside me. I would be remiss in not mentioning my beloved dog Badi, for your company in my every walk and your boundless emotional support, no matter how much you shed.

Leppäkoski, 05.12.2022

**Sy Nguyen-Ky**

# Contents

# List of Figures

# Abbreviations

| | |
|---|---|
| AHU | Air handling unit |
| ASHRAE | American Society of Heating, Refrigerating and Air-conditioning Engineers |
| BIM | Building information modelling |
| BMI | Body mass index |
| BMS | Building management system |
| CAV | Constant air volume |
| CEN | European Committee for Standardisation |
| CFD | Computational fluid dynamic |
| COVID | Coronavirus disease (caused by the SARS-Cov-2 virus) |
| CV(RMSE) | Coefficient of variation of the root mean squared error |
| DACH | D — Deutschland (Germany), A — Austria, CH — Confœderatio Helvetica (Switzerland) |
| DCV | Demand-controlled ventilation |
| DOE | Department of Energy |
| DTS | Dynamic thermal sensation |
| EN | European Standard |
| ET | Effective temperature |
| ET | Equivalent temperature |
| EU | The European Union |
| FEMP | Federal Energy Management Programme |
| IESD-FIALA | FIALA model from the Institute of Energy and Sustainable Development, De Montfort University Leicester |
| FINVAC | The Finnish Association of HVAC Societies |
| FMI | Finnish Meteorological Institute |
| FPC | Fiala thermal Physiology and Comfort |
| HIS | Heat stress index |
| HR | Heart rate |
| humindex | Humidity index |
| HVAC | Heating, ventilation, and air-conditioning |
| IAQ | Indoor air quality |
| ICV | Interactive cascade ventilation |
| IEA SHC | International Energy Agency Solar Heating and Cooling |
| IoT | Internet of Things |
| IPMVP | International Performance Measurements and Verification Protocol |
| ISO | International Standard Organisation |
| LIIKU | Liikuntatilojen sisäilman ja sisäympäristön laatu ja mahdolliset vaikutukset työntekijöiden hyvinvointiin ja terveyteen [Indoor air and indoor environment quality and the possible impacts to the well-being and health of the occupants] |
| LVI | Lämmitys, vesi, ja ilmanvaihto [Heating, water, and ventilation] |
| M&V | Measurement & verification |
| MET, met | Metabolic equivalent of task |
| MOE | Ministry of the Environment |
| MRT | Mean radiant temperature |
| NASA | The National Aeronautics and Space Administration |
| NMBE | Normalised mean bias error |
| PIR | Passive infrared sensor |

# 1 Introduction

## 1.1 Introduction to the LIIKU Project

In Finland, the culture of physical activity has greatly changed in the last decades regarding the practising environment: less outdoors and more indoors [1]. For that reason, the need for built sports facilities has also increased over time. At the same time, the attention to their functionality and performance from the public has been on the rise. Indoor sports facilities can be operated all year round and do not depend on outdoor conditions. In moderate and cold climate regions such as Finland, due to the shortened accessibility to outdoor sports, a majority of people spend their time training and practising different types of sports indoors. This magnifies the importance of adequate and functional indoor sports facilities to ensure the public's participation in sports and regular physical activities. During the last decades, creating and maintaining a good indoor environment in indoor sports facilities have posed real challenges to engineers and researchers, as it involves many trans- and interdisciplinary professionals [2]. The size, shape, structure, and design of an indoor sports facility depend crucially on the sports it serves, the main users, and the context it operates. For example, a gymnasium inside a school or university differs markedly from a national Olympic volleyball courtyard. Nevertheless, the ultimate role it holds is ubiquitous: to create a safe and comfortable environment for sportspeople.

Figure 1. Yrjönkatu swimming pool, the oldest public indoor swimming pool in Finland, which is cherished with its historical, architectural and artistic values, reprinted from [3].

LIIKU [Liikuntatilojen sisäilman ja sisäympäristön laatu ja mahdolliset vaikutukset työntekijöiden hyvinvointiin ja terveyteen] project (no. 200068), funded by the Finnish Work Environment Fund, aims at seeking new information from experimented and measured indoor air (chemical, microbiological, and particulate matters) and indoor environment quality (ventilation, noise, and space usability). Furthermore,

the factors that determined the quality of the indoor environment and their possible impacts on the well-being and health of the space users (sports players, staff) are also studied. Aalto University acts as the implementing organisation, together with the Finnish Institute for Health and Welfare (THL) and the Finnish Institute of Occupational Health (TTL). Other bodies in cooperation in the implementation of this project include Vaasa University, Tampere University of Applied Sciences, University of Eastern Finland, Queensland University of Technology, International Laboratory for Air Quality and Health (ILAQH), University Properties of Finland Ltd, Eurofins Expert Service Oy, the Finnish Society of Indoor Air Quality and Climate, Liikunnan ja Terveystiedon Opettajat ry (LIITO) [Sports and Health Science Teacher Association], Finnish Ministry of Social Affairs and Health, Finnish Ministry of the Environment, the Association of Finnish Local and Regional Authorities], the Building Information Foundation, the Finnish Olympic Committee, Aalto University Campus & Real Estate (ACRE), City of Espoo, City of Kerava, City of Helsinki, City of Vantaa. The 15 indoor sports facilities to be studied were offered by ACRE and the participating cities. The outcomes of this project are to be used as recommendations and working tools for the improvement of indoor air and indoor environment quality as well as the well-being and health of workers and users in indoor sports facilities. This thesis is part of the LIIKU project, covering the ventilation-related aspects of indoor sports facilities through a case study of one of the 15 sports facilities involved in the project, the Latokartano sports hall.

This work aims at investigating the factors contributing to a well-functioning demand-controlled ventilation system in indoor sports facilities, especially with regard to the thermal sensation of sports players or exercisers. To obtain that, the thesis revolves around these three focal points:

(i) How have the thermal responses of people in sports environments been assessed and predicted?

(ii) What are the ventilation requirements and the factors affecting the functionality of demand-controlled ventilation in indoor sports facilities?

(iii) What can be learnt from the performance of the DCV system in the Latokartano sports hall?

In particular, the methods to assess and predict human thermal responses in sports environments will be screened and examined in Chapter 2. The current ventilation requirements from the Finnish building regulation as well as recommendations from guidelines and international sports associations will be compiled in Chapter 3. Chapter 4 introduces the indoor climate and energy simulation of one of the two halls of the Latokartano sports centre, the model calibration process, and a discussion of the simulation result with the thermal comfort taken into consideration. Conclusions drawn from the performance of the indoor conditions and heating energy

consumption as well as the identified challenges in the operation of the demand-controlled ventilation system of the studied sports hall are presented in Chapter 5.

## 1.2 Limitations

This work was done partially during the COVID-19 lockdown and partially during the post-COVID period when the re-openings of the sports facilities participating in the project still had to follow the strict guidelines issued by the authorities. A questionnaire regarding the operation and maintenance practicalities of the ventilation systems was distributed to the sports hall maintenance workers during the autumn. The response rate was remarkably low (8%); thus, the subjective data and its analysis were left out of the preliminary research plan. In addition, the measurement of the demand-controlled airflow rate in the sports halls was not realised because at the time all the ventilation systems were required to be running at their maximum capacity (more details are described in Section 4.2). Subsequently, this part of the work was removed from the thesis's original scope.

# 2 Human Thermal Responses in Indoor Sports Facilities

This chapter emphasises the fact that humans are and must be the central subject in the design and operation of indoor sports facilities. The interconnection between human's perception of comfort and the controlled indoor environment designated for sports activities is attributable to various factors. Amongst those, ventilation and thermal comfort will be particularly discussed in the latter sections of this chapter. It is indispensable to mention the pragmatic compromise between the performance of sports facilities and their energy consumption amidst the 2021 global energy crisis [4], as well as the alternative use purposes of sports facilities and especially the temporary change of use during the COVID-19 pandemic.

## 2.1 Overview

Regular physical activity serves as a strong foundation for a healthy heart, body, and mind. Worldwide, it is estimated that every fourth adult does not obtain enough physical activity to the levels recommended by the WHO [5]. The WHO suggests that adults should exercise at least 2.5 to 3.0 hours of moderate-intensity aerobic physical activity or at least 75 to 150 minutes of vigorous-intensity aerobic physical activity or equivalent [5]. With the recent COVID-19 pandemic, the significance of physical activity has increased considerably from public awareness due to the multiple lockdown periods imposed around the world. It is once again confirmed that the healthiness and well-being of individuals greatly enhance public health, the prevention of diseases across the population, and the competitiveness of a society [1, 6]. The global life expectancy has increased by 6.6 years between 2000 and 2019, while the global healthy life expectancy (disability-free life expectancy) increased just by 5.5 years. Noticeably, the years living healthy were not prolonged but only the mortality rate was reduced. This means that people live longer with a longer period of living with disability [7]. Thus, to exercise regularly is the key to bridge the gap between the two numbers.

Whilst doing physical exercise, the body experiences an increase in the respiratory rate, corresponding to the raised metabolic rate. It is observed that inhalation is done through the mouth more often than through the nasal passage, which is known as the filter for the air entering the lungs. As a result, the body is put to expose to the largest amount of pollutants through breathing, when the pollutants and tiny particles can be transported to the deepest part of the respiratory tract. Consequently, exercising in bad air quality can possibly put one at a health risk rather than improving their health [8]. Therefore, good indoor air quality should be ensured in such indoor sports facilities, so to minimise the effects of air contaminant exposures on the sports players and athletes. Ventilation is one of the effective

measures to control indoor air quality. However, the ventilation in the context of indoor sports facilities is more complicated than in other spaces because they are characterised by the high occupancy rate and the variety of physical activity intensities undergoing inside the space. In this regard, ventilation in indoor sports facilities must be designed and implemented in a way which ensures an adequate IAQ, at the same time maintains the thermal comfort of the athletes or the exercisers.

The next parts of this chapter serve as a buffer zone between the ventilation system and its contributions to the IAQ as well as thermal comfort in indoor sports facilities. As mentioned before, indoor sports facilities are characterised by a high and unstable human occupation rate with increased human-stemmed pollutants. The sports performance of the athletes or exercisers indoors is partly determined by the environment the activity takes place. IAQ and thermal comfort, as well as how the human body perceives and responds to different indoor conditions during practising sports will be discussed closely. To understand thoroughly these mechanisms is to lay a strong foundation to establish a more effective ventilation strategy in indoor sports facilities.

## 2.2 Human Thermal Comfort Approaches

Everyone perceives the thermal environment surrounding them differently. This has been studied across several scientific fields. Humans body can effectively adapt to a broad range of surrounding conditions thanks to its autonomic thermoregulation, including adjusting skin blood flow, shivering in the cold, and sweating in the heat. Humans can also make changes to their surroundings in order to minimise any discomfort by behavioural regulation, i.e., consciously exercising to increase their activity level when it feels cool, taking off some pieces of clothes when it feels warm, or opening the window to increase the wind flow. To systematically classify human thermal comfort viewpoints, Fantozzi and Lamberti identified in [2] the three main thermal comfort approaches: engineering, physiological, and psychological approaches. The engineering or physical approach considers the human body as a heat-exchanging object in the thermal environment; thus, thermal comfort can be achieved once the human body reaches a heat balance state. The physiological approach focuses on the responses of the human body to the changes in the thermal environment, whether it is an autonomic thermoregulatory response (using mechanisms occurring within the body) or behavioural response (using mechanisms from the environment outside of the body), or both, see Figure 3. The last one, the psychological approach, is proved to be the most bothersome approach, as it relates to both the human's physical and physiological aspects, at the same time it has to deal with the individual's personal experience and expectations. Psychological thermal adaptation is one of the factors which prevent the design of an indoor environment from achieving absolute satisfaction for everyone in the same space due to the differences among the individuals. Therefore, in practical design, optimal comfort is referred to as the comfort which satisfies the greatest percentage of occupants [9].

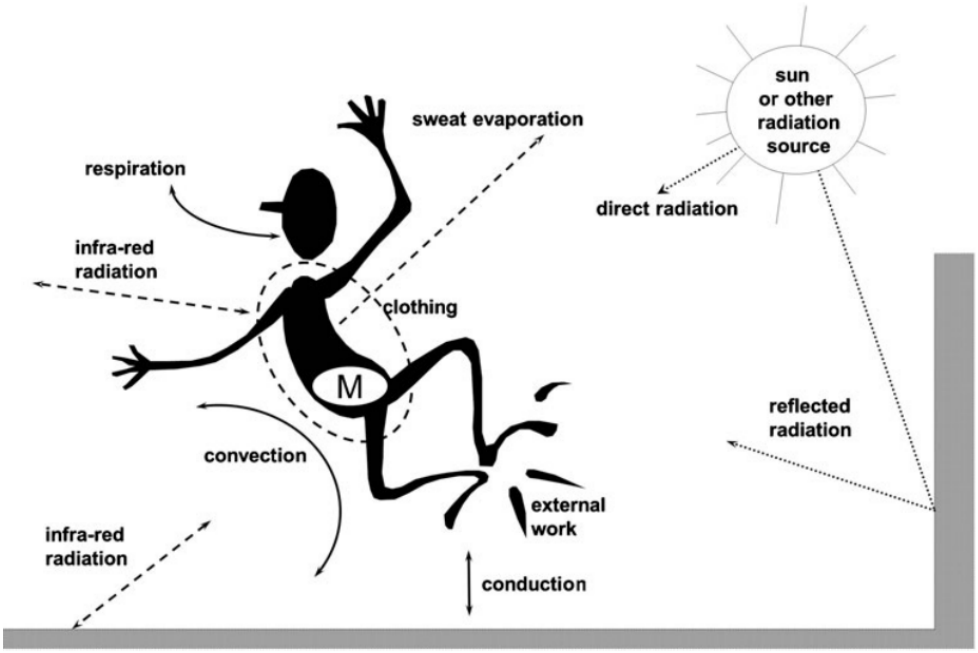


Figure 2. The human heat budget, reprinted from [10] after [11].

**The engineering approach** analyses the heat balance of the human body in exchange with their surroundings, i.e., the heat production, heat consumption, and the heat transferred to the environment. The heat balance is described in Equation 1 according to [10]. Fundamentally, this is the first theorem of thermodynamics applied to the human body's heat production and losses. The illustration of the heat avenues in exchange with the human body is provided in Figure 2. This approach considers the meteorological factors, the human activity level, and clothing. Nonetheless, the physiological variables which implicitly control the heat fluxes such as the sweat rate, skin temperature, skin wettedness, etc. are not mentioned. This equation motivates later research on the human thermoregulation systems, or later, the construction of human physiological models.

$$M - W - [Q_H(T_a, v) + Q^*(T_{mrt}))] - [Q_L(e, v) + Q_{SW}(e, v)] - Q_{Re}(T_a, e) \pm S = 0 \quad (1)$$

where M is the metabolic rate, W is the mechanical power, S is the rate of heat storage, Q's are the peripheral (skin) heat exchanges: $Q_h$ is the turbulent flux of sensible heat, $Q^*$ is the radiation budget, $Q_L$ is the turbulent flux of latent heat (passive diffusion water vapour through the skin), $Q_{SW}$ is the turbulent flux of latent heat (sweat evaporation), except the $Q_{Re}$, which is the respiratory heat flux (sensible and latent), and the thermal environmental parameters: $T_a$ is the air temperature, $T_{mrt}$ is the mean radiant temperature, $v$ is the air speed relative to the body, and $e$ is the partial vapour pressure.

**The physiological approach** deals with the ways the human body reacts to adapt to the changing thermal environment. The human body has its own

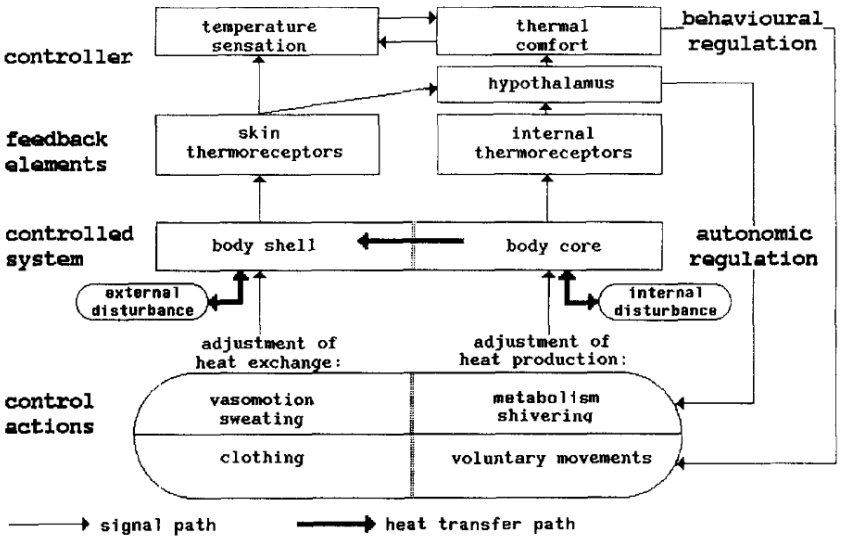


Figure 3. Schematic diagram of autonomic and behavioural thermal regulation in humans, reprinted from [12].

thermoregulatory mechanisms in order to keep the core temperature typically at around 37°C, or within the normothermic range of 36 °C to 40 °C [13] – these are referred to as the active system in thermoregulation. These mechanisms are triggered to cool the core down once there is surplus heat generated by the body, or to heat the core up when there is more heat loss to the environment than the heat produced in the body. When the body temperature increases to over 40 °C, it enters the hyperthermic condition. If the body's thermoregulatory mechanisms fail to lower the core temperature down to around 37 °C, and it exceeds the upper threshold temperature of 43°C, it is no longer reversible, a.k.a, fatal. In a similar but opposite manner, hypothermia is the condition when the body temperature drops below 35 °C, and the lower threshold temperature is 25 °C. In humans, regarding the thermal perception system, the thermoreceptors reside immediately about 0.2–0.5mm under the skin, with more cold receptors found near the skin surface than hot receptors. Also, the number of cold receptors is about 3.5 times more than hot receptors. The organ in the brain which receives the signals from the receptors and controls the thermal condition of the body is called the hypothalamus. Regulation of the blood flow to the skin is an important and most often used method to regulate body temperature. When the cold receptors send the signal and the hypothalamus receives it, the blood flow in the skin blood vessels is reduced by vasoconstriction so as to minimise the heat loss to the environment. This «insulation» process can be as effective as putting on a heavy sweater. Likewise, the blood flow is increased when there is excess heat in the body core by vasodilatation, thus boosting the heat transfer from the inner body to the environment. The boosted blood flow can be up to 15-fold more in extremely warm conditions compared to the blood flow at rest. In hot regulation, sweating is also a common mechanism to remove heat from the body by evaporation through the skin. Sweat glands secrete sweat either directly

through the skin surface or indirectly through the hair follicle or both. In favourable conditions with low relative humidity and high air velocity, the skin surface can still be dry even at high sweat secretion rate as all the sweat evaporates immediately. In less favourable conditions, most often observed in a moderate and hot climate, when the demand for cooling is high and consequently the sweat secretion rate increases, the sweat will spread to the area around the sweat glands and causes areas of wet skin. The proportion of the wet skin covered by sweat is called «skin wettedness». Increasing skin wettedness is associated with discomfort, regardless of the changes in body temperatures, according to Gagge in [14]. Fukazawa et al. in [15] later confirmed Gagge's hypothesis and even established a linear relationship between skin wettedness and thermal discomfort. Another study by Vargas et al. in 2018 [16] also concluded that skin wettedness plays an important role in thermal behaviour during exercise and recovery.

## 2.3 The Classic Fanger Model and the Criticism

During the 1960s, the prosperity followed by the stock market boom could be seen in many major countries. Corporations merged and became larger, while the workforce gradually moved from farms and assembling lines to office desks [17]. Offices witnessed significant growth, and workers desired better indoor environments [18]. HVAC engineers and architects were looking for methods and tools to predict the thermal comfort of the occupants, thus improving the quality of their design. At that time, the topic started to attract more and more researchers, amongst whom, Professor Ole Fanger is one of the most important contributors in this field – the thermal comfort study. His most influential work is the predictive model of whole-body thermal comfort, which was the result of numerous empirical studies based on real human participants dressed in standardised clothing, doing certain tasks, and being exposed to chamber-controlled conditions. His goal was to predict the optimum combination which provides comfort for the largest possible percentage of occupants by analysing the most impacting variables and introducing them in a human heat budget model. The predicted mean vote (PMV) was introduced as an index which represents the thermal votes of the occupants on a standard scale within a defined combination of thermal environment variables, activity level, and clothing. The index has been internationally accepted and brought into engineering practice ever since, including major international and national standards, such as the ISO and the ASHRAE. Together with the predicted percentage of dissatisfied (PPD), often used parallel, the PMV model has become the design guideline and is still popular in indoor climate assessment and prediction today. The mathematical equations of the PMV and PPD are briefly revisited in Equations 2 and 3. The detailed reference value tables for the parameters can be found elsewhere, for example in [19] or in [20].

$$
\begin{aligned}
PMV = &\left[0.303\exp\left(-0.036M\right)+0.028\right]\Big\{(M-W)\\
&-f_{cl}h_c(T_{cl}-T_a)-3.96\cdot10^{-8}f_{cl}\left[(T_{cl}+273)^4-(T_{mrt}+273)^4\right]\\
&-3.05\cdot10^{-3}\left[5733-6.99(M-W)-p_a\right]-0.42\left[(M-W)-58.15\right]\\
&-1.7\cdot10^{-5}M\left(5867-p_a\right)-0.0014M\left(34-T_a\right)\Big\}
\end{aligned}
\tag{2}
$$

where $M$ is the metabolic rate in $\mathrm{W\,m^{-2}}$, $W$ is the activity level in $\mathrm{W\,m^{-2}}$, $f_{cl}$ is the clothing surface area factor (dimensionless), $h_c$ is the convective heat transfer coefficient in $\mathrm{W\,m^{-2}\,K^{-1}}$, $T_{cl}$ is the temperature at clothes level in ℃, $T_{mrt}$ is the mean radiant temperature in ℃, $p_a$ is the partial vapour pressure in Pa, $V_a$ is relative velocity in $\mathrm{m\,s^{-1}}$, and $I_{cl}$ is the clothing insulation in clo.

$$
PPD = 100 - 95\exp\left(-0.03353PMV^4 - 0.2179PMV^2\right) \quad [\%] \tag{3}
$$

Figure 4 depicts Fanger's PPD as a function of PMV with the bold continuous line. It can be seen that Fanger's PPD is minimum around the neutral vote, and the PPD is symmetric over the vertical line $PMV = 0$. ISO 7730:2005 suggests that PPD should be kept around 0 with a tolerance of ±0.5 to ensure indoor thermal comfort. Moreover, it should be used attentively for PMV values out of the range $[-2;+2]$ due to the fact that the model was developed from empirical chamber settings, as notified by Fanger in his dissertation. Specifically, on the hot side ($PMV > +2$) significant errors were foreseen by the Professor [18]. As a consequence, his model was then the subject of many other validation studies through laboratory experiments.

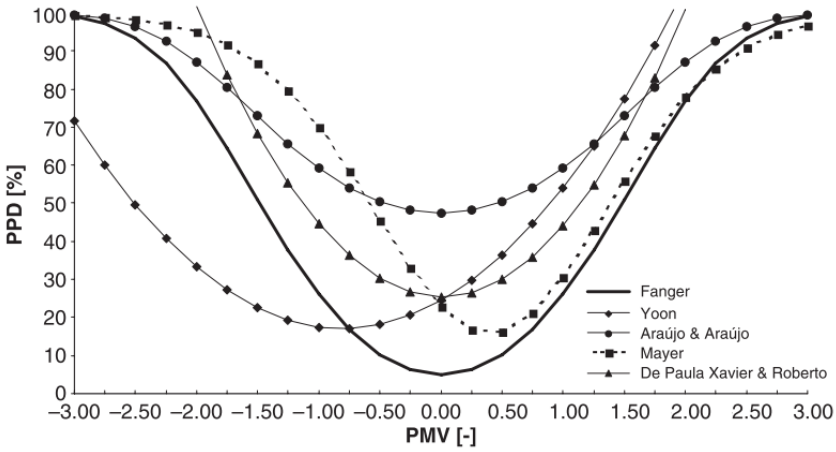


Figure 4. The PPD as a function of PMV from different studies, reprinted from [18] with corrections[2].

Over fifty years in practice, Fanger's PMV model has been validated, and gotten both endorsed and doubted by other studies. They showed discrepancies

[2]minus signs in front of positive votes on the horizontal axis were removed from the original figure.

from various perspectives, including the applicability in terms of geographic range, types of buildings, and input parameters [18]. The reliability and correspondence of the model were questioned when applying it to realistic cases in real life, where the subjects can be far away from being «standardised» and meteorological parameters can be totally deflected from the chamber conditions. Despite the fact that Professor Fanger had addressed that the model could be used in tropical climates, further research was still needed [21].

Validation studies from both laboratory and field settings illustrated that disagreement in the correlation between the PMV and the PPD does exist compared to Fanger's. van Hoff listed in [18] four studies from Korea, Germany, and Brazil (2 studies) and graphed their different PMV-PPD relationships in Figure 4. Fanger's model was thus proved to be reliable only within certain limits. To this end, the ISO 7730:2005 sets a range of input parameter validity range [19], as shown in the second column of Table 1. Humphreys and Nicols in [22] conducted an uncertainty analysis in the PMV with the ASHRAE's data set. They discovered that the stated ISO's intervals would cause considerable biases in the PMV and that the actual bandwidths of the parameters which produced the «correct» PMV («within acceptable bias» PMV) are narrower. As a result of the analysis, they defined the «bias-free» range of input parameters, which is shown in the third column of Table 1. It can be seen that the proposed interval for the activity level for minimal bias is realistically applicable to only resting and sitting office activities ($M < 1.4$ met), according to the metabolic rate measurement by indirect calorimetry by Zhai et al. in [23]. The same study also concluded that ISO and ASHRAE standards overestimated the metabolic rates of sitting, standing, and walking activities. The values for metabolic rate units for different activities are often taken from the two standards to predict thermal comfort by the PMV model. One other debating point is thermoneutrality and the preferred thermal sensation. Numerous independent study settings across several Asian countries and in different seasons were compiled in the same study by van Hoof. They revealed that (a) Fanger's thermoneutrality is not essentially ideal for a large number of people, that (b) it is common to have thermal preferences not right at Fanger's neutrality, but asymmetrically around that, and that (c) for a considerable amount of occupants, their thermal comfort is not unaccomplished when the thermal sensation votes fall out of the recommended range $[-1; 1]$.

The applicability of Fanger's model to buildings with and without air-conditioning was also doubted. de Dear et al. in [24] pointed out that there were evident discrepancies in the thermal sensations of occupants in air-conditioned buildings, naturally ventilated buildings, and hybrid ventilated buildings. In addition, they also found that the sensitivity of people in air-conditioned buildings with respect to temperature changes was higher than that of those in naturally ventilated buildings, up to two times. Since the PMV model does not fully capture the thermal adaptation of the occupants, de Dear et al. concluded that its application cannot be made to naturally ventilated buildings. They proposed afterwards an adaptive thermal comfort model for use in naturally ventilated buildings, which was then incorporated into ASHRAE

Table 1. Suggested intervals of input parameters by Humphreys and Nicol [22], reprinted from [18].

| Parameter | ISO 7730:2005 [19] | Humphreys and Nicol [22] | |
|---|---|---|---|
| | | PMV free from bias if | Comment |
| Clothing insulation | $0 - 2$ clo | $0.3 < I_{cl} < 1.2$ clo (chair included) | Overestimating of warmth of people in lighter and heavier clothing, serious bias when clothing is heavy. Little information exists for conditions when $I_{cl} < 0.2$ clo. |
| Activity level | $0.8 - 4.0$ met | $M < 1.4$ met | Bias larger with increased activity. At 1.8 met overestimation sensation of warmth by 1 scale unit. |
| «Hypothetical heat load» | | $M \cdot I_{clo} < 1.2$ units of met.clo | Serious at 2 units. |
| Air temperature | $10 - 30$ °C | | Overestimation warmth sensation $t_a > 27$ °C. At higher temperatures bias becomes severe. Upper limit $t_a$ approx. 35 °C in [19]. |
| Mean radiant temperature | $10 - 40$ °C | | |
| Vapor pressure or relative humidity | $0 - 2.7$ kPa or $30 - 70$ | | Suggested bias becomes important if $p_a > 2.2$ kPa. |
| Air velocity | $0 - 1$ m/s | $v_a < 0.2$ m/s | Overestimation warmth sensation $v_a > 0.2$ m/s. Underestimation cooling effect increased $v_a$. |

55 as an optional assessment method alongside the PMV method by Fanger. This approach is established based on extensive field studies, assuming that people will adapt to the thermal conditions whenever there are risks of discomfort. Only two variables are involved – indoor and outdoor temperatures – to determine the occupants' «acceptability limits». The foundation of this approach relies heavily on the occupants' behavioural adaptation, while physiological adaptation and psychological adaptation are not discussed. This approach is said to have narrow applicability and modest coverage to a vast part of the building stock across different climate regions, namely cold and moderate zones. It was noted by de Dear and Brager in [25] that buildings with a large number of occupants who do not have control over their indoor environment are ruled out under this approach. The latest version of ASHRAE 55 (2020) states clearly the applicability conditions of both methods [20]. Therefore, the use of either Fanger's model or the adaptive model should be selective and purposed-based.

Until today, in thermal comfort assessment methods in buildings, it is undeniable that Fanger's model is still the most commonly applied one. This half-a-century-old approach is widely used in practical studies and design, as well as being taught at universities and to professionals as the most important method for evaluating thermal comfort. However, the growth of computational power, as well as the development of new simulation tools, have called for a higher level of detail with a wider range of input parameters, and most importantly, non-uniform, transient thermal conditions. The easy availability of measurement devices, data transfer, storage, and processing have enabled the re-evaluation and improvement of the old models as well as the development of the new ones, with a higher level of complexity and a higher range of use. With relevance to thermal comfort assessment or prediction of exercisers in indoor sports facilities, Fanger's model is hardly applicable. This is due to the fact that in sports environments, the sports exercisers' time-averaged metabolic rates are classified as high ($M \geq 2.0$ met, [20]) in most sports activities. This opens up the application of other human thermal comfort models. The next section will introduce

and delve deeper into the physiological approach in thermal comfort study and the development of different physiological models.

## 2.4 Human Thermal Physiological Models

Since the 1970s, following Fanger's whole body thermal comfort model, there have been multiple other established models to represent the thermal physiological interactions of the human body and body parts with the surrounding environment [2, 26]. These models try to simulate the way the human body temporally adapts to external stimuli. They consider more closely the peripheral and the metabolic heat exchange with the body by explicitly adding more relevant meteorological and anatomical variables, thus predicting the thermal response of humans. One example of the physiological response is that, when exposed to freezing cold air without thick clothes, a person might start to shiver (as it leads to a higher metabolic rate) and the blood flow under their skin is reduced by vasoconstriction (as it lowers the heat loss to the surroundings through radiation and convection by making the skin temperature lower). Two other thermoregulation mechanisms in humans are sweating and vasodilatation.

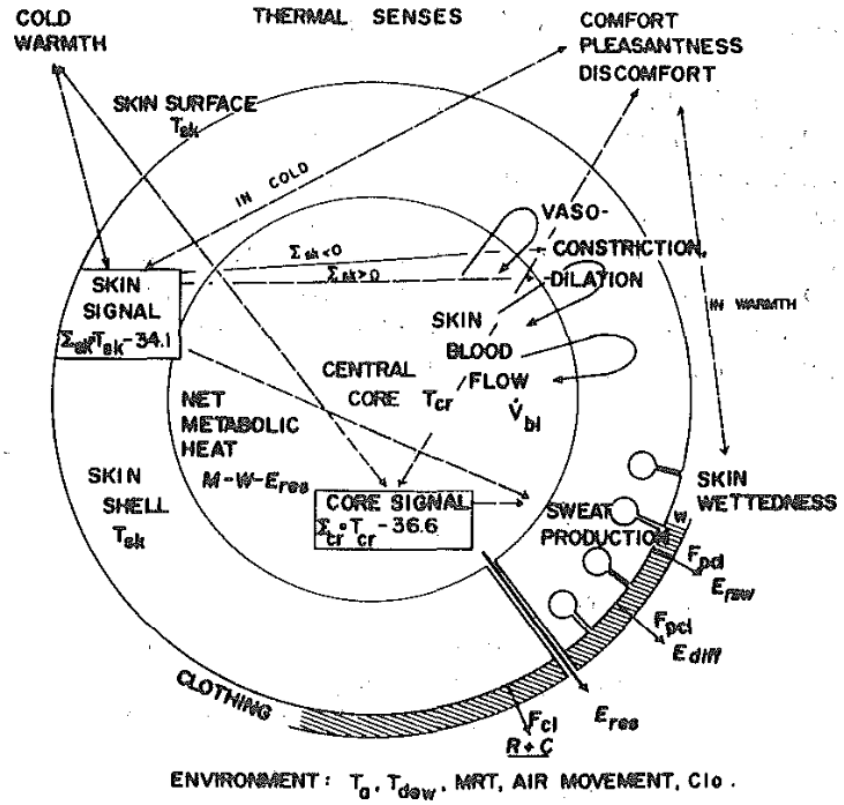


Figure 5. The concentric shell model – the Pierce two-node model, reprinted from [27].

The most simple nodal model, developed at the John B. Pierce Foundation at Yale University, is so called the «Pierce two-node model» by Gagge et al. It was first published in 1971, and the revised version with the rewriting of Fanger's PMV equation and the introduction of several other thermal indices was published in 1986 [14, 27]. The model includes both the passive system and the controlling system. The Pierce model analytically divides the human body into two isothermal, concentric shells with distinct masses. The inner one represents the core where all the metabolic heat is considered to be generated. The outer skin represents the interface of the human body with the environment, where all peripheral heat exchange happens. The original figure illustrating the shell model of «man» is reprinted as Figure 5 from the publication on ASHRAE Transactions in 1971. The skin and the core temperatures act as the controllers for the human physiological responses to the surroundings, i.e., the regulatory sweating, skin blood flow, and shivering, which were described in the controlling system section of [27].

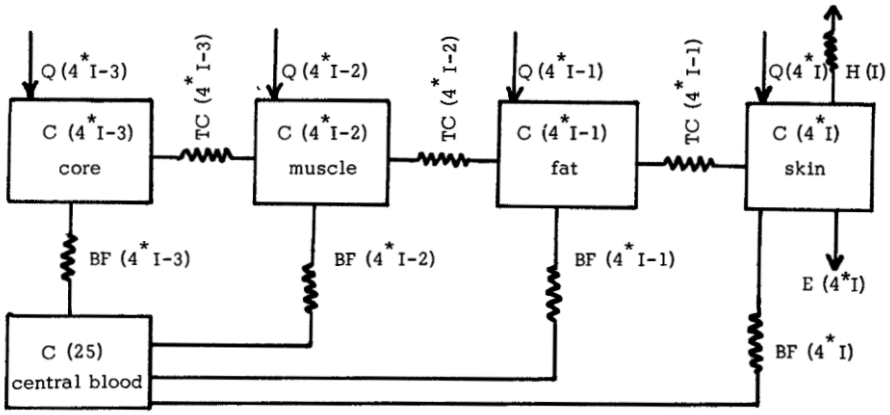


Figure 6. Schematic diagram of the interrelations amongst the four concentric layers of Segment I in the original Stolwijk model, reprinted from [28].

Another early complex multi-node model which was originally developed at NASA to be used in aerospace applications was published by J. A. J. Stolwijk in a NASA Contractor Report in 1971 [28]. He also revealed that the model was already implemented on an analogue computer in 1966, which he called the «forerunner» of this 1971 model. The model divides the human body into six segments, each segment is composed of 4 layers and one central blood pool. The objective of this model is to predict the thermal response and sensation of space travellers so as to develop suitable protection systems for them in the deep space environment. Stolwijk raised the advantage of his mathematical model as «they can be made to communicate with models of technical systems» [28]. A schematic illustration of the four compartments of segment I of the Stolwijk model is reprinted in Figure 6. Stolwijk model is the foundation of numerous other multi-segmental, multi-nodal, transient, non-uniform thermo-physiological models, which were validated with experimental data or thermal manikin experiments. Amongst those, IESD-FIALA and Tanabe 65MN are the two

remarkable evolvements of the Stolwijk model. Table 2 summarises the characteristics of novel thermo-physiological models. State-of-the-art models are developed with a higher level of accuracy by focusing more on multi-element models integrated with advances in human physiological research and increased computing power. Creating or selecting an appropriate human thermophysiological model to study thermal comfort as well as indoor condition monitoring is a challenging task, yet, by that, a correspondingly satisfactory result will be obtained in return.

To repeat once again, although being applied extensively in building science, Fanger's model is used in steady-state and uniform environments, and it does not take into account explicitly the active thermoregulation of the human body, such as vasoconstriction, vasodilatation, sweating, and shivering. Therefore, the model has low applicability in transient and non-uniform conditions or conditions further away from thermal neutrality, e.g., during sports activities or within vehicular environments. This could lead to considerable bias results if carelessly used in such cases. For instance, in Gagge's two-node model, mean body temperature was used as a quantified indicator to examine the thermal behaviour associated with thermal discomfort. The mean body temperature in this model is an equally weighted value of skin temperature and core temperature. Moreover, in a recent study by [16] in 2018, an empirical study was conducted and the results proved that sweating and subsequently skin wettedness are important contributors to thermal behaviour during exercise and recovery. It was also suggested that in cases when there is simultaneously an increase in body temperature and an expectation of sweat generation such as during sports activities, skin wettedness should also be included in the indicator as a weighted component. Noticeably, it was concluded that the contribution of skin wettedness to the thermal regulation behaviour is more significant than both the mean skin temperature and the core temperature. Even, the proposed weighting factor for skin wettedness is much greater than those for the mean skin temperature and core temperature added together. This is noteworthy when it comes to examining the thermal comfort in indoor sports facilities because in most indoor sports disciplines, except water sports, sweating and sweat accumulation are almost always observed along with raised body temperature. At the same time, it suggests that a model which includes thermophysiological control of the human body (active and automatic thermoregulation) should be chosen in sports-related studies.

For those reasons discussed above, a more appropriate comfort model should be used in sports-related facilities, instead of the PMV, namely multi-node models such as the Pierce two-node model, the Tanabe 65MN, the UC-Berkeley model (Zhang model), or the FIALA model. These thermal comfort models were introduced in several thermal comfort simulation tools such as the ABICS open-source software, including the Tanabe 65MN and the Zhang 2003 models, written by J. Hussan at the Auckland Bioengineering Institute, University of Auckland [31]; the Theseus-FE, a commercial tool by ARRK Engineering GmbH, including the FIALA-FE (modified FIALA), Zhang's local comfort models, and Fanger's models [32]; JOS-3 python package by Takahashi et al.[33]; Design Builder, including the Fanger's, Pierce

Table 2. Summary of several thermo-physiological models, partly adapted from [29, 30]).

| Author(s) (year)<br>Model alias | Characteristics | Environmental conditions | Human body description | Active and passive systems |
|---|---|---|---|---|
| Fanger (1974)<br>Fanger model | 1 segment<br>1 node | steady-state and uniform | n/a | no active system |
| Stolwijk (1971)<br>Stolwijk model | 6 segments<br>25 nodes<br>4 layers | transient and non-uniform | «average» man | controlled by functions of two tissue temperature signals, hot/cold signal and rate of tissue temperature change signal |
| Gagge (1971–1986)<br>Gagge model | 1 segment<br>2 nodes<br>2 layers | transient and non-uniform | «average» man | controlled by changes in mean skin and body core temperature |
| Fiala (1999)<br>Fiala model | 15 segments<br>187 nodes<br>3 sectors<br>7 tissues | transient and non-uniform | «average» man | based on Stolwijk model |
| Tanabe (2002)<br>65MN | 16 segments<br>65 nodes<br>4 layers | transient and non-uniform | «average» man<br>physical parameters can be changed | based on Stolwijk model |
| Zhang (2002)<br>UC-Berkeley | unlimited segments<br>unlimited nodes<br>4 layers | transient and non-uniform | «average» man<br>physical parameters can be changed | based on Stolwijk model |

two-node, and the KSU models (Kansas State University model); or the JBODY web-based application by Energy Simulation Solutions Ltd. [34], with available web API. Nevertheless, it is important to emphasise that, none of the aforementioned multi-segmental, multi-nodal thermo-physiological models has been adopted by any international, or national standards, or guidelines, as an option for the assessment and prediction of local or whole-body thermal comfort. The next section will describe shortly the fundamental of the 65MN model and IESD-FIALA as a foundation for Chapter 4.

## 2.5 The Tanabe 65MN Model and its Succeeding Versions

The 65-node thermal regulation model was developed by S. Tanabe et al. based on the Stolwijk model. It was first published in 2001, updated the first time in 2013 under the alias JOS-2 [35], and the latest version JOS-3 of this model was published in 2013 by [33].

The model includes a passive and an active system. The human body is segmented into 16 parts, each consisting of four layers, each layer acts as 1 node, plus the central blood pool which is the 65th node of the model. The 65 MN model considers the heat transferred within the tissues in each segment by conduction and the heat exchange with the environment by convection, radiation, evaporation, and respiration. The heat transferred between the tissues with the blood flow in each layer is simplified as the heat transferred between the tissues and the central blood pool [36], see Figure 7a. This is one unsafe simplification of the original 65MN model, which was then improved and published in 2013 with a more detailed

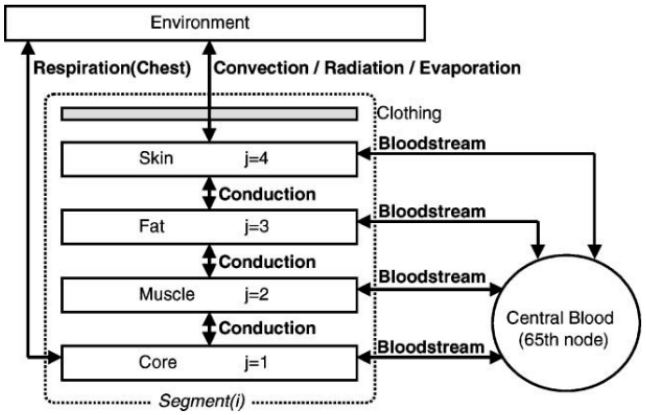


(a) Tanabe 65MN, reprinted from [36].

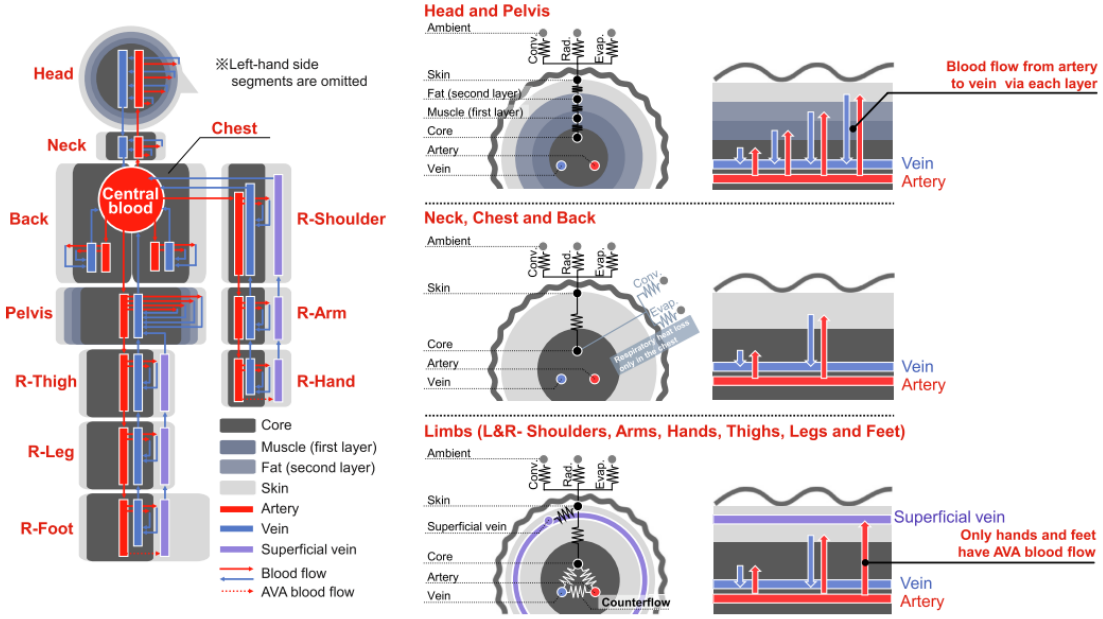


(b) JOS-3, reprinted from [33].

Figure 7. The Tanabe 65MN model and its latest version, JOS-3.

vascular system, so-called the JOS-2 model. Following that, the latest JOS-3 was introduced with the consideration of more physical and physiological parameters such as the ageing effect, brown adipose tissue activity, and shortwave solar radiation heat gain. The JOS-3 model consists of 83 nodes and the body temperatures were solved using the backward difference method, see Figure 7b. Most of the drawbacks of the previous version are improved extensively in this version. Through comparison of the model performance versus testing measurements on human subjects, the model was proved to have «higher accuracy in the prediction of heat production in young and older subjects and the mean skin temperature in older subjects [...] under cold environmental conditions» [33]. The model was implemented in open-source code in the form of a python package. The repository of the package can be found on GitHub at [37]. The use of JOS-3 model in python is exemplified in Appendix B.2.

## 2.6 The IESD-FIALA Thermal Comfort Model

The FIALA thermal comfort model was constructed by Fiala D., Lomas K., and Stohrer M. at the Institute of Energy and Sustainable Development (IESD), De Monfort University. The abbreviation IESD-FIALA refers to the original FIALA model published in 2001, to distinguish it from the later FIALA model versions such as the FIALA-FE, which is based on a finite element approach and allows the individualisation of human characteristic parameters [38]. The IESD-FIALA model consists of a passive system and an active system.

The internal energy of **the passive system** is balanced by the Pennes bioheat differential equation at the tissue level, Equation 4, which is also the core of the mathematical model of IESD-FIALA. An FDM scheme to solve Equation 4 was presented in [39], in which the partial derivatives with respect to radius were approximated by the central difference method and the derivatives with time by the Crank-Nicolson method.

$$\underbrace{k\left(\frac{\partial^2 T}{\partial r^2}+\frac{\omega}{r}\frac{\partial T}{\partial r}\right)}_{\text{conduction}}+\underbrace{q_m}_{\text{metabolism}}+\underbrace{\rho_{bl}w_{bl}c_{bl}\left(T_{bl,a}-T\right)}_{\text{convection}}=\underbrace{\rho c\frac{\partial T}{\partial t}}_{\text{change in storage}} \tag{4}$$

where $k$ is the tissue conductivity in $\mathrm{W\,m^{-1}\,K^{-1}}$, $T$ is tissue temperature in °C, $r$ is the radius in m, $\omega$ is a geometry factor (dimensionless): $\omega = 1$ for polar coordinates and $\omega = 2$ for spherical coordinates (head), $q_m$ is body metabolism in $\mathrm{W\,m^{-3}}$, and blood perfusion, which is a heat-convection term, where $\rho_{bl}$ is the density of blood in $\mathrm{kg\,m^{-3}}$, $w_{bl}$ is blood perfusion rate in $\mathrm{s^{-1}}$, $c_{bl}$ is heat capacitance of blood in $\mathrm{J\,kg^{-1}\,K^{-1}}$, and $T_{bl,a}$ is arterial blood temperature in °C, $\rho$ is tissue density in $\mathrm{kg\,m^{-3}}$, $c$ is tissue heat capacitance in $\mathrm{J\,kg^{-1}\,K^{-1}}$ and $t$ is time in s.

An average man was formulated as a humanoid, whose body is simplified as 15 body parts, either cylindrical or spherical (the head). Seven types of tissue layers were categorised based on the changes in body tissue properties distributed in each body part, including brain, lung, bone, muscle, viscera, fat and skin tissue layers. Every layer is then divided again into one or more tissue nodes. The body part is then sectorised into anterior, posterior, and inferior to take into account the asymmetric removal of bodily heat, due to, for instance, solar radiation, non-uniform clothes, sports garments, and hot or cold surface touching, see Figure 8. This segmentation, layerization, and spatial subdivision make the passive system highly anatomically, thermo-physically, and thermo-physiologically detailed [34].

The model takes into consideration the phenomena of human heat exchange that occurs within the body (i.e., blood circulation, metabolic heat production, conduction, and storage) and at the body periphery (i.e., free and forced convection, long- and shortwave radiation, clothing insulation, skin moisture evaporation, diffusion, sweat discretion, and sweat liquid storage).

Fiala et al. modelled the active system by simulating the responses of the

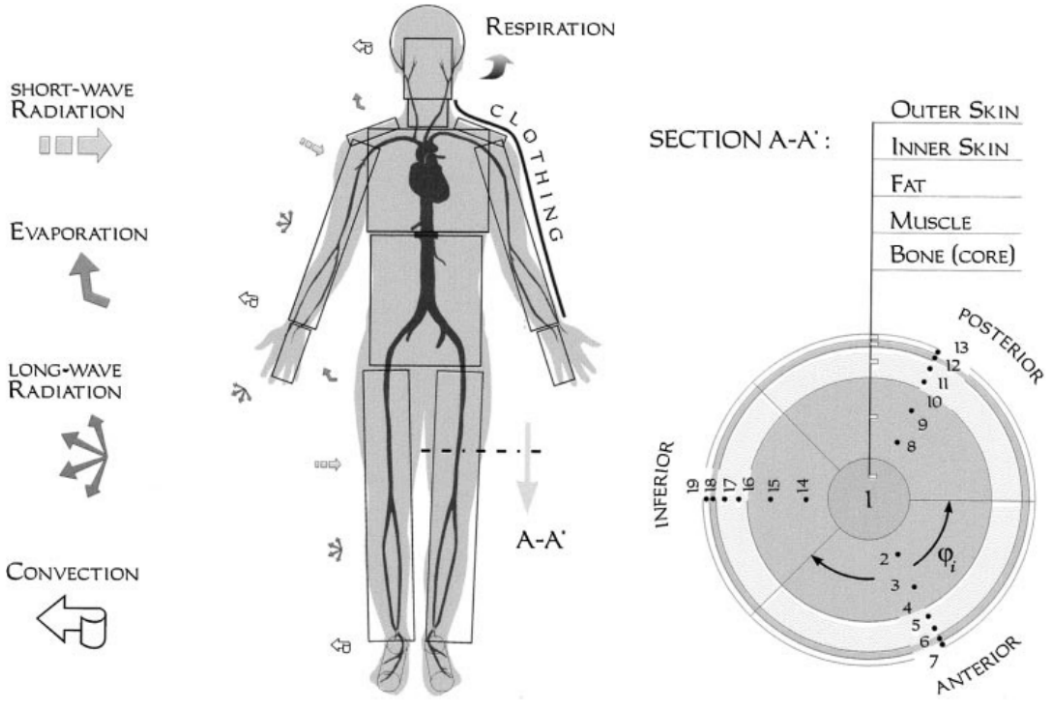


Figure 8. Schematic diagram of the passive system of the IESD-FIALA model, reprinted from [39].

human thermoregulatory system including the blood flow, i.e., controlling the surface heat loss by vasoconstriction and vasodilatation, the latent heat loss by sweat discretion, and heat production rate by shivering. Using data obtained from a wide range of steady and transient exposures, the active system was developed through regression analysis. The experimental measurements on mean and local skin temperatures as well as core body temperature spread from cold stress, cold, moderate, warm and hot stress conditions, and on over 2000 male and female subjects who were exercising at the intensities between 0.8 - 10 met [40, 41]. The model was validated with measured regulatory responses and showed good agreement. The model is thus capable of predicting the thermal responses of humans in real-world conditions and analysing the transient, non-uniform surroundings such as in vehicular environments, buildings, or even outdoors. That being said, the IESD-FIALA model corresponds to all the key aspects that Fanger's PMV model missed to provide in the study of thermal comfort in sports environments. Thus, it can be an alternative approach within the scope of this work.

The current version of the FIALA model is known as the **F**iala thermal **P**hysiology and **C**omfort (FPC) model version 5.3 [42]. The details of this version are not published, instead, it is commercialised in a human physiological and comfort simulation software by Ergonsim, a Germany-based company [43]. According to Roelofsen in [42], this version underwent noticeable changes, e.g., the standard male was replaced by a unisex person, and the body now has 20 compartments containing 366 tissue nodes.

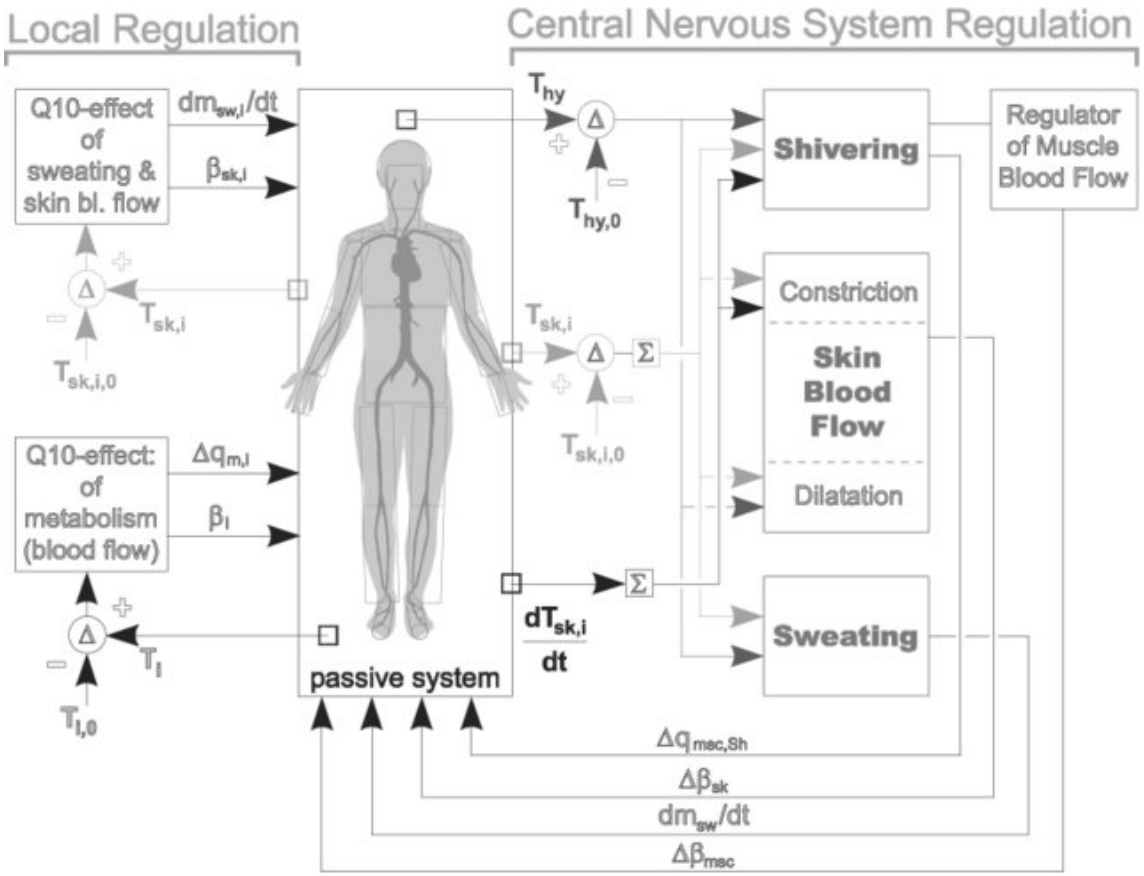


Figure 9. Schematic diagram of the active system of the IESD-FIALA model, reprinted from [40].

## 2.7 Carbon Dioxide Generation and Metabolic Rate Changes in Humans during Exercising

A building's main source of carbon dioxide is the respiration of its occupants. Carbon dioxide is produced by the human body and oxygen is consumed by the human body at a rate primarily determined by the size of the individual and the level of physical activity. In ASHRAE Handbook 2013, there is a detailed discussion of the relationship between activity level and carbon dioxide generation and oxygen consumption. The rate of carbon dioxide consumption in l/s is calculated using the formula in Equation 5.

$$V_{O_2} = \frac{0.00276 A_d M}{(0.23RQ + 0.7)} \qquad \text{l/s} \tag{5}$$

where $RQ$ is the respiratory quotient (dimensionless), $M$ is the metabolic rate per unit of the surface area of the human body in met, $A_d$ is the DuBois surface area from Equation 6 below, in $m^2$:

$$A_d = 0.2025 m^{0.425} l^{0.725} \tag{6}$$

where $m$ is the body mass in kg, and $l$ is the body height in cm.

In each individual, the quotient $RQ$ varies, depending on the person's physical conditions, activity level, and diet [44]. The range of $RQ$ is $[0.7; 1.0]$, at an estimated value of 0.83 for an average adult doing light or sedentary activities ($M < 1.5$ met) having a normal diet. The quotient increases proportionately to 1 for «extremely heavy exertion», about 5 met [44]. A person's rate of carbon dioxide production is determined by the definition of the $RQ$ as in Equation 7.

$$V_{CO_2} = RQ \cdot V_{O_2} \tag{7}$$

At a steady-state or lengthened period of work rate, it was observed that the breathing rate corresponds almost proportionately and immediately to the change in work rate. This was revealed by Casaburi et al. in their study in [45] on the different time constant between the breathing rate and the motor responses to exercise, see Figure 10. A phase lag and a reduction in the breathing rate amplitude in the shorter period of the varying work rate. This suggests that the provided diagram from ASHRAE 62.1 on the relationships among physical activity level, the breathing rate, oxygen consumption, and carbon dioxide production, should not be used for instantaneous assessment thereof, see Figure 11. Howbeit, it is a good source of information to use for rough estimation or in time-weighted averaging over a lengthened period of time.

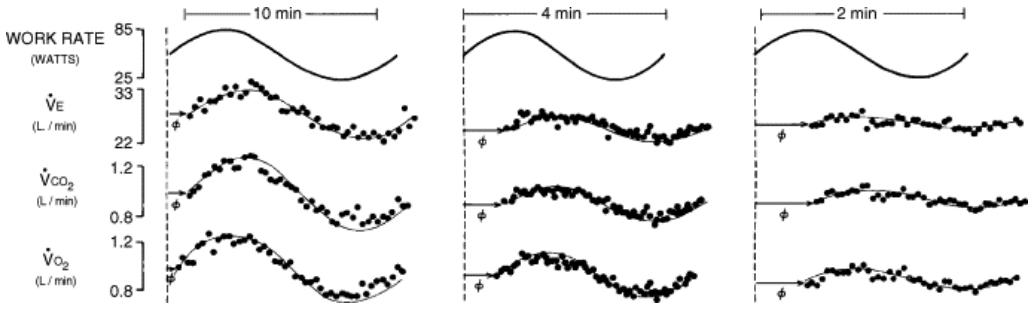


Figure 10. Breathing rate, oxygen consumption, and carbon dioxide production responses to sinusoidally varying work rate at different periods of 10 to 2 minutes in a person [45].

The Finnish Guidelines for the HVAC Design of Indoor Sports Facilities LVI-06-10600 provides an alternative method to estimate the carbon dioxide production of a person by multiplying the actual met level with the reference carbon dioxide production at the base level 1.0 met, as seen in Equation 8.

$$V_{CO_2} = \frac{V_{O_2(M=1)} \cdot M}{3600} \qquad \mathrm{L\,s^{-1}} \tag{8}$$

where the $V_{O_2(M=1)}$ is suggested to be taken at 20 $\mathrm{L\,h^{-1}}$ by [46].

It can be observed in various places within this topic that the human metabolic

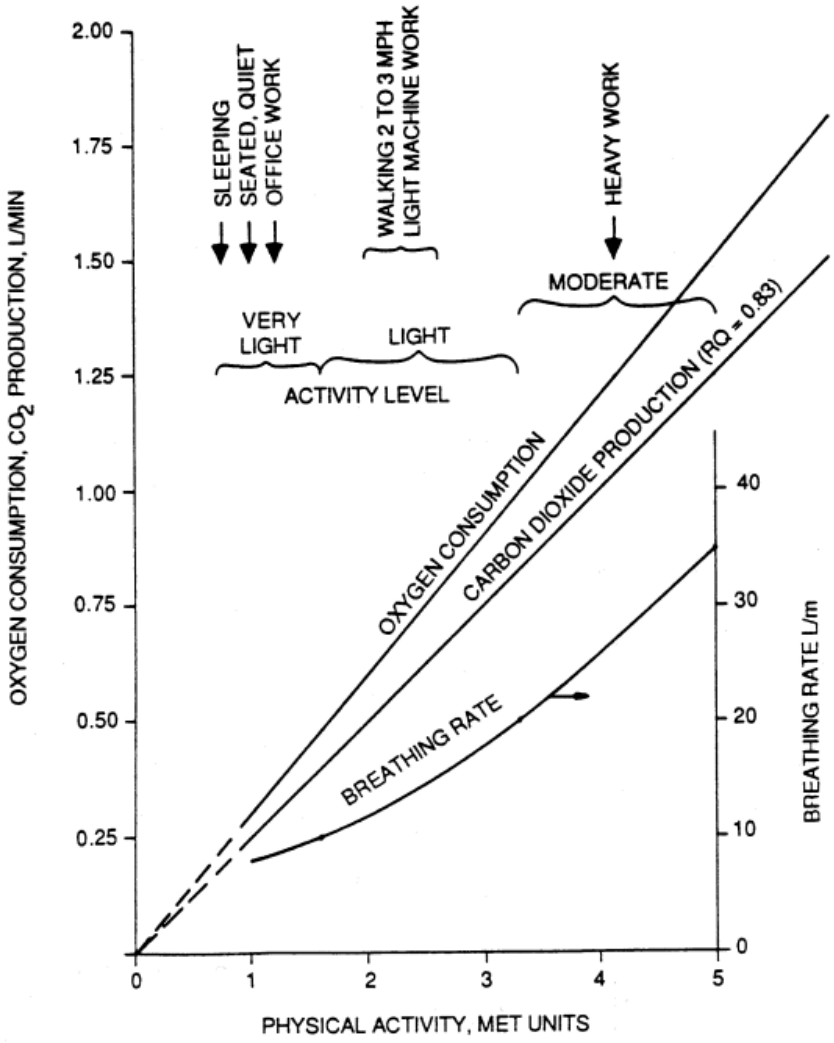


Figure 11. The relationship of oxygen consumption, carbon dioxide production, breathing rate, and physical activity level [47].

rate is involved in the determination and calculation of several other input parameters of the thermal comfort models. Tabulated reference values for metabolic rates in various defined activities are provided, usually by ranges or average values, for example, Table 5-1 in ASHRAE 55-2020 [20] or Annex B in ISO 7730:2005 [19]. The Finnish LVI 06-10600 Guidelines also present a similar table, but from different sources, see Appendix 1 of [46]. The latter gives more related information about the metabolic rates in sports and exercise activities than the former ones. In most cases where metabolic rates are not required to be measured accurately, the values from those tables suffice. However, ASHRAE warns in [44] that for an activity where $M > 3.0$ met, the values are prone to more significant error, as much as $\pm 50\%$. More importantly, the nature of sports and exercise activities is that the subject metabolic rates tend to exceed 3.0 met; thus, it is advisable to use the tabulated data very cautiously. For instance, physiological measurements might be needed, by various

direct or indirect methods, to estimate the metabolic rate. ISO 7730:2005 suggests that a time-weighted average is to be used in the PMV model if it is estimated from the previous one-hour period of activity [19].

ASHRAE Fundamental 2017 advises that estimating metabolic rate through RQ and the volumetric rate of oxygen consumption is satisfactorily sufficient, for a 10% error in RQ leads to $< 3\%$ error in the metabolic rate. The empirical formula for this method is presented in Equation 9.

$$M = \frac{21(0.23RQ + 0.77)Q_{O_2}}{A_D} \tag{9}$$

where $Q_{O_2}$ is the volumetric rate of oxygen consumption at STPD conditions in $\mathrm{mL\,s^{-1}}$, $A_D$ is the DuBois surface area in $\mathrm{m^2}$ as in Equation 6.

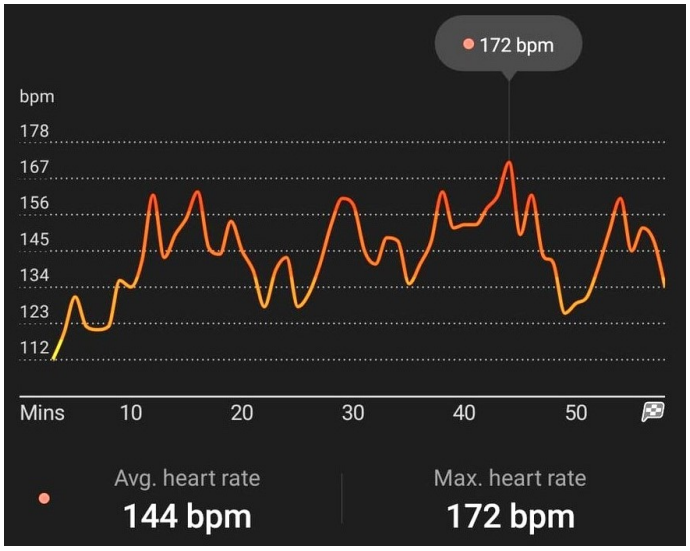


Figure 12. Heart rate log of an amateur football player during a 60-minute training session.

A workaround method is to estimate oxygen consumption through the heart rate (HR) measurement. This method is introduced in ASHRAE Fundamental 2017, using tabulated values of oxygen consumption corresponding to the heart rate at different levels of exertion from the research of Astrand and Rodahl, published in 1977 [48]. It is said to be less accurate by ASHRAE, for HR is not purely a physical meter but also a physiological and psychological one [44]. In the more academically updated ISO 8996:2021 Ergonomics of the thermal environment - Determination of metabolic rate, the standard defines four levels of methods for estimating the metabolic rate from the least to the most accurate. According to this scale, the aforementioned method through HR measurement is at level 3. The standards list the factors affecting the differences in the metabolic rate results using this level 3 method compared to recorded field data as follows: (a) a hot environment raises HR significantly, (b) stress and mental load oscillation leads to underestimation or overestimation of the actual metabolic rates, and (c) the fitness of the subjects

varies [49]. Despite the listed factors, the HR values reflect the «global strain of the person and therefore can be used to estimate the strenuousness of the task or job of the person» [49]. Annex C of the standard presents the procedure for estimating the metabolic rate based on recorded HR, based on the work of Malchaire et al., published in 2017 [50].

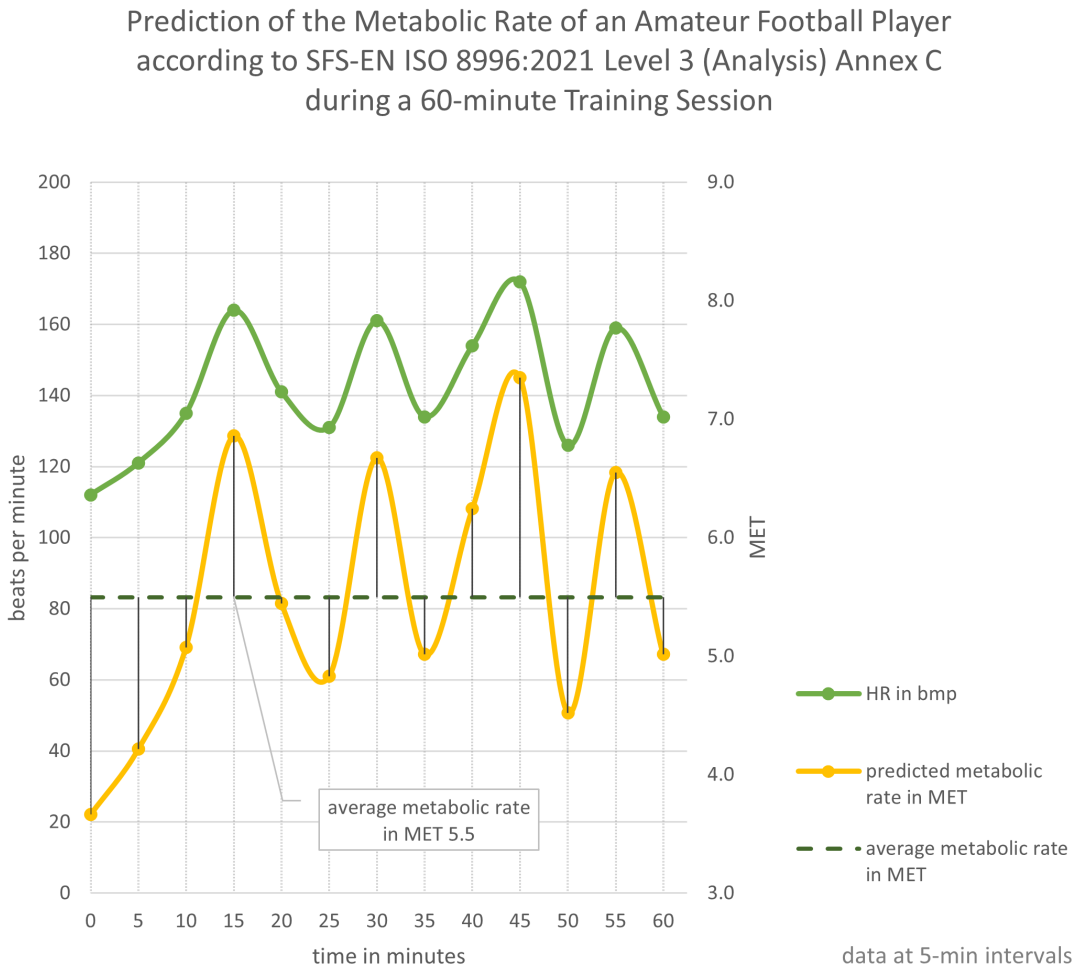


Figure 13. Metabolic rate in relation to the heart rate of an amateur football player during a 60-minute training session.

An example of the metabolic rate determination at level 3 (Analysis) according to Annex C of the ISO 8896:2021 is introduced as follows. The player is a 24-year-old male, slightly overweight by the BMI index. He was participating in a one-hour football training session. The session was short and there were several pauses. The HR of the subject was logged by a sports garment watch into a smartphone application as shown in Figure 12. Following the Annex C procedure, the metabolic rate was calculated and the result is shown in Figure 13. Detailed calculation of this example is presented in Appendix B.1. It can be seen that during the session, the HR of the subject fluctuates considerably, and subsequently does the metabolic rate. Dips in

both values can be observed during rest periods. It takes about 8 minutes during the warming-up period for him to get to 5.0 met, and no less than 5 minutes to get to the next met level. This observation is in line with the conclusion from the study of Ji et al. in [51], where the metabolic rate is calculated based on indirect calorimetry theory. The average metabolic rate of this player during the whole session is at 5.5 met, which is slightly above the lower limit of the range for football by the guideline [46], at 5–10 met. The dynamic changes in the metabolic rate of this sport player affected the thermal sensation. Therefore, in thermal comfort assessment and prediction of sports players or exercisers, momentary discomfort is unavoidable, e.g., during warming up or in between break periods.

## 2.8 Clothing and Sports Garments

Clothing on the human body acts as extra layers of heat and moisture resistance. Clothing participates directly in the balancing of the human heat budget, as described in Section 2.2. In sports environments, the sports disciplines usually decide or conventionally form a certain way of dressing for the athletes or players, depending strongly on the characteristics of the sport itself and the surroundings where it is played. For instance, beach volleyball apparel is accustomed to being seen with a pair of short bras and briefs on women, and a sleeveless shirt with short shorts on men. Skiing or snowboarding clothes are specialised by wind- and waterproof but light and breathable shell jackets, with beanie or helmet. The clothing and sports garments are to create and maintain a comfortable micro-climate between the human skin and the environment; thus, they contribute to the thermo-physiological comfort of the wearers during sports activities. It is undeniable that sports apparel bears remarkable importance when it comes to survival protection from the environment, e.g., mountain hiking or paragliding. Additionally, suitable, comfortable clothing can also improve athletic performance from a psychological perspective.

Clothing in thermal comfort models is considered as thermal insulation layers. ISO 9920:2007 presents in detail the methods for estimating the thermal insulation and water vapour resistance of a clothing ensemble [52]. In practice, the insulation value $I_{cl}$ in clo of complete ensembles from tables from e.g. ASHRAE 55, ASHRAE 62.1, ISO 7730:2005 [19, 20, 47] is adopted for convenience. This value of customised ensembles is also possible to be calculated with the empirical Equation 10 presented in ISO 9920:2007, where the properties of standardised clothes items can be found in Table B.2. The insulation values of some of the most common daily wear clothing ensembles are shown in Table 3.

$$I_{cl} = 0.161 + 09.835 \sum I_{clu} \tag{10}$$

where $I_{cl}$ is the insulation value of complete ensemble in clo, $I_{clu}$ is the insulation value of individual garments in clo.

In many sports disciplines, players or exercisers usually move continually

Table 3. Insulation values of common clothing ensembles, adapted from [52].

| Clothing ensembles | $I_{cl}$ | |
|---|---|---|
| | clo | $m^2\,K\,W^{-1}$ |
| Panties, T-shirt, shorts, light socks, sandals | 0.3 | 0.05 |
| Panties, petticoat, stockings, light dress with sleeves, sandals | 0.45 | 0.07 |
| Underpants, shirt with short sleeves, light trousers, light socks, shoes | 0.5 | 0.08 |
| Panties, stockings, shirt with short sleeves, skirt, sandals | 0.55 | 0.085 |
| Underpants, shirt, lightweight trousers, socks, shoes | 0.6 | 0.095 |
| Panties, petticoat, stockings, dress, shoes | 0.7 | 0.105 |
| Underwear, shirt, trousers, socks, shoes | 0.7 | 0.11 |
| Underwear, tracksuit (sweater and trousers), long socks, runners | 0.75 | 0.115 |
| Panties, shirt, skirt, thick knee socks, shoes | 0.8 | 0.12 |
| Panties, shirt, skirt, round-neck sweater, thick knee socks, shoes | 0.9 | 0.14 |
| Underpants, singlet with short sleeves, shirt, trousers, V-neck sweater, socks, shoes | 0.95 | 0.145 |
| Panties, shirt, trousers, jacket, socks, shoes | 1 | 0.155 |

during the training or playing period. The clothing items are not always attached to the human skin, not to mention the openings such as collars and cuffs. When performing movement, air from the environment can «blow» inside and increase or decrease the distance between the fabric and the human skin. This is described as the «pumping effect» of the body motion in the ISO standard [52]. When a person sweats, the secreted liquid is absorbed by the fabric until it is saturated. The absorbed liquid changes the thermal insulation and the vapour resistance properties of the clothing items, generally increasing heat loss and evaporation rate. The relative air movement effect on the thermal insulation and vapour resistance of clothing ensembles can be taken into account by using a correction factor. ISO 9920:2007 correction method takes the air velocity relative to the person and the walking speed as the two acting factors [52]. The correction factor for a dressed person in normal or light clothing (0.6 clo $< I_{cl} <$ 1.4 clo or 1.2 clo $< I_T <$ 2.0 clo) is presented in Equation 11. Note that this correction factor is to be used to correct the total insulation $I_T$. A back calculation is needed if one wishes to obtain the correction factor for the clothing insulation $I_{cl}$, based on the relation amongst the total insulation $I_T$, the clothing insulation $I_{cl}$, the clothing area fraction $f_{cl}$, and the air insulation $I_a$.

$$\text{corr } I_T = \exp\left[-0.281 \times (v_{ar} - 0.15 + 0.044 \times (v_{ar} - 0.15)^2 - 0.492 v_w + 0.176 v_w^2\right] \tag{11}$$

where corr $I_T$ is the correction factor for total insulation, $v_{ar}$ is the air velocity

relative to the person in $\mathrm{m\,s^{-1}}$, from 0.15 $\mathrm{m\,s^{-1}}$ to 0.35 $\mathrm{m\,s^{-1}}$, and $v_w$ is the walking speed in $\mathrm{m\,s^{-1}}$, from 0 $\mathrm{m\,s^{-1}}$ to 1.2 $\mathrm{m\,s^{-1}}$.

## 2.9 Thermal (Comfort) Indices

Over decades of thermal comfort study, researchers have developed new thermal comfort indices as means to assess and predict the human thermal sensation as well as the characteristics of the thermal environment. Other than the classic Fanger's PMV and PPD (and its mutated form ePMV), other thermal and thermal comfort indices include the effective temperature (ET, and its modified ET*), standard effective temperature (SET, and its modified SET*), the heat stress index (HSI), the humidity index (humindex), the universal thermal climate index (UTCI), the perceived temperature (PT), the operative temperature ($T_o$), the equivalent temperature (ET), the dynamic thermal sensation (DTS), and so on. Each of those has its own scope and field of use. Within buildings, the PMV and PPD are undeniably the most used for decades, as already discussed above. Amongst the listed ones, the dynamic thermal sensation (DTS) index was introduced together with the IESD-FIALA thermal comfort. The DTS was developed to predict the sensation of humans in discrete transient conditions, on a 7-point ASHRAE scale $[-3; +3]$ similar to the PMV.

**The Dynamic Thermal Sensation** was derived based on the observation in human physiology that human thermal sensation is a fusion of signals which are relevant to the skin and core temperatures. Fiala and Lomas in [40] quoted Benzinger in [53] that «the ideal thermal comfort [is the state where there] is the absence of punitive impulses from both [i.e., cutaneous and hypothalamic] receptor fields». They believe that «even when these conditions are not met, a state of "mixed" comfort can be reached». This can be noticed during exercising or changing of environments, where the elevated core temperature is balanced out by the cold surroundings. The signals from the hot receptors and from the cold receptors equalise each other and thus the subject might feel neither hot nor cold. A more familiar example in the context of Finnish sauna-goers is when they throw themselves into the snow or dip into the icy cold lake water straight from the sauna, a similar «mixed» comfort is reached. Fiala et al. developed the concept through extensive regression analysis on experiment results with 220 exposures, including sedentary and exercising subjects. The DTS model is formulated as in Equation 12.

$$DTS = 3 \times \tanh\left[\underbrace{a \cdot \Delta T_{sk,m}}_{F_1} + F_2 + \underbrace{\left(0.11\frac{dT^{(-)}_{sk,m}}{dt} + 1.91e^{-0.681t} \cdot \frac{dT^{(+)}_{sk,m}}{dt_{max}}\right) \cdot \frac{1}{1+F_2}}_{F_3}\right] \tag{12}$$

where a is 0.30 $\mathrm{K^{-1}}$ and 1.08 $\mathrm{K^{-1}}$ for $\Delta T_{sk,m} < 0$ and $\Delta T_{sk,m} > 0$ respectively,

$\frac{dT_{sk,m}^{(-)}}{dt} = 0$ for $\frac{dT_{sk,m}}{dt} > 0$, t is the time since the occurrence of the highest rate $\frac{dT_{sk,m}}{dt}$ and $F_2$ is calculated using Equation 13 below.

$$F_2 = 7.94 \times \exp\left(\frac{-0.902}{\Delta T_{hy} + 0.4} + \frac{7.612}{\Delta T_{sk,m} - 4}\right) \tag{13}$$

where $\Delta T_{hy}$ is the change in the core temperature (**hy**pothalamus).

It is worth noting that this DTS formula is specific to the IESD-FIALA model (the «original», developed during 1999-2003), as the later versions thereof (namely the FIALA-FE and FPC models) are not published. They also have their own modified DTS versions, however, Roelofsen in [42] compared the DTS between the original FIALA and the FPC version and concluded that the original DTS «does not fall short of the calculated results of the DTS equation in the current FPC model». In addition, after having been tested with three other experimental results from renowned studies in the field, the DTS model showed good agreement and potential [42]. Roelofsen also commented that the DTS model, even when applied to the Stolwijk model, would be relevant and helpful in professional practice within the built environment field. With all the advantages and drawbacks discussed throughout the classic PMV, the adaptive model, to the physiological model, it can be seen that in the thermal comfort study in sports environments, the IESD-FIALA thermo-physiological model and its DTS model have shown to be a better fit amongst all.

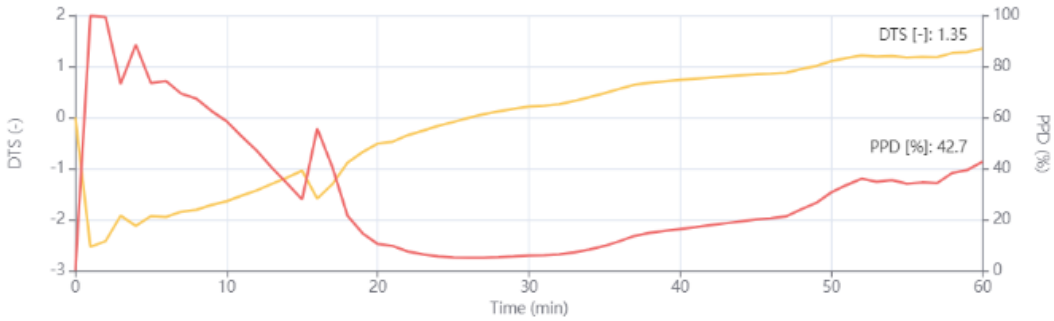


Figure 14. DTS of the exemplified football player if he would have played in Latokartano hall, indoor air 19℃, MRT 18.5℃, met profile as described in Section 2.7 and Appendix B.1.

The DTS model takes the air temperature, relative humidity, air velocity, clothing insulation, mean radiant temperature, and the person's metabolic rate as the boundary conditions. The example of the amateur football player described in Section 2.7 is further exemplified here for the application of the IESD-FIALA model in the calculation of the predictive DTS. Figure 14 illustrates the DTS and PPD as an inferred result calculated based on the training session of the football player. It can be seen that, in the beginning, the person would feel «slightly cold». After about 15 minutes of warming up, he would already feel «cool» and would start to take off some clothes layers. This leads to a brief dip in the DTS but it recovers

swiftly after, within about 3 minutes. The thermal sensation would increase toward the hot direction during the training session. Finally, at the end of the session, the player would feel slightly above «warm».

# 3 Ventilation in Indoor Sports Facilities and its Adequacy

This chapter emphasises how important it is to have good ventilation in the sports environment. The current regulations and guidelines on how to implement ventilation in sports facilities are also mentioned. The effects of the COVID-19 pandemic on sports venues are addressed in the following sections.

## 3.1 Regulations and Guidelines regarding the Indoor Conditions of Indoor Sports Facilities

Built sports facilities include outdoor venues, e.g., open golf fields and ski resorts, semi-outdoor edifices like track-and-field stadia, and indoor sports halls or complexes such as an indoor swimming pool (such as the one in Figure 1) combined with a weightlifting room. The definition of an indoor sports facility is not only limited to a space to do sports but also a venue for professional sports competitions or performances. In such cases, the spectator stand or seating area is often integrated, in addition to scoreboards and other auxiliary equipment such as a safety fence or glass partition. Each and every sport has its own requirements for the playing environment, which should provide the players not only adequate thermal conditions and good air quality but also maintain the unique traits of the sports. Some concrete examples are that in an ice hockey rink there should not be fog, in a badminton court there should not be air draught, and in a swimming pool, the water should not be too warm nor icy cold. Sports types are diverse; therefore, it is inappropriate or overbroad to have a common regulation or guideline for designing an indoor sports facility. It should be sports-type or sports-group-specific. Nevertheless, many countries and regions have set their own regulations on the minimum requirements for the indoor conditions and ventilation of indoor sports facilities to some extent. Certain international sports federations have also given their requirements for indoor thermal conditions to be maintained during the official games in the playing areas. Table 4 shows the air temperature, relative humidity, and maximum air velocity mentioned by some of the official international sports federations or associations recognised by the Olympic Committee [54].

In Finland, there are no statutory regulations specifically on indoor conditions or ventilation in sports facilities. The current Finnish *Decree of the Ministry of the Environment on the Indoor Climate and Ventilation of New Buildings 1009/2017* specifies only the minimum outdoor air rate to be 6 $\mathrm{L\,s^{-1}}$ per person during the occupancy period and to be 0.35 $\mathrm{L\,s^{-1}\,m^{-2}}$ floor area outside of the occupancy period. In addition, the instantaneous carbon dioxide concentration in indoor air during the occupancy period can be at the maximum 800 ppm above that of the outdoor air's concentration. At the requirement levels, the Finnish *Decree on Indoor Climate*

Table 4. Indoor air conditions to be maintained in the playing area given by sports federations and associations (adapted from [2]).

| **Federation or association** | **Air temperature** [°C] | **Relative humidity** [%] | **Maximum air velocity** [$\mathrm{m\,s^{-1}}$] |
|---|---|---|---|
| Aquatics (FINA) | 2°C higher than water temperature (water temperature 25–28°C) | - | - |
| Badminton (BWF) | 18–30 | - | $< 0.2$ |
| Basketball (FIBA) | 16–20 | $< 50$ | $<$ - |
| Curling (WCF) | 6–7 | controlled | no constant air movement |
| Gymnastics (IFG) | Humidex = 22–38 | | $< 0.2$ |
| Handball (IHF) | 15–22 (heated halls)<br>18–24 (cooled halls) | - | $< 1.0$ |
| Ice hockey (IIHF) | 6 | $< 70$ | - |
| Ice skating (ISU) | 6–12 | $< 70$ | - |
| Judo (IJF) | 17–26 | 30–40 | - |
| Table tennis (ITTF) | 12–25 | - | $< 0.1$ |
| Tennis (ITF) | 13–17 (winter)<br>6–8 below the external temperature (summer) | 55–60 | - |
| Volleyball (FIVB) | $> 10$<br>15–16 (for official competitions) | - | - |
| Wrestling (UWW) | 18–22 | - | - |

*and Energy Efficiency* is considered to be too coarse and insufficient for practical designing work [55]. However, in another currently valid Finnish Decree, the *Decree of the Ministry of the Environment on the Energy Performance of New Buildings 1010/2017*, it is mentioned that while calculating the calculated energy performance reference value (E-value) of the category «buildings for sports and physical exercise excluding swimming pools and indoor ice rinks», the outdoor airflow value should be 2 $\mathrm{L\,s^{-1}\,m^{-2}}$ and the heating and cooling limits should be respectively 18°C and 25°C. Amongst the HVAC-designer community, the withdrawn *D2 – Indoor Climate and Ventilation of Buildings Regulations and Guidelines 2012* is still being used as a reliable reference source. The guideline values for the outdoor air flow rate per person

and per metre-squared, as well as the air velocity regarding the sports facilities, can be found in Table 6 of Appendix 1 of the Decree. Part of Table 6 is translated and presented in Table 5.

Table 5. Guideline values for dimensioning ventilation in sports facilities during occupancy period (translated and reprinted from [56]).

| **Space / use purpose** | **Outdoor airflow** ($L\,s^{-1}\,pers^{-1}$) | **Outdoor airflow** ($L\,s^{-1}\,m^{-2}$) | **Air velocity** ($m\,s^{-1}$) |
|---|---|---|---|
| Fitness centre[1] | | 6 | 0.25 |
| Gymnasium[1] | | 4 | 0.25 |
| Sports hall[1] | | 2 | 0.25 |
| Spectator stand | 8 | | 0.25 |
| Swimming pool hall[2] | | 2 | 0.40 |
| [1] ventilation has to be controlled by demand<br>[2] moisture removal is the dimensioning factor, calculate it case by case | | | |

There are also several guidelines on the designing of ventilation in sports facilities from other professional associations and private information providers. For example, the HPAC card index «LVI-kortisto» from Rakennustieto Oy is a series of HVAC guidelines, covering from technical guidelines for designing, installation, and maintenance of HVAC systems, to the measurements of HVAC components or system performance [57]. The series also has several sport-specific guidelines for HVAC designing of the sports facilities, including swimming halls, indoor sports complexes, bowling halls, indoor ice rinks, gymnasia, dance floors, indoor tennis halls, and indoor boulder centres. These HVAC-cards are also referred to in another popular Finnish guideline – *The guidelines for ventilation design in buildings other than residential buildings* by the FINVAC Ry [58]. Amongst the aforementioned references, the HVAC-card «LVI-10600 Sisäliikuntatilojen LVIA-suunnittelu» [HVAC Design of Indoor Sports Facilities] provides the most detailed ventilation design values and the indoor condition values in sports facilities, by sports (excluding swimming pools and indoor ice rinks). Table 6 summarises the reference values used in HVAC designing practice from LVI-10600. Notice that some of the values are taken directly from the international associations or federations, which are presented in Table 4.

Table 6. Airflow rate and indoor condition guideline values by sports (reprinted from [46]).

| Sport | Activity level [met] | Supply airflow [$L\,s^{-1}\,m^{-2}$] | Supply airflow [$L\,s^{-1}\,pers^{-1}$] | Air velocity [$m\,s^{-1}$] | RH [%] | Target temperature [°C] | Required temperature [°C] | $CO_2$ concentration max [ppm] | Note! |
|---|---|---|---|---|---|---|---|---|---|
| gymnastics | 5–8 | 4 | 25 | 0.2 | | 18–20 | | 1200 | – magnesium dust removal to be considered |
| rhythmic gymnastics | 4–8 | 4 | 25 | 0.2 | | 18–20 | | 1200 | – high air velocity might affect the flying of the ribbons |
| competitive dancing | 6–12 | 4 | 30 | 0.2 | 35–60 | | | 1200 | |
| futsal | 5–10 | 2 | 30 | 0.2 | 35–60 | 20–21 | | 1200 | |
| basketball | 5–10 | 2 | 30 | 0.2 | 35–60 | 17–18 | 16–25 | 1200 | |
| floorball | 5–10 | 2 | 30 | 0.2 | | 17–18 | | 1200 | |
| handball | 5–10 | 2 | 30 | 0.2 | 35–60 | 18–24 | | 1200 | |
| volleyball | 3–6 | 2 | 25 | 0.2 | 35–60 | 17–18 | 16–25 | 1200 | |
| tennis | 4–8 | 2 | 25 | 0.2 | | 17–18 | | 1200 | |
| table tennis | 3-4 | 2 | 25 | <0.2 | | 20–21 | | | – high air velocity might affect the trajectories of the balls |
| squash | 5–10 | 2 | 30 | 0.2 | 35–60 | 18–20 | 15–25 | 1200 | |
| badminton | 3–8 | 2 | 25 | <0.1 | | 17–20 | | 1200 | – air velocity <0.1 m/s in the whole shuttling space<br>– building service equipment on the ceiling must not bother the observation of the shuttlecocks by their colours |
| wrestling | 6–12 | 4 | 35 | 0.2 | | 20–22 | 18–25 | 1200 | |
| judo | 6–12 | 4 | 35 | 0.2 | | 20–24 | | 1200 | |
| karate | 5–12 | 4 | 35 | 0.2 | | 20–24 | | 1200 | |
| boxing | 8–12 | 4 | 35 | 0.2 | | 20–22 | | 1200 | |
| taekwondo | 6–12 | 4 | 35 | 0.2 | | 20–22 | | 1200 | – building service equipment must not limit space height, min. 3 m |
| fencing | 5–10 | 2 | 35 | 0.2 | | 17–22 | 15–20 | 1200 | |
| athletics | | 2 | | 0.2 | | 18–20 | 16–18 | 1200 | – polyurethane tracks emit high VOCs |
| wall climbing | 5–10 | 4 | | 0.2 | | 18–20 | | 1200 | – magnesium dust removal to be considered |

## 3.2 Common Ventilation Design Practices in Indoor Sports Facilities

Sports facilities are characterised by the variable occupancy rate, intensive and rapid heat and human-stemmed emissions. Ball games such as basketball, volleyball or badminton require the halls to have high overhead space. This makes the air distribution inside the halls difficult due to the limited air throw lengths and widths of air devices in order to keep the air velocity under the threshold values. As each sport has its own requirements for the indoor conditions of the sports space, it is wise to group sports which have similar set-ups in terms of playing area; for example, ball games such as futsal, floorball, basketball, and volleyball can be played in one same high-ceiling hall, while martial arts such as taekwondo, judo, karate, and wrestling can be practised in the same space. In reality, because of the high financial investment of a sports facility and also the efficiency of land use, sports halls are often built to be versatile, i.e., to host as many sports as possible. Three badminton courts can easily fit well within a floor-ball rink; the same goes for a volleyball court. Sports halls used for teaching and training purposes are usually equipped with separation curtains so that several groups of students or athletes can train at the same time. Therefore, the design of air distribution in sports halls should also consider the predefined spaces according to the flexible use of the halls.

The goal of good air distribution inside a sports space is to provide balance and efficient ventilation without causing irritating draughts. This should be ensured during the whole occupancy period, also in case, the ventilation system is running at part-load or in case the supply temperature changes [46]. In addition, air distribution should not interfere with the performance of the athletes or the quality of the sports games. Badminton and rhythmic gymnastics are two examples of air-velocity-sensitive sports. In designing ventilation in sports spaces hosting these sports, it is important to consider the air distribution not only in the occupancy zone but also in the overhead zone where the sports equipment involves. Sports facilities are mostly built to be used in official competitions and regular training, or in educational purposes. Ventilation solution in such multi-purpose sports halls is thus a compromise between the usage purpose and the sport played. It is also possible to distribute the air with air terminals which can flexibly alter its throw patterns by automation control when needed [46].

There are two important elements in designing a ventilation system: the maximum outdoor air flow rate and the air distribution solution. The Finnish guideline card LVI 06-10600 suggests dimensioning the outdoor air flow rate primarily based on the greatest number of occupants in the sports area, usually at times when there is competition with spectators, or at assembly events. This means that the maximum occupancy rate has to be taken into account already at the early preliminary design phase. If there is not sufficient initial information on this, then the dimensioning of the ventilation system will be based on the floor area [46]. Heat, moisture, carbon dioxide, and other metabolic impurities emitted into the space

increase together with the intensity of the physical activities of the sports players or athletes. Therefore, the demand for the ventilation air flow rate also increases. It is suggested in [58] that in large sports halls, ventilation has to be controlled by head counts and the corresponding metabolic rate by the sports, or by indoor air quality. Carbon dioxide concentration is overall a popular indicator of indoor air quality, which has been in use in the dimensioning as well as the control of the ventilation system of schools, restaurants, theatres, office spaces, and conference rooms [59]. Regarding this, the Finnish Ministry of Environment also provides official guidelines on the dimensioning of outdoor air flow rate on the basis of carbon dioxide emission, including a calculator for practical design work [60]. In the next chapter, there will be a more detailed discussion on the application of carbon dioxide concentration as an important IAQ index and its participation in ventilation system control.

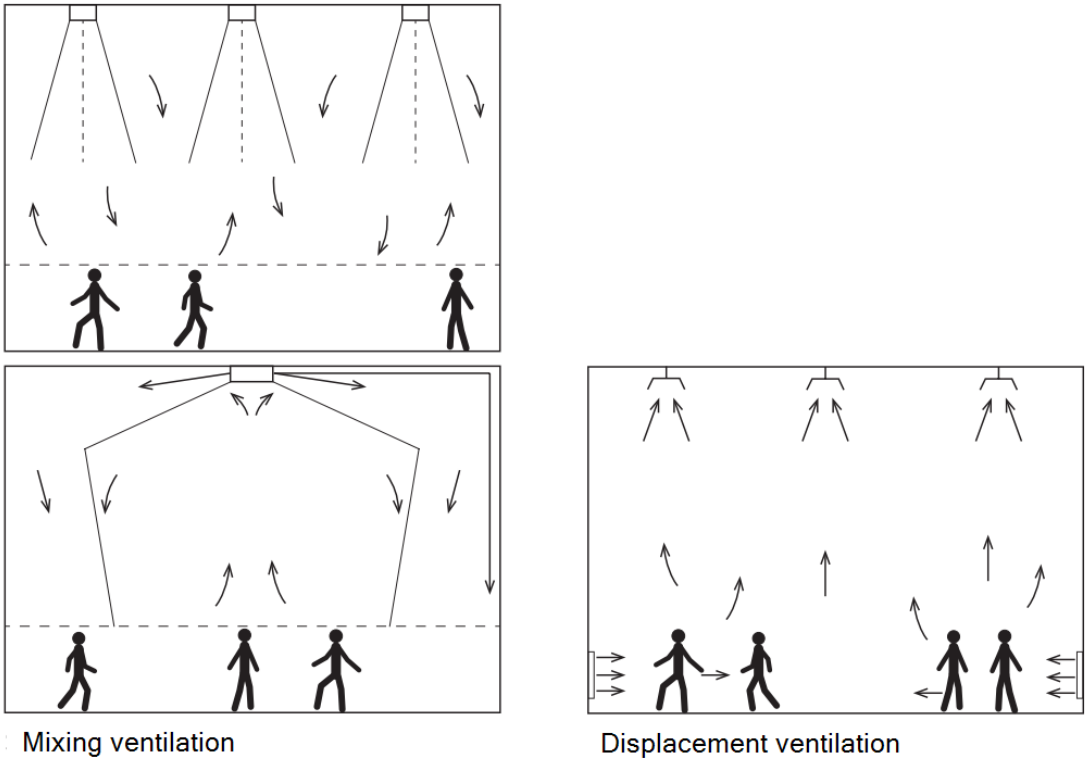


Figure 15. Principles of mixing ventilation and displacement ventilation in sports halls with high ceilings, reprinted from [46].

The guidebook LVI06-10600 [46] describes two common ways to ventilate sports facilities: displacement ventilation and mixing ventilation. Figure 15 reprinted from the guidebook briefly depicts the ideas of those two ways to distribute air. The physical meaning of displacement ventilation is to supply fresh and slightly cooler than the desired room temperature into the space with a low air velocity at a low height level such as from at the lower corners of the room or from the edges of the floor. The heat emitted from the sports players causes a convection flow towards the upper part of the space. The contaminants from the occupants will follow the convection airflow towards the ceiling, where the extract air devices

are installed. In this way, the air in the occupancy zone is kept at a lower level of contamination concentration than the upper part of the space, i.e., the overhead space till the ceiling. This way of ventilation suits well the context of sports spaces, where heat and impurities are emitted from the same source - the sports players. A vertical contaminant gradient and vertical temperature gradient are presented in the space [46, 61]. Displacement ventilation should be designed carefully, taking into consideration the heat load, the geometry of the space and the arrangement of the equipment or furniture. The second way mentioned, mixing ventilation, is simply to efficiently mix fresh supply air into the room air. Good locations of supply and extract air devices as well as suitable air throw pattern analysis result in higher mixing efficiency. It is noted in [46] that airflow should be designed in such a way that odours and impurities from sports players should not spread to other parts of the room in spaces with both sports play areas and other occupancy purposes, such as coffee shop.

Ventilation in sports facilities plays an important role because it directly relates not only to the thermal comfort of the athletes but also to the sport performance and the quality of the practice sessions or the games. In practice, the design of the ventilation system is not optimised simultaneously to achieve these two inseparable goals: thermal comfort and energy efficiency [26]. At the moment this thesis is being written, in the midst of the energy crisis, the second goal seems to weigh more heavily than ever. As concluded in the review paper [62], within the last two decades, there was an exponential increase in scientific publications on IAQ in physical exercise and sports practice areas. This reveals an immensely strong interest in the topic. The next sections will delve deeper into that connection and present some potentials on how to achieve both with an ideal compromise.

## 3.3 Potential Ventilation Practices in Indoor Sports Facilities

Most of the air distribution in existing indoor sports facilities in Finland follows either the aforementioned practice. Both the designers and the building owners might lean towards the presented guidelines and the experience of the previous cases. When existing design works without complaints over years, trust is built gradually on those certain solutions and thus, it becomes the convention. The most common combinations of heating and ventilation in sports halls are mixing ventilation with radiators or radiant panels or floor heating, and displacement ventilation with radiators or radiant panels. Existing frameworks and design tools which support the decision-making process are also the factors which somehow take over the space for a change. Recently, nozzle duct, or duct with direction adjustable nozzles, has come into practice in newly built sports spaces with mixing ventilation. Another mutant of this nozzle duct is the air socks or fabric duct with or without nozzles, see Figure 16. The advantage of these duct-shaped air distribution diffusers is the versatility in air throw pattern and the higher convertibility of the ductwork with regard to future changes. The principle of this air distribution method is still mixing ventilation. In

fact, this mode is not really well-mixed in many cases if not carefully designed or considered the large height of most sports halls.


(a)

(b)

Figure 16. (a) Fabric duct with nozzles in an indoor tennis court. Photo by Prihoda [63]. (b) Fabric duct without nozzle in an indoor climbing centre. Photo by FabricAir [64].

In fact, there are several other ventilation modes which are used in different applications as well as space types. Especially after the outbreak of SARS-CoV-2 in 2019, many research and literature review papers were published on the ventilation modes regarding thermal comfort, air quality, and pathogen risk control. Fan et al. in [65] reviewed and compared thoroughly various ventilation modes, the favourable operating environments, their characteristics, advantages, and disadvantages. Beyond the listed modes in the mentioned review paper, in 2021, Li et al. introduced and studied the thermal comfort of the occupants with the interactive cascade ventilation

(ICV) in [66, 67]. The idea of ICV is to supply fresh air into space through jet nozzles with different air temperatures and at different heights, see Figure 17. ICV was later studied in a chamber setting to test its space heating potential, airflow pattern, distribution, temperature response, and also draught rate in [68]. In ICV mode, the cooler air stream is placed slightly above the warmer air stream, oriented at a correspondingly steeper angle than the warmer jet's, thus suppressing the natural thermal buoyancy upwards of the warmer air stream. The expected air distribution layout is a controllable vertical temperature gradient of indoor air, where warmer air will reach the more sensitive body parts such as the lower leg and foot meanwhile cooler air is delivered to the body trunk, other upper parts, and the head, which prefers cooler temperature. The ICV solution was proved to be effective in both space heating and cooling modes, plus offering «excellent energy-saving and thermal comfort» [66]. Kong et al. also concluded that ICV demonstrates «strong feasibility and superiority in space heating» compared to displacement ventilation and mixing ventilation through their chamber tests. It is worth noting that in both studies the test settings were typical office layouts, where the ceiling height was less than 3 metres and the occupants were not experiencing heightened metabolic rates. Nonetheless, the portrait of the ICV method through [66, 67, 68] still sheds light on the potential of its in the application of sports halls and sports spaces, where the high ceiling is often the factor making up the unuseful heating energy.

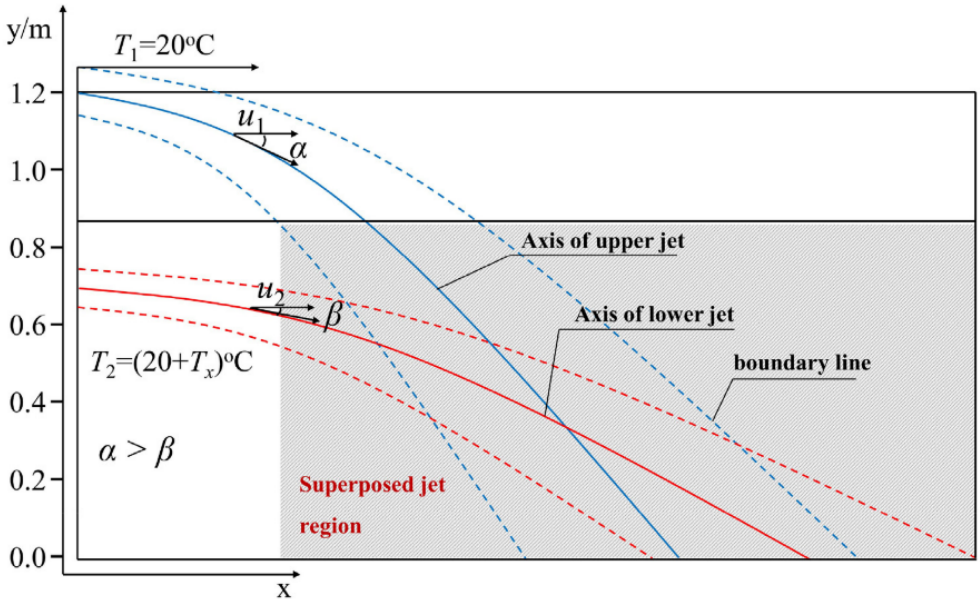


Figure 17. Arrangement and characteristics of air jets in ICV, reprinted from [67]. NB.: The heights of the jets and the supply air temperatures are limited to the scope of the experiment presented in [67] only and are subjected to vary case by case.

Inspired by the ICV concept for the suppression of the warm air layer by the cool air, the Latokartano sports hall 1 was exemplified. The jets were arranged on the two longer sides of the hall with the extract terminals along the middle line on the ceiling. A simple 2D CFD simulation is done via the fluid simulation software

Flowsquare+ (or «FSP»). It is an easy-to-use tool with simple boundary condition definitions which was developed and optimised for 64-bit Windows OS [69]. FSP has its own result visualisation viewer, but users can also post-process the output files through Paraview for further visual animation or analysis. Figure 18 illustrates the pattern of the temperature distribution and air velocities created by the jets. It can be seen that in the occupancy zone ($H \leq 2$ m) the warm air is trapped near the floor level while the cooler air flow is circulating in the overhead space. The table under the figures specifies the jet characteristics used in the 2D CFD simulation.

Overall, through the sketchy application of the concept into the Latokartano sports hall sali 1, it is noticed that the ICV solution has strong potential as a novel ventilation method in sports halls with high ceilings. However, open questions which require further detailed investigation remain: (i) due to the asymmetry of the jet and extract terminal location during the geometry construction and meshing, the above simulation results did not truly reflect the design idea, i.e., the air velocity distribution is slightly too low on the right-hand side of the Figure 18b – this non-uniform air velocity distribution might affect ball games (volleyball, basketball) and particularly badminton games; (ii) in the occupancy zone, draught appears here and there; (iii) the pattern is based on maximum ventilation airflow, in case of DCV, the part-load behaviour and pattern of the jets might dramatically change and it would affect the desired effect. All in all, one should bear in mind that this quick and simple simulation serves only as a brief glimpse into the applicability of ICV in sports halls with high ceilings. The results presented do not hold any conclusive proof of the solution.

## 3.4 Inspection of the Ventilation Systems

A properly functioning ventilation system contributes not only to a good indoor climate but also to the efficient use of heating, cooling, and electrical energy in buildings. To assure adequate ventilation, it is equally important to conduct a systematic, recurring inspection of the whole system. For the time being, the inspection of building ventilation systems is not enforced by law in Finland. On the other hand, Swedish legislation has made it obligatory since 1991, so-called the «Mandatory Ventilation Inspection» [70]. In addition to the first inspection carried out before it is deployed, interim inspections are scheduled to be done by certified personnel by law, either every 3 or every 6 years depending on the types of the buildings [70]. The law enforcement might have led to a difference in the percentage of buildings with indoor air issues in the public sector between the two countries: about 10% in Sweden versus 60% in Finland [71]. In May 2021, the guideline «Inspection of Ventilation» was published by the Finnish Ministry of Environment, as ordered by the «Terveet Tilat 2028» («Healthy Premises») public project. The project as a whole is a 10-year programme aiming at rejuvenating public buildings and improving the treatment as well as revitalising those who suffered from indoor air problems [72].

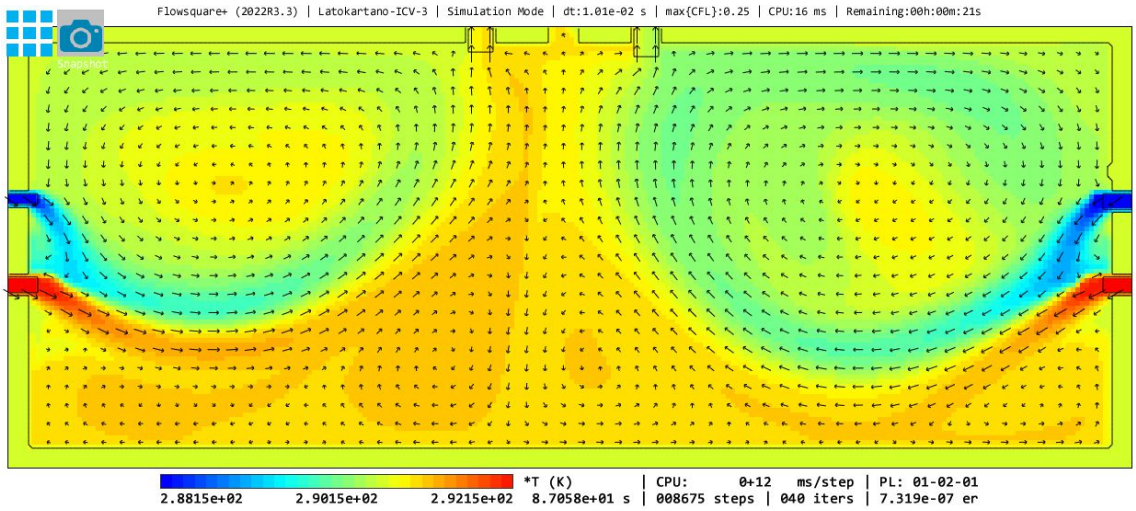


(a) T in Kelvin

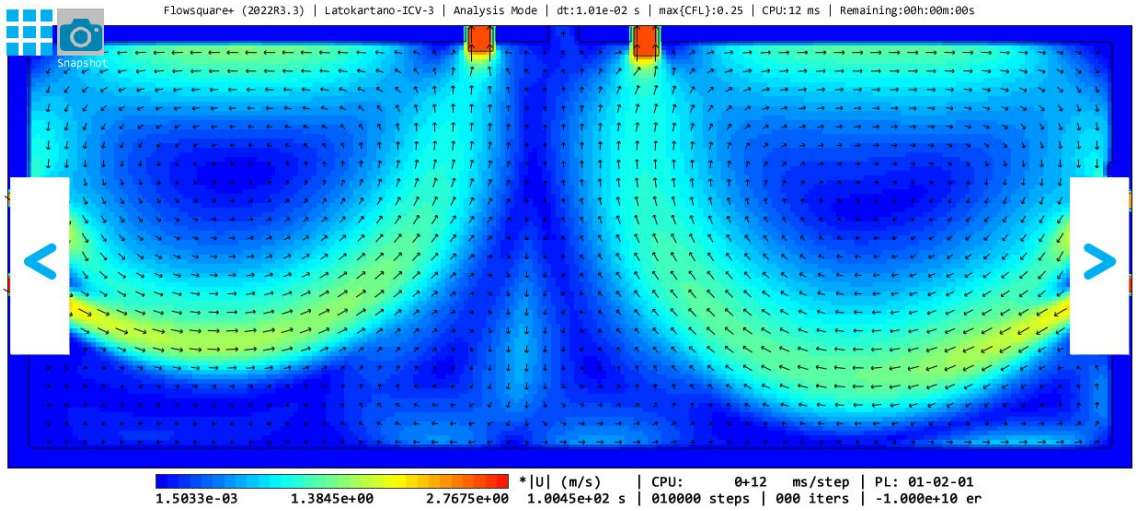


(b) Velocity in m/s

| Jet | Tilt angle ° | Air flow $\mathrm{L\,s^{-1}}$ | Air velocity $\mathrm{m\,s^{-1}}$ | Air temperature °C | No. of jets | Jet height m |
|---|---|---|---|---|---|---|
| Upper | $\alpha = 35°$ | 75 | 2.3 | 15 | 22 | 5.5 |
| Lower | $\beta = 30°$ | 110 | 2.7 | 19 | 22 | 5.0 |

Figure 18. Simple 2D CFD simulation of the ICV concept applied into the geometry and the design air flow rate of the Latokartano hall (sali 1).

The Finnish guideline categorises the inspection of the ventilation system into three levels: recurring inspection (3–5-year interval), examination (5–10-year interval or when needed), and investigation (when needed but usually under 10 years). Each level has its own scope of checking areas as well as the depth of the methodologies used. The inspected areas include documentation, condition and functionality, usage and maintenance, hygiene and cleanliness, fire safety, automation control, indoor environment, and energy efficiency. The recurring inspection is

suggested to be between 3 to 5 years depending on the types of the ventilation system, i.e., complicated and prone to faults such as VAV systems with supply and return air should be inspected every 3 years, while CAV systems, extract only, local extract system or natural ventilation system could be inspected every 5 years.

A flowchart describing the ventilation inspection process is shown in Figure 19. The assessment of the inspection process is divided into three classes: E, H and K. Class E stands for «not in order», which means that the detected faults are to be repaired without delay, and a follow-up inspection has to be carried out no later than 6 months after the inspection date. The faults, according to their impacts on the buildings, can be marked with the letter L if there is a need for further examination (level 2) or investigation (level 3). Class H suggests that the system is functional but there are minor faults to be fixed without delay and there is no need for a follow-up inspection since those items will be checked in the next inspection. Finally, class K means that the system works well: the condition, functionality, and cleanliness are good and there is no need for further actions. Building stakeholders should be aware of the result of the inspection so that needed actions are taken timely. The guideline also draws clear lines between the inspectors and the clients, their responsibilities and tasks. The inspectors are required to be proficient in the inspection process as well as to have a broad knowledge of the ventilation system and its relevant fields. At the moment, there has not been existing certification for such professionals in Finland yet, since the project is still in progress. Regarding the client side, it is of great importance that the procurement of the inspection service is prepared carefully, ideally by persons in the field. HVAC design engineers are the ones who suit well into this role [70].

Indoor sports facilities with DCV systems belong to the group of buildings which should be inspected every 3 years if adhering to the newly-published guideline. Regular inspection of the ventilation system in such premises would eventually improve the lifespan of the system components, assure the functionality of the system as well as maintain good indoor conditions for the sports players, the students, the exercisers, as well as the staff working in the buildings. Although the regulation at the moment does not require mandatory inspection, the introduction of the guideline bears the meaning of awareness spreading. Once the stakeholders of the buildings – owners, maintenance and working staff, visitors, etc. – realise the significance of a well-functioning ventilation system, from the thermal comfort, and the smell, to the noise, the draught feel, etc., they will appreciate adequate ventilation inspections. Economical savings as well as carbon footprint mitigation through effective risk management and preventive action plans with regular ventilation inspections are great assets to the building owners; especially in the case of public buildings such as the studied indoor sports facilities within the LIIKU project, they are the cities and municipalities.

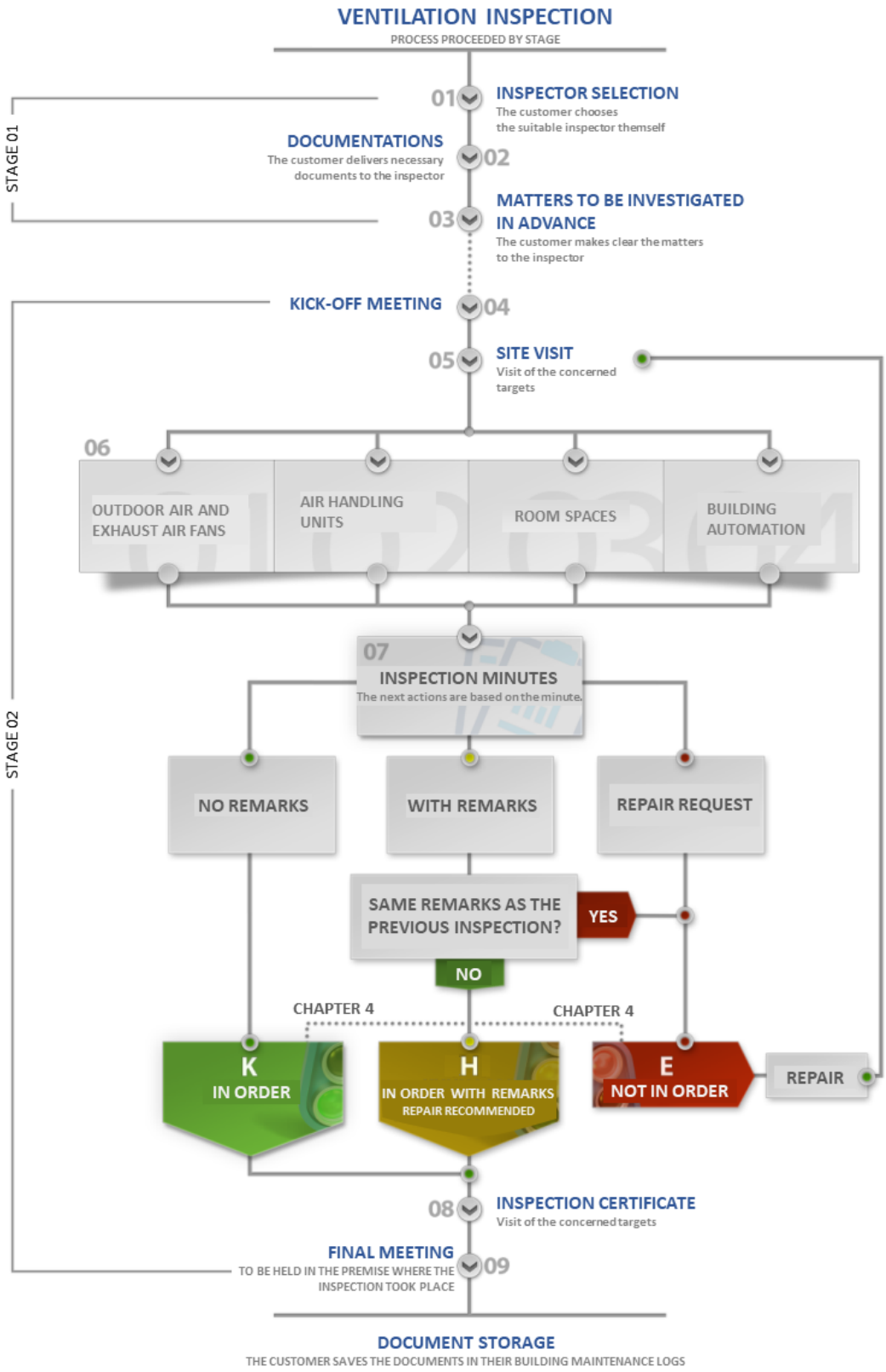


Figure 19. Ventilation inspection process from the Finnish MOE Guideline, reprinted from [73]. English translation by the author.

## 3.5 Demand-controlled Ventilation System, its Control, and its Adequacy

Demand-controlled ventilation (DCV) is a subset of variable air volume (VAV[3]), opposite to constant air volume (CAV). Even the simplest ventilation system with air volume changes according to an operation time timer on a fan is considered a VAV system. Therefore, in terms of terminology, it is important to specify the control strategy of a ventilation system in order to call it DCV. Mysen, Schild and Cablé in the «Demand-controlled ventilation - requirements and commissioning» guidebook define DCV as the «VAV systems which control the airflow rate according to a demand measured in the room, and not according to a preset value» [74]. The demand can be assessed based on one or several measurements at the room level, for example, the usage time of the buildings, the presence of the occupants, the indoor air temperature, the carbon dioxide concentration, and the VOC concentration. Table 7 presents the pros and cons of each control parameter. The control principle of a DCV system can be based on one or a combination of several parameters; in reality, the timer, the carbon dioxide concentration and room air temperature are used together the most often [4].

Regarding different DCV systems, it is possible to classify them based on the underlying control principles. Mysen et al. in [74] listed four main control principles of DCV, as illustrated in Figures 20–23.

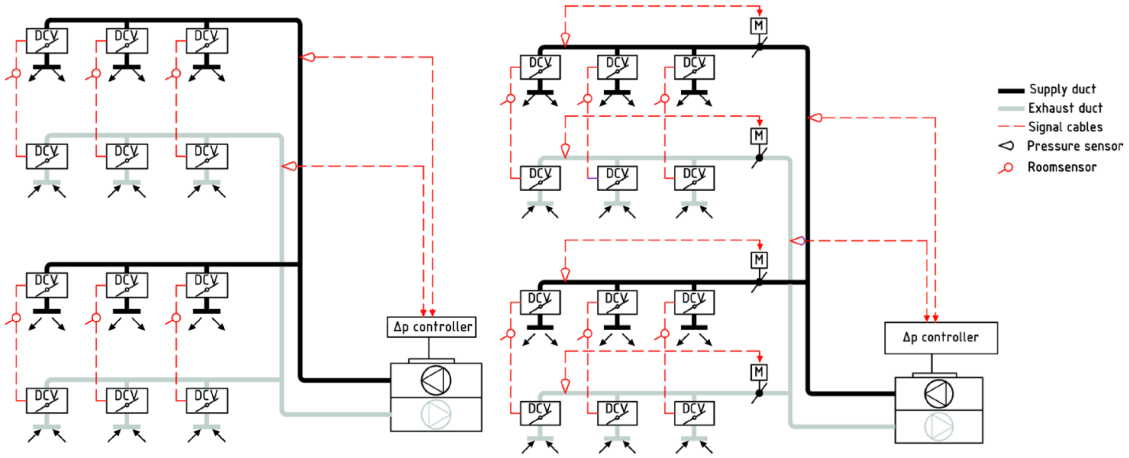


(a) Without branch dampers

(b) With branch dampers

Figure 20. Principle diagram for pressure-controlled DCV, reprint from [74].

A majority of old or existing DCV systems are pressure-controlled. It is

[4]VAV might be defined differently by different ventilation component manufacturers, e.g., Swegon defines VAV as «the system adjusts the airflow over an operating time but may only be adapted to temperature or air quality», and DCV as «the system adjusts the airflow over time and allows adaptations to be made on a variety of different factors» [75]. Meanwhile, Lindab brochures use interchangeably «VAV» and «DCV», sometimes with a slash «VAV/DCV» [76].

Table 7. Common control parameters for DCV, adapted from [77].

| Control parameter | Advantages | Disadvantages |
|---|---|---|
| Usage period | Affordable, nowadays available as the basic function of fans or AHUs | Fixed schedules, not flexible for changing situation |
| Presence | Low cost, long lifespan (PIR sensors) | Limited possibility for gradual control according to actual occupancy, e.g., in meeting room, open space office, etc. |
| | Sensitive to fine movements (microwave sensors), suitable for odd space shapes with obstacles | |
| | Low cost, high accuracy (smart video camera) | Possible personal privacy violation, misuse of collected video data |
| Air temperature | Low cost, long lifespan | Only DCV according to heat load |
| Relative humidity | Low cost, long lifespan | Measurement range depends strongly on the sensing method |
| Carbon dioxide concentration | Gradual demand-control according to actual occupancy in classrooms, meeting rooms, open space offices, etc. | Require frequent calibration to ensure precision over time. Large differences in measuring principles and measuring methods induce large discrepancies in the quality of the measurements |
| VOC concentration | Possibility to predict a theoretical $CO_2$ level | Unclear/hardly applicable requirements for VOC in relation to DCV. Cannot be controlled or calibrated. Accuracy as a $CO_2$ not well documented. |

the most simple DCV system layout. One drawback of this control principle is that the fan would be unnecessarily throttling at part-load conditions. This is because the static pressure at the sensor locations is maintained by adjusting the fan speed through the controller. Furthermore, the location of the damper affects the controlling results, i.e., if it is not sensitive enough to recognise the change in the demand in one room and the fan speed is not adjusted accordingly to change the total airflow, the distribution of the air through other dampers are affected unwantedly. One solution is to have branch dampers as shown in Figure 20a where the zone dampers keep the minimum pressure in the AHU on par with the room dampers' working ranges. This way the throttling is avoided, although the controlling is not the most efficient. Pressure-controlled DCV systems are no longer recommended to be commissioned nowadays due to those drawbacks, instead, other optimised systems with bus communication are used in newly-built buildings [76].

The static pressure reset principle (SPR DCV) has similar zone dampers as the branched version of the pressure-controlled DCV, except that there are pressure sensors before the critical room terminals of each branch. The SPR controller regulating the pressure setpoint for the AHU fan should be so that at least one of the critically located dampers is fully opened, see Figure 21. By this, the duct pressure is prevented to surge unnecessarily.

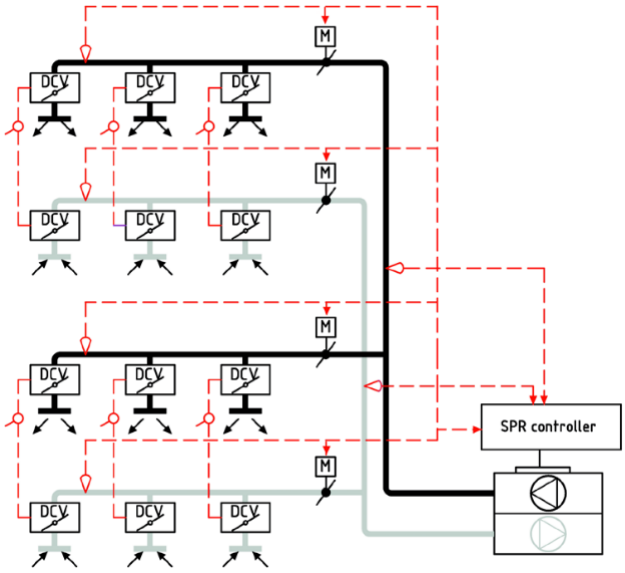


Figure 21. Static pressure reset DCV principle diagram, reprint from [74].

In the damper-optimised DCV system, the principle is to collect the information about damper position and current airflow rate from all the VAV dampers to the controller. The output signals will be so that at least one damper is at the maximum open position, which should be at the most critical position (index position) in order to minimise the fan power at the minimum load. Sub-branching could be done similarly to the above cases to increase controllability in larger systems, as shown in Figure 22b. Alternatively, to programme the damper controlling in the BMS is to simplify the physical components, which means reducing the investment expenses.

The last control principle of the DCV system is the variable supply air device,

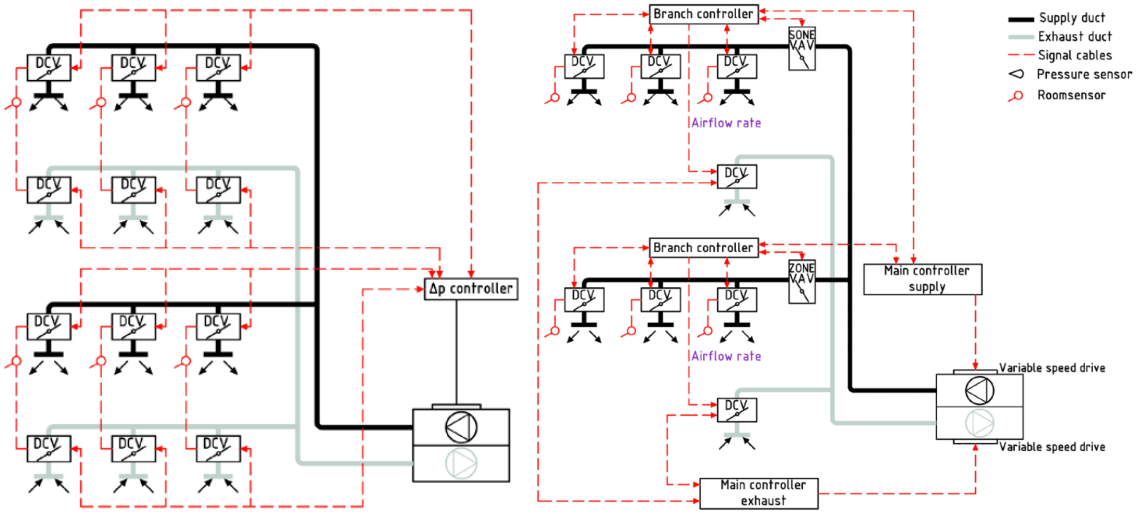


(a) Without branch dampers (b) With branch dampers

Figure 22. Damper-optimised DCV principle diagram, reprint from [74].

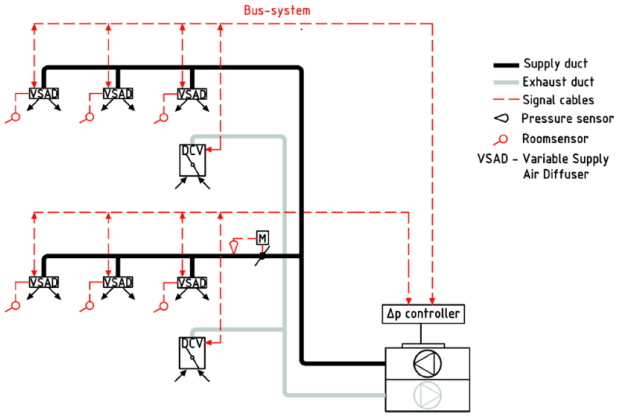


Figure 23. Damper-optimised DCV principle diagram, reprint from [74].

a.k.a. the VSAD-DCV, where the VAV dampers, the plenum (box) and the diffusers are integrated into modules. Other aliases for this system are the VAV box and the VAV terminal unit. VSAD-DCV systems are vastly aimed at pressure independence. The module can communicate with the controller via a bus system. In the last couple of years, VSAD-DCV has been developed extensively thanks to wireless technology. This reduces significantly the amount of cable routing and commission work is generally cheaper. The main idea of this principle is similar to the optimised-damper DCV, which is to have one maximum open VSAD and one fully open damper on the extract side. With the current omnipresence of IoT sensors, the VSAD-DCV is expected to overtake all the previous DCV systems by improving communication and reducing the number of physical components as well as cabling in the buildings. For instance, the WISE ecosystem by Swegon covers the physical components, the data transferring, the control setup and the user interface SuperWISE, as the service can also be provided as a full package [78].

DCV systems are meant to reduce energy consumption through the adjustment of the unnecessary airflow rate. Compared to conventional CAV systems, DCV systems are more complicated in terms of controlling and the number of components. Therefore, it requires careful design, accurate commission, and attentive maintenance. Although it is often seen via the ventilation system suppliers the advertisements about the great potentials of DCV systems, multiple DCV systems were reported not performing as planned due to various reasons in one or several aforementioned stages [79]; subsequently, the savings effect could not be seen while the indoor air condition requirements were not met.

## 3.6 Frequent Reasons for Inefficient and Ineffective Ventilation Systems

Despite the high potential for energy savings, many implemented DCV systems do not work as expected. A study by Zhao et al. revealed that out of the monitored DCV systems in eight public buildings in Southern Finland, only one system worked to the design specifications [80]. In another case, 11 out of 22 school buildings equipped with DCV systems in Oslo, Norway were classified as «malfunctioning» after having undergone a spot-checking procedure in a field study by Mysen et al. [79]. These studies have shown that in reality, there still exists a huge gap between the theoretical and the actual DCV systems, which leads to less-than-expected energy savings. Throughout the studies, the most common faults, defects, or shortcomings from the design, commission, operation, and maintenance stages of the DCV systems were summarised from [73, 79, 80, 81] as below.

During the design and commission stages:

(i) Airflow-related components: air terminals, control dampers, and airflow measurements are not correctly sized. Minimum and maximum airflow rates, required pressure drop over the dampers, working range of dampers, safety distance downstream, etc. are not considered thoroughly.

(ii) Control principles vs airflow rate range: a large system without sub-branching would cause control difficulties. Operational airflow rates do not meet the design airflow rates. Unclear control strategies.

(iii) Design, commission, and maintenance are not consistent: commissioned system differs from the design due to changes in the procurement process (influenced by product price, availability, contractor, etc.). Changes were not documented, and as-built drawings were not carried over.

(iv) Wrong locations for sensors: planned locations for sensors were not realised due to furniture or other building service equipment which was not visible during the design process. Sensed values are not effectively represented the conditions of the room, e.g., temperature sensors placed too close to a heat source.

(v) Inadequate design documentations (cf. Item iii): copycats of standard schemes, unspecified setpoints, control principles were not properly described, vague user manuals, etc.

(vi) Final system balancing and checking were skipped during commissioning.

During the operational stage:

(vii) Insufficient documentation, instructions, and manuals from the previous stages (cf. Item v).

(viii) Re-balancing of the system was undone after a change, e.g., in occupancy rate, space re-arrangement, etc.

(ix) Dirt-covered air pickup crosses or damper blades which lead to the shifted calibration of the airflow measuring devices.

(x) Maintenance staff is incapable of covering all aspects of the ventilation system since they are getting more and more complicated.

(xi) No regulation on mandatory inspections, so, as long as there is no complaint, the faults will not usually be detected and fixed.

## 3.7 Auxiliary Uses of Indoor Sports Facilities

Many indoor sports facilities were not originally built as sports spaces in the first place but as an auxiliaries. It can often be a bomb shelter, emergency centre, or natural disaster shelter. The chances or the times the listed facilities are utilised are minimal; therefore, it is more resource-efficient to have them operated as places for people practising sports and exercising in normal situations. In Finland, numerous bomb shelters were built in the 60s and the 70s which are now operating as sports spaces. Most often they are underground structures which were built into the bedrock. One example of the Finnish bedrock shelters is the Kuusankoski shelter in Kouvola with a capacity of almost 5000 people, which hosts a ballgame hall and a 100-metre sprinting track, see Figure 24. Other famous examples are the underground swimming pool Itäkeskus in eastern Helsinki or the Hakunila shelter in Vantaa which accommodates a gym and a sprinting track. The ventilation of such facilities has to follow both the required air flow rate and the blast-proofing characteristic of the sheltering structures. These depend strongly on the design occupant capacity of the facilities as well as their protecting classification.

In rare occasions such as the COVID-19 global health crisis, sports centres have been repurposed into testing and vaccination centres or temporary hospitals in many countries around the world, from China to Brazil. Some of them were put into complete closure. At the peaks of the mortality rate, they were even transformed into morgues and mortuary cold rooms. Buildings which serve in the public health sector are often required to meet a higher ventilation standard in order to prevent the spread of airborne pathogens, not to mention the SARS-CoV-2, which turned out to be a pandemic. In such cases, the ventilation system might not be able to provide sufficient fresh air, due to which the heightened risk of infection might occur. Sports facility sometimes functions beyond the scope of their normally expected uses. In the disastrous human stampede on Halloween 2022 in Seoul, the Wonhyoro sports centre was used as a storage and lost-and-found centre for the victims' belongings. The items rescued from the site of the incident amounted to 1.5 tonnes and were spread systematically on the floor, awaiting their owners or family and friends of

Figure 24. A running track inside the Kuusankoski bedrock shelter in Kouvola. Photo by Antro Valo / Yle, March 2022 [82]

the owners to come to pick them up. The items were with dirt, blood stains, and unavoidably sweat and tear [83, 84].

Indoor sports halls can be seen as spacious indoor areas where multiple social activities or emergencies can be hosted inside. The ventilation system in an indoor sports facility might therefore often miss serving the unforeseeable or unexpected purposes of use during rare occasions. It is also possible that the facility is transformed into some other purposed building after a period of being in operation as a sports venue, for example in its first or second major renovation. For that reason, the design decision should be made thoroughly already at the initial stage of the construction project, whether or not or how likely the use purpose would be changed, how flexible the building would be, or at which level of convertibility the building should be. This may later help ease the space rearrangement, as well as the overall cost of the transformation work. In the context of the ventilation system, it means that, for example, extra airflow capacity might be set aside, or extra free space might be reserved for a future extra air handling unit and ductwork.

# 4 Latokartano Sports Hall Indoor Condition Simulation

Amongst the sports facilities in the LIIKU project, the Latokartano sports hall was chosen to be studied more closely, particularly its demand-controlled ventilation system and the indoor conditions of one of its two ball game halls.

## 4.1 Building Information

«Latokartanon Liikuntahalli» – Latokartano Sports Hall – Key information:

- Year of construction: 2010
- Address: Agronominkatu 26, 00790 Helsinki
- Gross floor area: 3360 $m^2$
- Facilities: two ball game halls and one gymnasium, locker rooms and showers, reception, toilets


Figure 25. Latokartano sports hall. Photo by LPV arkitehdit Helsinki [85].

Latokartano sports hall is a public sports venue under the ownership and maintenance of Helsinki City. It was built in 2010 in an emerging residential

neighbourhood in the northeastern part of the city, surrounded by parks and other outdoor sports facilities, see Figure 25. The building as a whole has two ball game halls, a gymnasium, a staff area, other auxiliary rooms, and locker rooms and showers which also serve the visitors of the nearby outdoor courts and football fields. The main sports which are played in the halls are floorball, handball, futsal, volleyball, and basketball. One of the halls, «sali» 1 – the west hall, is reserved for the adjacent Latokartano comprehensive school during the days, for which it is equipped with a point elastic sports floor. It is a soft coating in the form of a vinyl mat placed on a concrete surface, ideal for installation in small sports halls for children, nursery schools and kindergarten indoor playgrounds [86]. The other hall, «sali» 2 – east hall, has an area elastic floor, which is a harder coating on top of the underfloor layers, providing better absorption of sports motion and thus, more suitable for multi-sport purposes, see Figure 26. The construction of the Latokartano sports hall utilised building information modelling (BIM), which was built from the preliminary design stage [85].

Figure 26. Latokartano sports hall, southern side. Photo: «Latokartanon liikuntahalli / Palloilusali 2» by Aki Rask / City of Helsinki [87].

The chosen hall for the modelling and simulation is the «sali 1», which is the one for the school's use during schooldays (08–16) and other reserved activities after school hours and in the evening. This hall includes a sports equipment room which extrudes to the outside of the northern wall of the hall. The dimensions of the hall are 42.03 metres in length, 23.55 metres in width, and approximately 8.60 metres in height, see Appendix C for the floor plan. There is a partition curtain wall to divide the hall into two parts when needed in training sessions and physical education lectures. The number of visitors strongly depends on the booked time

slots, the sports disciplines, the time of the year, and the school schedules. The studied hall has a floor area of approximately 890 $m^2$. The design outdoor airflow in the hall is 3960 $L\,s^{-1}$, which is about 4.45 $L\,s^{-1}\,m^{-2}$.

## 4.2 Limitations on the Data Measurement and Acquisition

Information and data acquisition is of utmost importance in order to model and simulate the indoor climate and energy of buildings, from the structural to the maintenance perspectives. There were a number of difficulties during the collection of this building's technical documentation and operation data:

(a) Compared to a typical service life of 20 to 30 years of a sports facility before it is renovated or demolished, this Latokartano sports hall is quite new. However, the plan drawings, type drawings, detail drawings, system descriptions, and inspection minutes of the structural, automation, and electrical design were not available, neither in electronic nor in physical formats from the archive of the city. Only the ventilation plan drawings, architecture plan drawings and elevation views, architectural site drawings, and screenshots from the building management system (BMS) for the automation of ventilation, heating, lighting, and alarm are available.

(b) Although the building was designed with the demand-controlled ventilation system, due to the COVID-19 pandemic, the City of Helsinki has decided to change the DCV to CAV mode according to the guidelines of the WHO until further notice since October 2020 [88, 89]. This principally means that the effect of the DCV was not observable within this work, and subsequently, the assessment of the adequacy of the DCV system in the Latokartano sports hall.

(c) The logging of the automation variables and measured values is faulty. It showed not to store data until 23.08.2022. The reason was unknown according to the maintenance people at the time the data retrieval was made. Ventilation and automation measurements were collected during 23.8.–16.9.2022, and the chosen period to be used in the simulation and calibration is 10.9.–16.9.2022, during which the missing data proportion is the minimum. Except for the outdoor air temperature and the carbon dioxide concentration, all other series witnessed a significant percentage of missing data on an hourly basis, at the minimum 29.9% up to 64.9%, see Appendix A for the summary of the missing data proportion of the collected measured data.

(d) It is worth noting that the average air temperature of the two halls is calculated as the arithmetic mean from four sensors, two in each hall. One of the four is placed too close to a heat source, therefore, its value is always about 2.8–3.6℃ higher than the other three. The average air temperature of the halls is used to adjust the heating setpoint in the halls, as well as the supply air

temperature from the AHU. This measurement error subsequently causes a chain of inaccuracy and unexpected control effects in the system. The compensation for this measurement error was performed in the model calibration and also the average room air temperature in the hall, see Appendix A.

## 4.3 Simulation Tools

IDA ICE by EQUA Simulation AB was used in the modelling of the Latokartano sports hall. It is widely used for whole building simulation, energy and indoor climate condition simulation, parametric study, optimisation, and plant modelling and simulation. The tool is popular the most in the DACH and Nordic regions because it supports the localisation in most of those countries and the local language interfaces. It also provides a number of extensions, including the ASHRAE 90.1, boreholes, daylight, ice rinks and pools, and most recently, the CFD extension. This dynamic simulation software has been validated and certified against several guidelines and standards such as ASHRAE 140-2004, CEN Standard EN 13791, CEN Standard EN 15255- and 15265-2007, IEA SHC Task 34, and TM 33 [90]. Along with IDA ICE, pre- and post-processing of data (such as weather files and schedules, calculation of calibration indices) were done using R.

## 4.4 Model Construction and Calibration

In the construction of the Latokartano ICE model, basic geometry, building structures, and HVAC systems were limited to only the studied hall («sali 1»), as mentioned above. Adjacent walls to the other part of the building were considered adiabatic. Figure 27 depicts the 3D view of the studied hall in IDA ICE, with empty buildings bodies representing the other parts of the buildings.

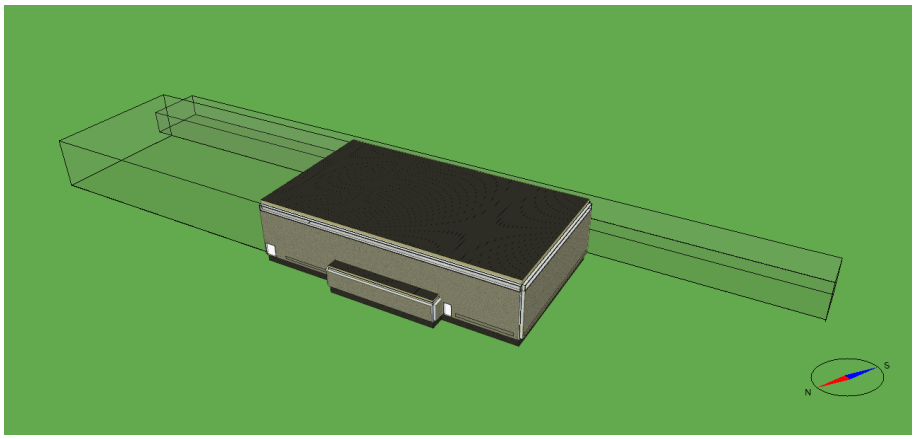

Figure 27. A 3D view of the Latokartano hall 1 modelled in IDA ICE.

Due to the lack of structural drawings of the venue, the modelling of the

building elements and windows was mostly based on the Finnish building codes for the U-values and on observations for the element material layers. The precise internal height of the hall was not known because of the lack of cross-section drawings and they were estimated by the projection from taken photos. Otherwise, the floor plan gave sufficient details for the modelling of the room. The studied hall has a small equipment storage which protrudes from the northern external wall, two external doors, and clerestory windows on top of the two external walls, see Figure 27. Appendix C provides the floor plan, the ventilation drawing, and the screenshots from the automation system for the AHU serving the studied hall, for example in Figure 28. Ventilation in the hall is typical mixing ventilation with 18 supply air terminals arranged in three identical groups and 3 extract air terminals located close to the internal wall. The free height of the hall is about 8.5 metres. Occupancy schedules were retrieved from the public reservation calendar from the booking system of the City of Helsinki. The weather data during the period used in the calibration process was taken from the two nearest weather stations from the Finnish Meteorological Institute (FMI). Air temperature, relative humidity, wind direction, and wind speed measurements were from the Malmi Airport station, while the diffuse radiation and direct solar radiation were from the Kumpula station. This is due to the fact that neither of the two stations collects all the six weather parameters required in the IDA ICE weather file. The observations were then replaced with the values in the Helsinki reference weather file in IDA ICE at the corresponding hours, see Appendix A for the process.

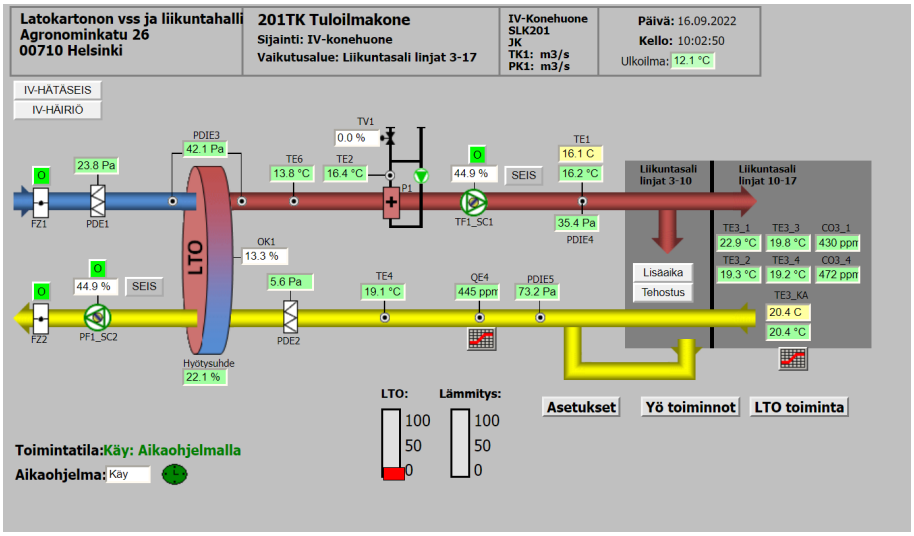


Figure 28. Screenshot from the BMS showing the AHU 201TK which serves the two halls.

The heating and ventilation setpoints and control were modelled according to the settings from the automation interface in the BMS. Heating setpoints change according to the outdoor air temperature, which can be seen in Figure 29a. The hall is equipped with a DCV system with room air temperature and carbon dioxide concentration as the main driving factor during occupancy hours. In addition, the supply air temperature setpoint is controlled with a cascade mode, with its maximum

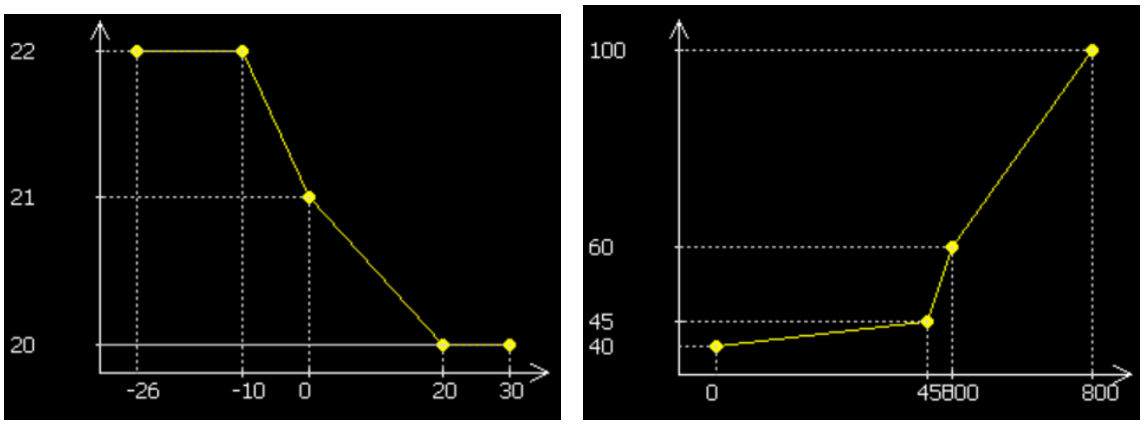


(a) $T_{\text{air,room}} = f\left(T_{\text{air,outdoor}}\right)$ (b) $u_{\text{fan}} = f\left(C_{\text{CO}_2}\right)$,[%]

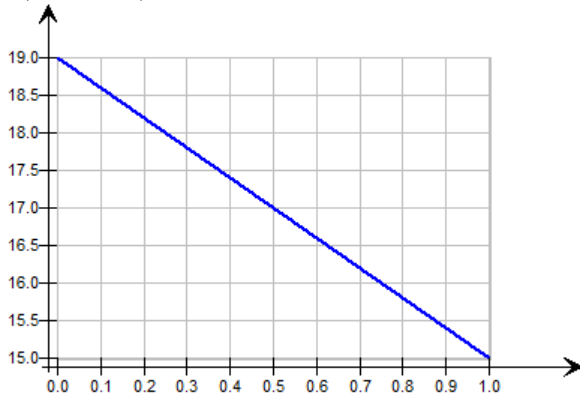


(c) $T_{\text{air,supply}} = f\left(u_{\text{air,return}}\right)$

Figure 29. Current setpoint curves of the DCV system in the sports halls appeared in the BMS interface.

value at 19℃ when the room air heating setpoint is at 22℃, corresponding to the coldest outdoor air temperature, and its minimum value at 15℃ when the room air heating setpoint is at 20℃, as shown in Figures 29c and 30a. The average room air temperature heating setpoint of the hall is thus at 21℃. The nighttime ventilation mode is also in operation in this AHU. Nighttime «outdoor air flush» will be turned on whenever one of the four room air temperature sensors in the two halls exceeds 22℃, the outdoor air temperature is 3℃ cooler than the room temperature (i.e., the arithmetic mean of the four) and higher than 13℃. It will be turned off when the room air temperature drops below 19℃ or the outdoor air temperature is 2℃ cooler than the room air temperature, whichever condition fills first. The nighttime «air flush» flow is meant to cool the space down with free air cooling. It can also be seen from the screenshot in Figure 28 and 31b the room air temperature measurement abnormality mentioned in Item d of Section 4.2 at the TE3_1. The AHU was running on the «boosting» mode at its maximum air flow rate according to the city guideline as mentioned in Item b of Section 4.2. With all the available information about the AHU, it is modelled in IDA ICE in the closest possible to the actual one, as shown in Figure 31. Note that the values in Figure 31 are the values after calibration.

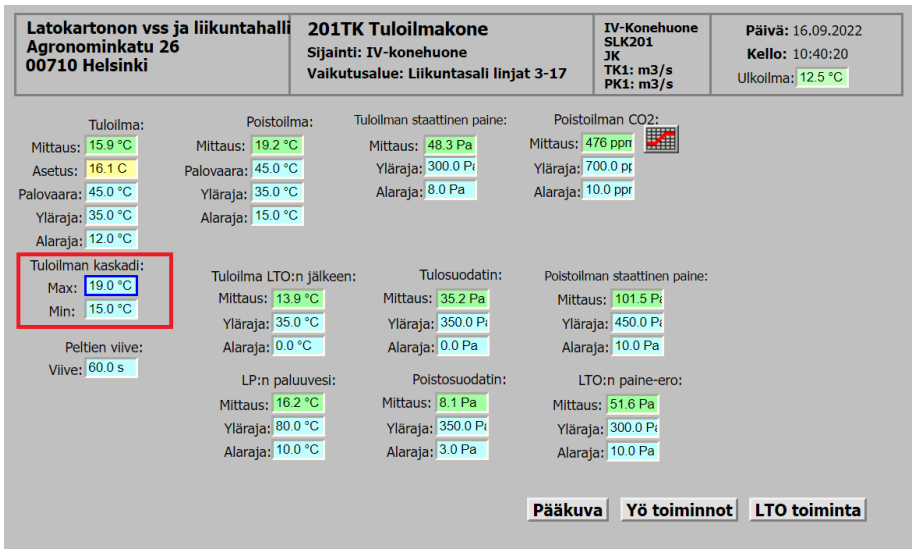


(a) Cascade settings of supply air temperature in the red box.

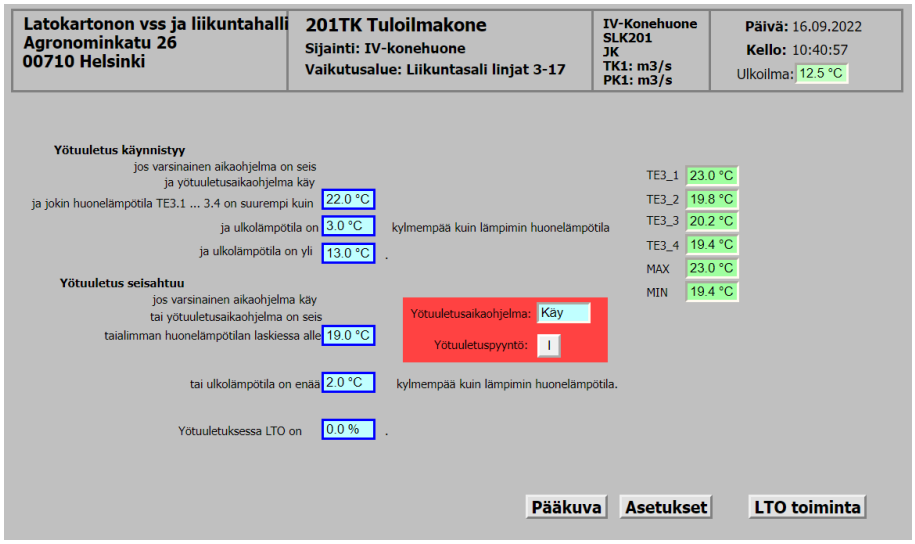


(b) Nighttime ventilation mode is ON.

Figure 30. Screenshots from the BMS show the control settings of the DCV system.

To create a baseline model, the model was calibrated using the hourly calibration method with measured indoor air conditions. ASHRAE Guideline 14-2014 – Measurement Of Energy, Demand, And Water Savings describes "calibration" as the "process of reducing the uncertainty of a model by comparing the predicted output of the model under a specific set of conditions to the actual measured data for the same set of conditions" [91]. The input parameters were set firstly based on the existing technical drawings and documentation, after that, they were manually modified to account for the errors in the observation collection mentioned in Section 4.2. Fit-the-graph technique was used to preliminarily calibrate the model by manual iteration of the most sensitive input parameters before the statistical indices were used to verify the calibration. Two indices, which were benchmarked by several renowned measurement and verification (M&V) guidelines, were employed. They

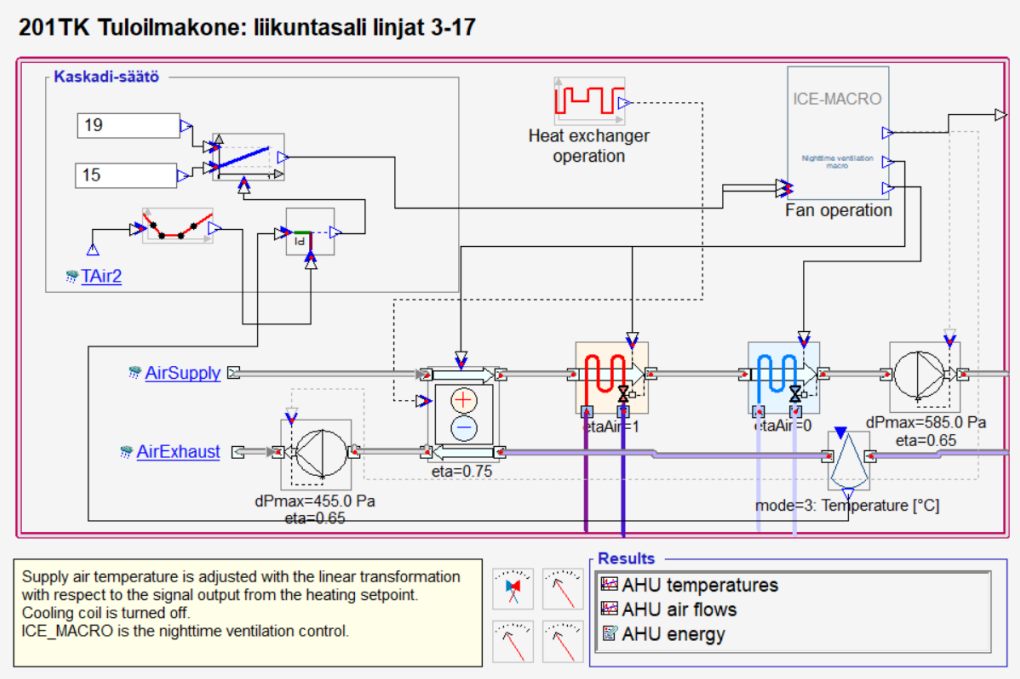


(a) AHU 201TK

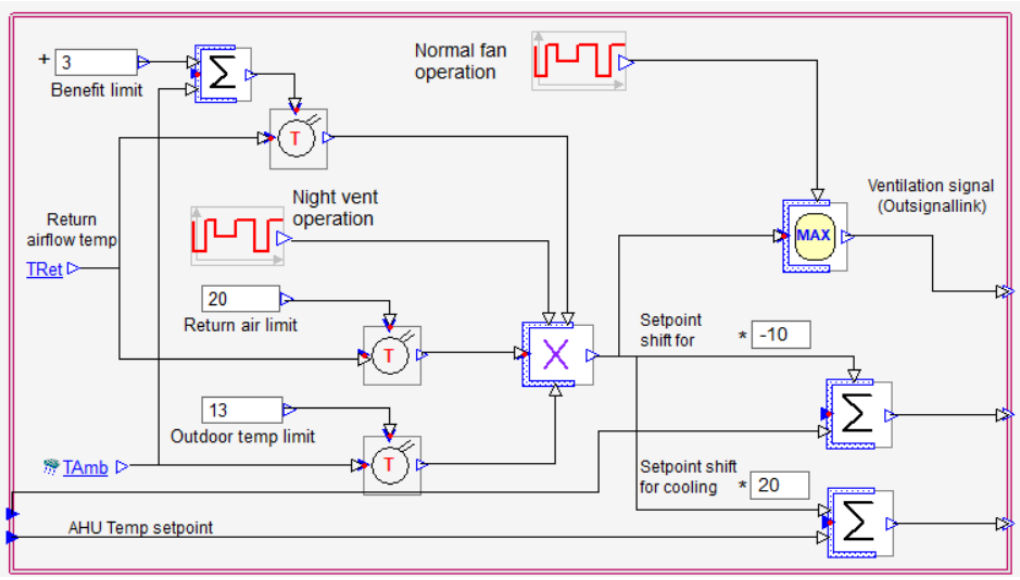


(b) Nighttime ventilation control macro.

Figure 31. Modelling of the automation control in IDA ICE.

are the coefficient of variation of the root-mean-square error [CV(RMSE)] and the normalised mean bias error (NMBE). The formulae for the two are presented in

Equations 14 and 15.

$$\text{CV(RMSE)} = \frac{1}{\bar{y}} \times \sqrt{\frac{\sum_i^n (y_i - \hat{y}_i)^2}{n-1}} \tag{14}$$

$$\text{NMBE} = \frac{\sum_i^n (y_i - \hat{y}_i)^2}{(n-1) \times \bar{y}} \tag{15}$$

where $y_i$ is the measured value at instance i, $\hat{y}_i$ is the simulated value at instance i, n is the number of data points, and $\bar{y}$ is the mean of the measured values.

In addition to ASHRAE 14-2014, the two other popular M&V guidelines, for instance, the option D of the International Performance Measurements and Verification Protocol (IPMVP) version 2016 (Efficiency Valuation Organization, 2016) and the US Department of Energy's (DOE) Federal Energy Management Program (FEMP) version 4.0 2015 (Federal Energy Management Program, 2015) [92, 93], also use CV(RMSE) and NMBE for calibration verification. They used to have their own benchmark values but in the later versions, they refer directly to the values given by ASHRAE Guidelines 14, see Table 8. The reliability of the model is enhanced through hourly calibration but only needed if they are followed by studies with high accuracy requirements, for example, in the prediction of energy consumption, automation controls, fault diagnosis, etc. Otherwise, performing hourly calibrations requires greater effort and time; hourly simulations also consume more processing power [93]. A flowchart presenting the basic steps of model calibration is reprinted from the guideline IPMVP Core Concepts 2016 in Figure 32.

Four variables were used to calibrate the model. They are the supply, return, and mean room air temperatures, and the carbon dioxide concentration in the hall. The main adjustments were made at the control curves of the supply air temperature and the heating setpoint temperature to reflect the actual performance of the AHU system due to the measurement error. Remarkably, the room temperature measurement error dragged down the setpoint room air temperature compared to the designed setpoint in Figure 29a, see also Item d of Section 4.2. Nighttime ventilation condition values were also modified accordingly in the same way due to the measurement error. The number of occupants in the hall is set to be on average at 25 people with the metabolic rate level at 3.0 met. This is due to the fact that most of the sports sessions during the calibration period were the school use and non-adult group training sessions in handball, soccer, and gymnastics.

The modelled values of the four variables from the calibrated model were compared to the measured data graphically and statistically, as shown in Table 8 and Figure 33. It can be seen that the model displays acceptable agreement with the actual performance of the indoor condition of the simulated hall. Therefore, it is considered calibrated.

The supply air temperature setpoint curve after calibration is shown in Figure 34. The average heating setpoint of the room air temperature is 19℃. Compared to

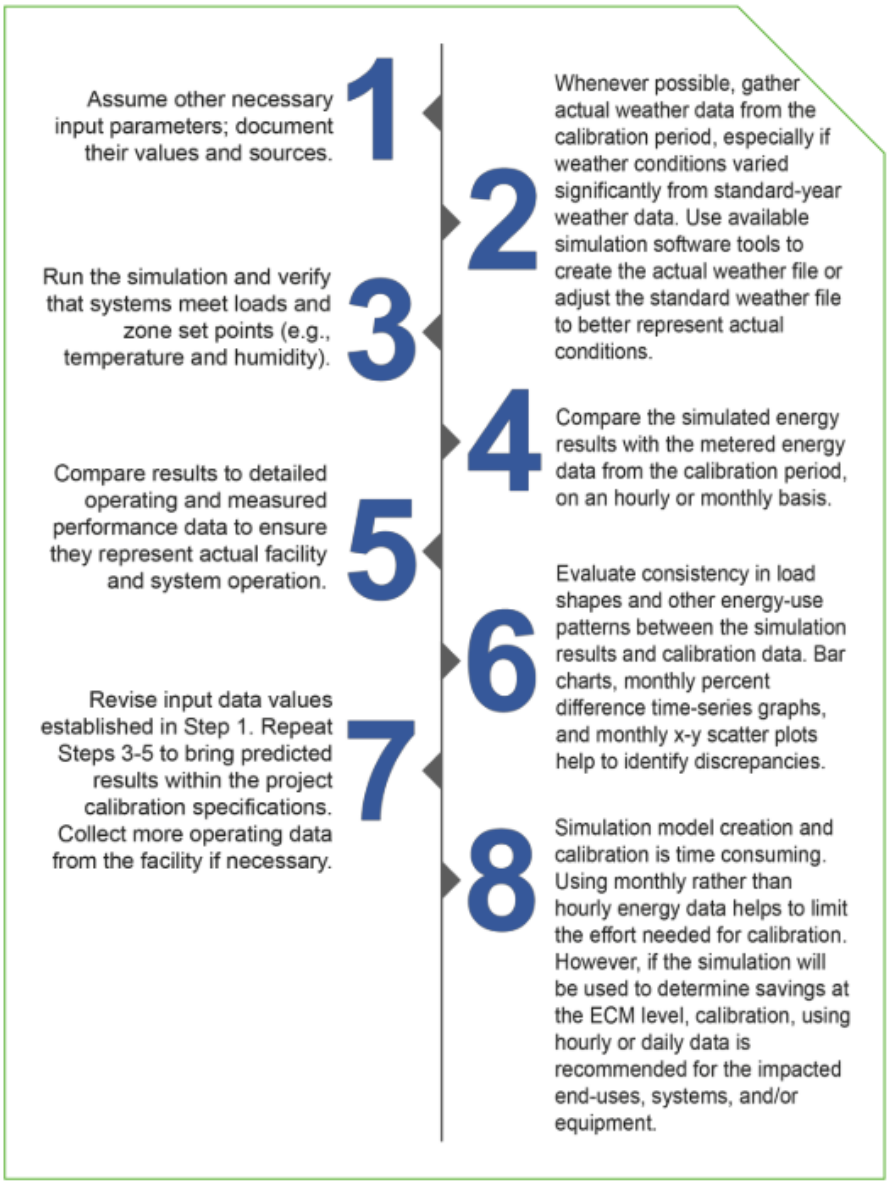


Figure 32. Calibration steps in a nutshell, reprinted from [93].


Figure 33. Calibration result

Table 8. Calibration results versus benchmark values by ASHRAE 14-2014

| | Calibrated model | | Calibration criteria by ASHRAE 14-2014 | | Note |
|---|---|---|---|---|---|
| Index in % | CV(RMSE) | NMBE | CV(RMSE) | NMBE | |
| Supply air temperature | 4.35 | -8.75 | 30 | ±10 | passed |
| Return air temperature | 1.34 | -2.02 | | | passed |
| Mean room air temperature | 0.62 | 0.26 | | | passed |
| $CO_2$*concentration* | 20.23 | 0.27 | | | passed |

the mentioned level of room temperature of 18℃ in indoor sports facilities in the Finnish building regulations 1010/2017, the average setpoint of this sports hall is about 1℃ higher.

## 4.5 Simulation Cases

The calibrated model was then used to simulate different other indoor air condition setpoints and to estimate the heating energy consumption in those cases. It was noticed that the actual current setpoint curve of the air temperature in the sports hall is at 18 to 20℃. This is about 2 to 4°C higher than the **required temperature** for

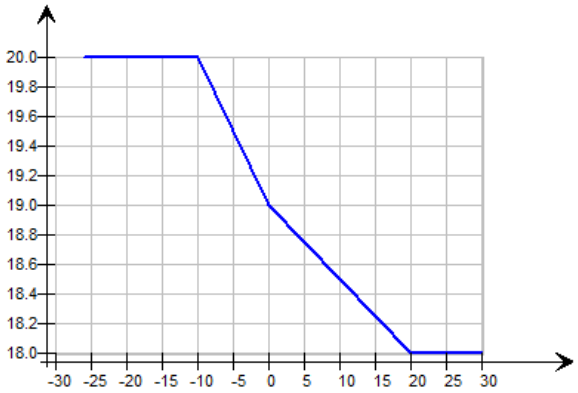


Figure 34. Calibrated room air temperature setpoint curve in the hall.

basketball and volleyball, and about 1 to 2°C higher than the **target temperature** for basketball, floorball and volleyball, see Table 6. For that reason, the two cases to be simulated in this post-calibration study would be about experimenting with lower indoor air temperature setpoints as follows:

(i) case 1: offset the heating setpoint curve down 2°C, number of occupants is 15 at a metabolic level rate 5.0 met, and

(ii) case 2: offset the heating setpoint curve down 3°C, number of occupants is 15 at a metabolic level rate 5.0 met.

A lower number of occupants at a higher metabolic rate were proposed in order to infer the approximate performance of a «ballgame» hall, as the studied hall only hosts educational sessions from 08–16 on weekdays. The nighttime ventilation settings and the airflow control based on carbon dioxide concentration however stayed unchanged. The indoor air conditions such as the mean air temperature in the hall and the relative humidity will be used as the boundary conditions in the study of the thermal comfort of the occupants. The DTS value will be calculated with the JBODY web application which was built based on the IESD-FIALA thermal comfort model. Corresponding to the 7-point scale of thermal sensation votes, the proposed criteria for acceptable thermal comfort of the sports players or exercisers are as follows:

(i) the warming up period lasts maximum 15 minutes, during which the sports players could have more clothes layers and could feel «cold», after that, the occupants should not feel «cool» even with fewer clothes layers (DTS $\geq -2$).

(ii) the occupants should not feel beyond «warm» at the end of the session (DTS $\leq 2$).

To predict the thermal comfort of the sports players, the simulated indoor conditions (mean air temperature, mean radiant temperature, air velocity, and relative humidity) from the two cases were applied to a typical 90-minute training session,

inspired by the example presented in Section 2.7 and Appendix B. The monthly average indoor air temperature and relative humidity in the coldest month (Feb) and the warmest month (Aug[5]) are used as the «reference» coolest and warmest indoor conditions for the prediction of the occupant's thermal comfort, as shown in Table 9. The average metabolic rate trend during this session is that it increases from 3.0 to 5.0 met within the warming-up period (15 minutes) and assumably remains unchanged until 5 minutes before the end of the session, to 4.0 met. This is because the halls are used mainly for playing ball games (volleyball, handball, basketball, floorball, futsal), although it also hosts gymnastics and other less intensive sports such as gymnastics sometimes. Therefore, there will be another two reference cases to test the extremes of thermal comfort, as follows:

(a) In the coolest conditions of the three cases, which are the conditions of the **offset 3℃ case**, the metabolic rate profile will be decreased to represent occupants participating in lower activity level sports such as aerobics or gymnastics (maximum 3.0 met). This is referred to as the «cold extreme case».

(b) Likewise, in the warmest conditions, the profile will be increased to represent intensive game-play sessions (maximum 7.0 met), respectively called the «warm extreme case». This will use the indoor condition values of the **baseline case**.

The summary of the air conditions and metabolic rate profiles is shown in Table 9 as per each case. Regarding the clothing, the same clothing setup is applied to all cases: during the warming-up period total clothing insulation value is 0.9 clo (e.g., briefs, ankle-length socks, sports shoes, sports trousers, long-sleeve shirt plus a thick sweater), after that the value is step-changed to 0.6 clo (e.g., the sweater is taken off). This «forced» step change will subsequently create a dip in the DTS value. The human to be studied is a standard male as described in the IESD-FIALA model, see Section 2.6.

## 4.6 Simulation Results and Discussion

Regarding the heating energy, the annual consumption in the three cases is presented in Table 10. Predictably, when decreasing the indoor air temperature of the hall, the heating energy consumption will also decrease. In the case the heating setpoint curve is offset 2℃ the consumption reduces from 98.1 kWh/($m^2$a) to 85.0 kWh/($m^2$a), corresponding to 13.3% compared to the current setpoint. In a similar manner, the other case of offsetting 3℃ appears to bring up to 18.4% heating energy savings per year, or approximately 18.1 kWh/($m^2$a). This reduction in heating energy can be translated into operational cost savings, which bears significant meaning in the context of an energy crisis [4]. The City of Helsinki already announced in November 2022

[5]Every year the halls are closed from the third week of June until the end of July. Therefore, these two months are ruled out.

Table 9. Indoor air conditions used in the thermal comfort prediction of the sports players and exercisers.

| | Coolest conditions | | Warmest conditions | |
|---|---|---|---|---|
| | Air temp ℃ | RH % | Air temp ℃ | RH % |
| Baseline case | 19.7 | 20 | 20.7 | 58 |
| Offset 2℃ | 17.7 | 22 | 20.0 | 60 |
| Offset 3℃ | 16.7 | 24 | 19.8 | 61 |

(a) Air temperature and relative humidity input for each case

| | Metabolic rate in met | | | | |
|---|---|---|---|---|---|
| Time in minute | 0 | 5 | 15 | 85 | 90 |
| Cold extreme case | 2.0 | 3.0 | **3.0** | 2.0 | 2.0 |
| Other cases | 3.0 | 4.0 | **5.0** | 4.0 | 4.0 |
| Warm extreme case | 3.0 | 4.0 | **7.0** | 5.0 | 5.0 |

(b) Metabolic rate profiles.

that the energy savings measures include lowering the indoor temperature in their offices, and indoor sports facilities except swimming pools, youth centres, cultural centres, and museums; optimising ventilation more closely to the operation time and demand; shorter Christmas lighting season; dimming street lights, etc. [94, 95]. The simulation result of this work brings more specific, quantitative estimates of the level of reduction so that they can help assist in the decision-making of the authority.

Table 10. Annual heating energy and potential savings in cases of lowered temperature set point curve in the Latokartano sports hall.

| | AHU heating kWh/a | Space heating kWh/a | Total heating energy kWh/a | Specific heating energy kWh/(m$^2a$) | Change |
|---|---|---|---|---|---|
| current setpoint | 55366 | 43010 | 98376 | 98.1 | – |
| offset 2℃ | 47004 | 38252 | 85256 | 85.0 | 13.3% |
| offset 3℃ | 43253 | 37013 | 80266 | 80.0 | 18.4% |

In terms of thermal comfort, Figure 35 graphs the DTS of the standard male during a 90-minute training session in the Latokartano sports hall 1 in the listed cases, during the coolest and warmest conditions. The dashed orange rectangular box depicts the allowable range of the DTS values according to the criteria mentioned in the previous section. It is apparent that the DTS values fulfil the defined criteria in all cases with typical metabolic profiles (ballgames – playing or training), both in the coolest and the warmest condition. The player feels **slightly below cool** at the beginning of the session, gradually warms up, and at the end of the session, they feel **slightly warm**. The dips at minute 15 are due to the reduction in the clothing layers, as described before. In the coolest conditions, regarding the extreme case, if the player participates in lighter sports such as gymnastics ($M_{max} = 3.0$ met), they

are predicted to feel still below «cool» until the 17th minute. The thermal sensation gradually increases towards neutral and reaches **slightly above neutral** at the end of the session. On the other hand, in the warmest conditions, for the extreme case, the players who intensively practice or play the games ($M_{max}$ = 7.0 met) would feel **slightly beyond warm** at the end of the session.

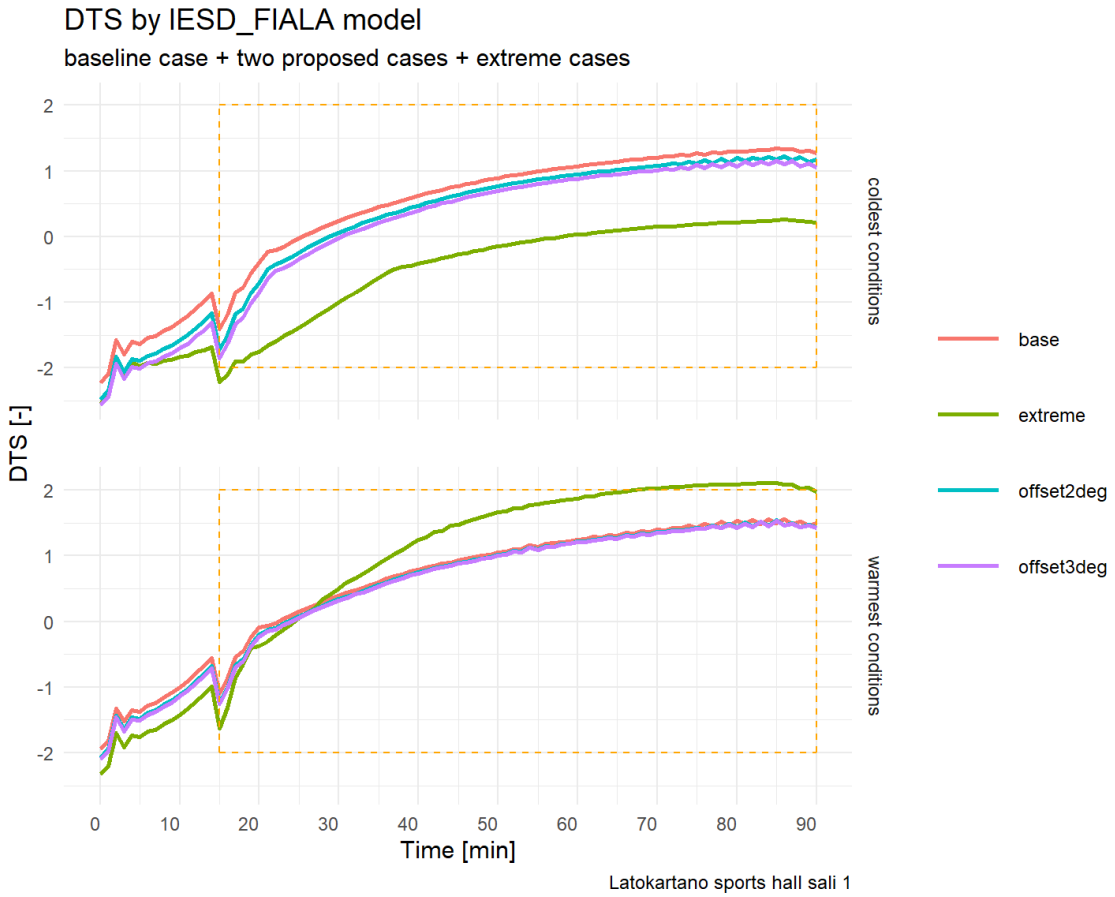


Figure 35. DTS of the occupants simulated from the baseline case, the two proposed cases, and the reference extreme cases.

In the context of the defined cases and criteria for the acceptable thermal sensation, it was found that the effect of reducing the indoor air temperature 2 to 3℃ from the current setpoints does not affect the thermal comfort of the players and exercisers in the sports halls. However, it is worth noting that lower air temperature leads to higher relative humidity regarding the same moisture load. Although the monthly average relative humidity does not significantly surpass the recommended indoor air limit (60%), it does oscillate above that threshold diurnally for several weeks of the year. During the end of summer until mid-autumn, the water vapour in the air is already high, and together with the moisture load from the occupants, it heightens the indoor relative humidity. If persisting, this could lead to an increased risk of mould and microbial growth in the space, e.g., condensation in structural layers or at cold bridges. Detailed relative humidity graphs from the simulated cases can be found in Appendix D.

Under a tight schedule to complete this work, the author acknowledges the following shortcomings in the research design and methodology, in addition to the aforementioned ones in Section 4.2:

(i) The data for the model calibration was collected for only a short period. It should be longer, for example, two to three weeks and ideally one period from each season of the year. This way the model is tested against various outdoor conditions; subsequently, once it is calibrated, it will perform more stably and reliably.

(ii) The thermal comfort prediction depends greatly on the number of players or exercisers, duration of the sports session, the intensity of the sports, clothing level, age group, and physical condition. These factors are principally difficult to be generalised. Thus, the prediction varies case by case and is subject to significant deviation. In this work, the dominant sports discipline (ballgames) and player group (young adults) were chosen to be studied.

(iii) The determination of the acceptable thermal comfort criteria is based on personal experience as a sports player. There should be a more scholarly method to define the range of the thermal sensation vote at different stages of a sport practising or playing session, which might remarkably influence the athletic performance of the sportspersons.

# 5 Conclusion

This work has reviewed the human thermal comfort models which could be applied in sports environments. In addition, the common ventilation solutions in indoor sports facilities were also introduced, especially demand-controlled ventilation and the factors influencing its adequacy and efficiency were investigated. An indoor climate and energy model of one of the halls of the Latokartano sports centre was constructed and simulated with different indoor air temperature setpoints. The IESD-FIALA thermal comfort model was employed to predict the thermal sensation of the sports players and exercisers, so to suggest the optimal indoor conditions for sports practising environments without compromising on energy consumption and indoor air quality.

Conventional thermal comfort models are inapplicable in indoor sports environments due to the high activity level of the occupants. In search of a more appropriate human thermal comfort assessment and prediction methodology, thermo-physiological models were found to have great potential. The employment of such models, e.g., JOS-3 or IESD-FIALA, yields more accurate predictive thermal sensations of the sports players and exercisers as they explicitly model the physiological aspects of the human body. The results from those models assist in the optimal HVAC design practice in transient, non-uniform thermal environments which are typically found in sports environments. Multi-nodal, multi-segmental thermal regulation models can also be combined with CFD simulation to study more closely the whole body thermal comfort as well as the local thermal discomfort of the sportspersons.

The ventilation system in the studied indoor sports facility complies with the current regulation in terms of maximum designed airflow, at 4.45 $\mathrm{L\,s^{-1}\,m^{-2}}$ which is more than twice the required airflow rate 2 $\mathrm{L\,s^{-1}\,m^{-2}}$. The building is equipped with a DCV system based on carbon dioxide and temperature measurements. The carbon dioxide concentration inside the hall is well controlled by the DCV system. However, the efficacy of its automation control and maintenance practice leave numerous doubts and needs for further investigations. Challenges in the inspection, operation, and maintenance of the ventilation systems which might pose high risks to the performance of the buildings were spotted. It was due to the SARS-CoV-2 transmission risk mitigation guidelines from the authority that further examination of the functionality of the DCV systems was not accomplished, for the airflow rate is set to be at the maximum for the time being until the next guidance.

From the modelling and simulation of the Latokartano sports hall 1, it was proven that lowering the temperature setpoints by 2℃ during the occupancy period could reduce the energy consumption by 13%, at the same time maintaining the thermal comfort for the sports players or exercisers in the hall. Even a lower indoor air temperature does not hurt their thermal comfort, however, it would lead to increased relative humidity ($\geq 60\%$) during summer and autumn, which might pose a higher risk for mould and microbial growth if not controlled timely. The simulation

cases considered also the extremities when a sport discipline with a lower activity level was played in the hall in the coolest possible conditions and when a heated match was played in the warmest possible conditions. The results revealed that only in the case of intensive gameplay in the warmest conditions the players would feel slightly beyond «warm» on the 7-point thermal sensation scale at the end of the games or training sessions. This strongly reinforces the proposals for lower indoor air temperature in indoor sports facilities compared to the suggested values from the guidelines.

To ensure the adequate performance of the ventilation system in sports facilities, a number of measures are suggested. A thorough inspection of the system, including ductwork, air flow handling components, automation control, minimum and part-load performance tests, etc. should be carried out already at the commissioning phase of the project, regardless of whether it is the renovation of an existing sports building or a newly-built. Detailed documentation yet simple and easy-to-follow instructions for maintenance work should be emphasised during the design and commissioning. Regular inspection and scheduled maintenance are indispensable. In addition, the upkeep of the maintenance log should be made compulsory. In regards to the management side, sports facilities owners and managers should consider spending more resources on regular training of the maintenance staff, especially whenever there is a change in personnel. One way to prolong their tenure is to provide more appreciation and motivation for the maintenance workers. Besides, the utilisation of smart control and visualised building metrics through IoT with a dashboard on the BMS would make building automation and control more efficient, transparent, and user-friendly. Reliable real-time predicting models trained on collected data of that building would improve the control algorithms with time and improve the overall performance of the building.

# References


[1] Sosiaali- ja terveysministeriö [Finnish Ministry of Social Affairs and Health]. *Muutosta liikkeellä! Valtakunnalliset yhteiset linjaukset terveyttä ja hyvinvointia edistävään liikuntaan 2020 [On the move – national strategy for physical activity promoting health and wellbeing 2020]*. 2013.

[2] Fabio Fantozzi and Giulia Lamberti. Determination of thermal comfort in indoor sport facilities located in moderate environments: An overview. *Atmosphere*, 10(12):1–27, 2019.

[3] Discovering Finland. Yrjönkadun uimahalli Helsinki. https://www.discoveringfinland.com/fi/destination/yrjoenkadun-uimahalli/. Accessed: 2022-12-02.

[4] International Energy Agency. Global energy review 2021 - assessing the effects of economic recoveries on global energy demand and $CO_2$ emissions in 2021. Technical report, 2021.

[5] World Health Organization. *WHO Guidelines on Physical Activity and Sedentary Behaviour*. 2020.

[6] World Health Organization. Promoting sport and enhancing health in European Union countries: a policy content analysis to support action. Technical report, 2009.

[7] World Health Organization. Global health estimates: Life expectancy and leading causes of death and disability – Technical paper WHO/DDI/DNA/GHE/2020.1-.3. Technical report, 12 2020.

[8] A. J. Carlisle and N. C.C. Sharp. Exercise and outdoor ambient air pollution. *British Journal of Sports Medicine*, 35(4):214–222, 2001.

[9] Stefano Corgnati, Manuel da Silva, R Ansaldi, Ehsan Asadi, J Costa, and Marco Filippi. *Indoor Climate Quality Assessment*, volume 14. 2011.

[10] Gerd Jendritzky, Richard de Dear, and George Havenith. UTCI-Why another thermal index? *International Journal of Biometeorology*, 56(3):421–428, 2012.

[11] George Havenith. Individualized model of human thermoregulation for the simulation of heat stress response. *Journal of Applied Physiology*, 90(5):1943–1954, 2001.

[12] J. L.M. Hensen. Literature review on thermal comfort in transient conditions. *Building and Environment*, 25(4):309–316, 1990.

[13] Beker Braian M, Cervellera Camila, Vito Antonella De, and Musso Carlos G. Human Physiology in Extreme Heat and Cold. *International Archives of Clinical Physiology*, 1(1), 2018.

[14] L. G. Gagge, A. P., Fobelets, A. P. and Berglund. A standard predictive Index of human reponse to thermal enviroment. *American Society of Heating, Refrigerating and Air-Conditioning Engineers*, 92(92(2B)):709–731, 1986.

[15] Takako Fukazawa and George Havenith. Differences in comfort perception in relation to local and whole body skin wettedness. *European Journal of Applied Physiology 2009 106:1*, 106(1):15–24, jan 2009.

[16] Nicole T. Vargas, Christopher L. Chapman, Blair D. Johnson, Rob Gathercole, and Zachary J. Schlader. Skin wettedness is an important contributor to thermal behavior during exercise and recovery. *American Journal of Physiology - Regulatory Integrative and Comparative Physiology*, 315(5):R925–R933, nov 2018.

[17] U*X*L American Decades. The 1960s business and the economy: Overview. https://www.encyclopedia.com/social-sciences/culture-magazines/1960s-business-and-economy-overview. Accessed: 2022-11-09.

[18] J. van Hoof. Forty years of Fanger's model of thermal comfort: Comfort for all? *Indoor Air*, 18(3):182–201, 2008.

[19] International Organization for Standardization. *ISO 7730:2005 Ergonomics of the Thermal Environment: Analytical Determination and Interpretation of Thermal Comfort Using Calculation of the PMV and PPD Indices and Local Thermal Comfort Criteria*. International standards. ISO, 2005.

[20] Refrigerating American Society of Heating and Air-Conditioning Engineers. *Thermal Environmental Conditions for Human Occupancy: ANSI/ASHRAE Standard 55-2020 (Supersedes ANSI/ASHRAE Standard 55-2017) Includes ANSI/ASHRAE Addenda Listed in Appendix N*. ASHRAE, 2021.

[21] Poul O Fanger et al. Thermal comfort. analysis and applications in environmental engineering. *Thermal comfort. Analysis and applications in environmental engineering.*, 1970.

[22] Michael A. Humphreys and J. Fergus Nicol. The validity of ISO-PMV for predicting comfort votes in every-day thermal environments. *Energy and Buildings*, 34:667–684, 7 2002.

[23] Yongchao Zhai, Minghui Li, Siru Gao, Liu Yang, Hui Zhang, Edward Arens, and Yunfei Gao. Indirect calorimetry on the metabolic rate of sitting, standing and walking office activities. *Building and Environment*, 145:77–84, 11 2018.

[24] Richard de Dear, Gail Brager, and Cooper D. Developing an Adaptive Model of Thermal Comfort and Preference - Final Report on RP-884. *ASHRAE Transactions*, 104, 01 1997.

[25] Richard de Dear and Gail Schiller Brager. The adaptive model of thermal comfort and energy conservation in the built environment. *International Journal of Biometeorology*, 45(2):100–108, 2001.

[26] Cristiana Croitoru, Ilinca Nastase, Florin Bode, Amina Meslem, and Angel Dogeanu. Thermal comfort models for indoor spaces and vehicles - Current capabilities and future perspectives. *Renewable and Sustainable Energy Reviews*, 44:304–318, apr 2015.

[27] Adolf P Gagge. An effective temperature scale based on a simple model of human physiological regulatory response. *ASHRAE Transactions*, 77:247–262, 1971.

[28] J A Stolwijk. A mathematical model of physiological temperature regulation in man. *NASA Contractor Report*, CR-1855:77, 1971.

[29] Daniel Wölki. *MORPHEUS : Modelica-based implementation of a numerical human model involving individual human aspects*. Dissertation, RWTH Aachen University, Aachen, 2017.

[30] Katarina Katić, Rongling Li, and Wim Zeiler. Thermophysiological models and their applications: A review. *Building and Environment*, 106:286–300, 9 2016.

[31] Jagir R. Hussan and Peter J. Hunter. Comfort simulator: A software tool to model thermoregulation and perception of comfort. *Journal of Open Research Software*, 8, 2020.

[32] Human Thermal Model – FIALA-FE. https://www.theseus-fe.com/simulation-software/human-thermal-model. Accessed: 2022-10-14.

[33] Yoshito Takahashi, Akihisa Nomoto, Shu Yoda, Ryo Hisayama, Masayuki Ogata, Yoshiichi Ozeki, and Shin ichi Tanabe. Thermoregulation model JOS-3 with new open source code. *Energy and Buildings*, 231:110575, 1 2021.

[34] JBODY Web API. https://www.jeplus.org/wiki/doku.php?id=docs:jbody:start. Accessed: 2022-10-14.

[35] Yutaka Kobayashi and Shin Ichi Tanabe. Development of jos-2 human thermoregulation model with detailed vascular system. *Building and Environment*, 66:1–10, 8 2013.

[36] Shin Ichi Tanabe, Kozo Kobayashi, Junta Nakano, Yoshiichi Ozeki, and Masaaki Konishi. Evaluation of thermal comfort using combined multi-node thermoregulation (65MN) and radiation models and computational fluid dynamics (CFD). *Energy and Buildings*, 34(6):637–646, 2002.

[37] TanabeLab. Github - tanabelab/jos-3. https://github.com/TanabeLab/JOS-3. Accessed: 2022-10-16.

[38] Daniel Wölki, Christoph Van Treeck, Yi Zhang, Sebastian Stratbücker, Sandeep R. Bolineni, and Andreas Holm. Individualisation of virtual thermal manikin models for predicting thermophysical responses. *12th International Conference on Indoor Air Quality and Climate 2011*, 1:432–437, 2011.

[39] Dusan Fiala, Kevin J. Lomas, and Martin Stohrer. A computer model of human thermoregulation for a wide range of environmental conditions: the passive system. *Journal of Applied Physiology*, 87(5):1957–1972, 1999.

[40] D Fiala and K J Lomas. The dynamic effect of adaptive human responses in the sensation of thermal comfort. *Moving Thermal Comfort Standards into the 21st Century, Conference Proc.*, pages 147–157, 2001.

[41] Dusan Fiala, Kevin J. Lomas, and Martin Stohrer. Computer prediction of human thermoregulatory and temperature responses to a wide range of environmental conditions. *International Journal of Biometeorology*, 45(3):143–159, 2001.

[42] Paul Roelofsen. A comparison of the dynamic thermal sensation between the modified Stolwijk model and the Fiala thermal physiology and comfort (FPC) model. *Intelligent Buildings International*, 12(4):284–294, 2020.

[43] Ergonsim. Human thermal modelling. http://www.ergonsim.de/. Accessed: 2022-11-30.

[44] ASHRAE. *2017 ASHRAE fundamentals (SI)*. 2017.

[45] Richard Casaburi, Brian J Whipp, Karlman Wasserman, William L Beaver, and Sankar N Koyal. Ventilatory and gas exchange dynamics in response to sinusoidal work. *Journal of Applied Physiology*, 42(2):300–301, 1977.

[46] Rakennustieto Oy. *LVI 06-10600 Sisäliikuntatilojen LVIA-suunnittelu [LVO 06-10600 Heating, ventilation, air conditioning and automation design of indoor sports facilities]*. Number 13. 2018.

[47] ANSI ASHRAE. ASHRAE Standard 62.1-2022. Ventilation and Acceptable Indoor Air Quality. *American Society of Heating, Refrigerating, and Air-Conditioning Engineers, Inc.: Atlanta, GA*, 2021.

[48] Per-Olof Åstrand and Kaare Rodahl. *Textbook of work physiology : physiological bases of exercise*. New York (N.Y.) : McGraw-Hill, 2nd ed. edition, 1977.

[49] International Organization for Standardization. *ISO 8996:2021 Ergonomics of the thermal environment — Determination of metabolic rate*. International standards. ISO, 2021.

[50] Jacques Malchaire, Francesca Romana d'Ambrosio Alfano, and Boris Igor Palella. Evaluation of the metabolic rate based on the recording of the heart rate. *Industrial health*, 55(3):219–232, 2017.

[51] Wenjie Ji, Maohui Luo, Bin Cao, Yingxin Zhu, Yang Geng, and Borong Lin. A new method to study human metabolic rate changes and thermal comfort in physical exercise by CO2 measurement in an airtight chamber. *Energy and Buildings*, 177:402–412, 2018.

[52] International Organization for Standardization. *ISO 9920:2007 Ergonomics of the Thermal Environment: Estimation of thermal insulation and water vapour resistance of a clothing ensemble*. International standards. ISO, 2007.

[53] Theodor Hannes Benzinger. The physiological basis for thermal comfort. *Indoor climate*, pages 441–476, 1979.

[54] International Olympic Committee. International Sports Federations (IFs) with Olympic Recognition. https://olympics.com/ioc/international-federationshttps://www.olympic.org/ioc-governance-international-sports-federations. Accessed: 2022-03-27.

[55] Seppänen, Olli, Säteri, Jorma, and Ahola, Mervi. Finnish guidelines of ventilation rates for non-residential buildings. *E3S Web Conf.*, 111:02015, 2019.

[56] Ympäristöministeriö [Finnish Ministry of Environment]. *D2 Suomen rakentamismääräyskokoelma – Rakennusten sisäilmasto ja ilmanvaihto [D2 Finnish building regulation – Indoor climate and ventilation in buildings]*. 2012.

[57] Rakennustieto Oy. LVI-kortisto [hvac-cards]. https://www.rakennustieto.fi/palvelut/tietoa-rakentamiseen/kortistot/lvi-kortisto. Accessed: 2022-09-29.

[58] FINVAC Ry. *Opas ilmanvaihdon mitoitukseen muissa kuin asuinrakennuksissa [Guidelines for ventilation dimensioning in non-residential buildings]*. 2020.

[59] ASHRAE/ANSI. *Standard 62.1-2019, Ventilation for Acceptable Indoor Air Quality*. 2019.

[60] Ympäristöministeriö [Finnish Ministry of Environment]. *Laskentaopas – Tilan ulkoilmavirran mitoitus hiilidioksidikuormituksen perusteella [Calculation guidelines – Outdoor air dimensioning based on carbon dioxide load]*. 2018.

[61] Elisabeth Mundt, Hans Martin Mathisen, P. V. Nielsen, and Alfred Moser. *Ventilation Effectiveness*. REHVA, 2004.

[62] Alexandro Andrade, Fábio Hech Dominski, and Danilo Reis Coimbra. Scientific production on indoor air quality of environments used for physical exercise and sports practice: Bibliometric analysis. *Journal of Environmental Management*, 196:188–200, 2017.

[63] Prihoda s.r.o. Fabric diffusers in sports facilities – Prihoda Fabric Ducting and Diffusers. https://www.prihoda.com/en/applications/pools-sports-halls-and-fitness-centres/. Accessed: 2022-11-06.

[64] Fitness / Sports Centers - United Kingdom FabricAir. https://www.fabricair.com/uk/applications/fitness-sports-centers/. Accessed: 2022-11-06.

[65] Man Fan, Zheng Fu, Jia Wang, Zhaoying Wang, Hanxiao Suo, Xiangfei Kong, and Han Li. A review of different ventilation modes on thermal comfort, air quality and virus spread control. *Building and Environment*, 212(November 2021):108831, 2022.

[66] Han Li, Jinchao Li, Man Fan, Zhaoying Wang, Wei Li, and Xiangfei Kong. Study on the performance of interactive cascade ventilation oriented to the non-uniform indoor environment requirement. *Energy and Buildings*, 253:111539, 2021.

[67] Han Li, Zhaoying Wang, Jinchao Li, Leilei Wang, Xiangfei Kong, and Man Fan. Study on thermal comfort of interactive cascade ventilation based on body multi-node thermal demand. *Energy and Buildings*, 273:112404, 2022.

[68] Xiangfei Kong, Zhaoying Wang, Man Fan, and Han Li. Analysis on the performance of interactive cascade ventilation for space heating based on non-uniform indoor environment demand. *Building and Environment*, 219(April):109244, 2022.

[69] Nora Scientific Co. Ltd. Flowsquare+ – the free and handy computational fluid dynamics software. https://fsp.norasci.com/en/index.html. Accessed: 2022-10-29.

[70] Lars Ekberg. Inspection of ventilation systems. *REHVA Journal 02/2021*, pages 14–18, 2021.

[71] Olli Seppänen. Terveet tilat -tietoisku: Ilmanvaihdon katsastusopas. https://finvac.org/iv-katselmukset/. Recorded interview. Accessed: 2022-11-23.

[72] Valtioneuvoston kanslia. Terveet tilat 2028 -ohjelma. https://tilatjaterveys.fi/ohjelma. Accessed: 2022-11-24.

[73] Ympäristöministeriö [Finnish Ministry of Environment]. *Ilmanvaihdon katsastusopas - Hallittua sisäilmastoa [Ventilation inspection guidelines – Controlled indoor climate]*. Helsinki, 1st edition, 2022.

[74] Mads Mysen, Peter G. Schild, and Axel Cablé. *Demand-controlled ventilation - requirements and commissioning*. SINTEF Academic Press, 2014.

[75] Demand-controlled ventilation - increased comfort and lower costs. https://www.swegon.com/knowledge-hub/technical-guides/we-explain-demand-controlled-ventilation/. Accessed: 2022-11-29.

[76] Lindab Ventilation. *VAV & DCV Solutions*. 2016.01 edition, 2021.

[77] Cathrine Grini and Tore Wigenstad. *LECO. Behovstilpasset ventilasjon. Hvordan får man alle brikkene på plass? [LECO. Demand-controlled ventilation. How do you get all the pieces in place?].* SINTEF akademisk forlag, 2011. Prosjektrapport / SINTEF Byggforsk 73.

[78] Swegon. A complete solution for the optimal indoor climate. https://www.swegon.com/siteassets/4-guides/technical-guides/demand-controlled-ventilation/wise-quick-guide-8p.pdf, 2022. Accessed: 2022-11-30.

[79] Mads Mysen, Sverre Holøs, Kari Thunshelle, Aileen Yang, Ole-Hugo Sandsnes Vik, Tore Fredriksen, and Peter G Schild. Control Procedure for Demand Controlled Ventilation Performance. In *Roomvent & Ventilation 2018*, pages 115–120, 2018.

[80] Weixin Zhao, Simo Kilpeläinen, Wertti Bask, Sami Lestinen, and Risto Kosonen. Operational Challenges of Modern Demand-Control Ventilation Systems: A Field Study. *Buildings*, 12(3):1–15, 2022.

[81] Risto Kosonen. Performance Challenge of Demand-based Ventilation. http://www.scanvac.eu/uploads/9/4/5/2/94521553/kosonen_risto_performance_challenge_of_demand_response_ventilation__nordic_ventilation_forum.pdf. Presentation presented at the Nordic Ventilation Forum (webinar), 2022-09-21. Accessed: 2022-10-14.

[82] Grekula Vesa. Sotilaallinen uhka ja väestönsuojelu ovat nyt pääosassa – viranomaiset harjoittelevat useita samanaikaisia kriisejä itärajan pinnassa [the military threat and civil defense are now in the lead – the authorities are practising several simultaneous crises at the eastern border]. https://yle.fi/uutiset/74-20003309. Accessed: 2022-11-05.

[83] BBC News. South Korea Halloween crush: The lost belongings in pictures. https://www.bbc.com/news/world-asia-63467914. Accessed: 2022-11-05.

[84] Reuters. South Korea Halloween crush victims' belongings fill quiet lost-and-found centre. https://www.reuters.com/world/asia-pacific/south-korea-halloween-crush-victims-belongings-fill-quiet-lost-and-found-centre-2022-11-01/. Accessed: 2022-11-05.

[85] LPV. Latokartanon Liikuntahalli [Latokartano sports hall]. https://lpv.fi/latokartanon-liikuntahalli. Accessed: 2022-10-15.

[86] Unisports AB 2022. Sports flooring  sports floor systems. https://www.unisport.com/sports-flooring. Accessed: 2022-10-21.

[87] Rask Aki and Helsingin Kaupunki. Latokartanon liikuntahalli / palloilusali 2 [latokartano sports hall / ballgame hall 2]. https://www.hel.fi/helsinki/fi/kaupunki-ja-hallinto/osallistu-ja-vaikuta/ota-yhteytta/hae-yhteystietoja/toimipistekuvaus?id=41075.

[88] Helsingin kaupunki [City of Helsinki]. Helsingin palvelurakennuksissa on tehostettu ilmanvaihtoa [Service buildings in Helsinki are ventilation-boosted]. https://www.hel.fi/fi/uutiset/helsingin-palvelurakennuksissa-on-tehostettu-ilmanvaihtoa, oct 2020. Accessed: 2022-11-19.

[89] Helsingin kaupunki [City of Helsinki]. Päätösasiakirja 210 / 17.09.2020 - Varautumisen toimeenpano koronavirus-tilanteessa Helsingin kaupungilla 9.9.-16.9.2020 [Decision deed 210 / 17.09.2020 – Implementation of precautions for the coronavirus situation in Helsinki city]. https://www.hel.fi/helsinki/fi/kaupunki-ja-hallinto/paatoksenteko/viranhaltijapaatokset/asiakirja?year=2020&ls=11&doc=Keha_2020-09-17_Kp_210_Pk&vdoc=U02100VH2. Accessed: 2022-11-19.

[90] EQUA Simulation AB. Validation & certifications - Simulation Software – EQUA. https://www.equa.se/en/ida-ice/validation-certifications. Accessed: 2022-11-28.

[91] ASHRAE Guideline 14-2014. Measurement of Energy, Demand, and Water Savings. *ASHRAE Guideline 14-2014*, 4:1–150, 2014.

[92] Federal Energy Management Program. MV guidelines: measurement and verification for performance-based contracts -Version 4.0. *U.S. Department of Energy*, 3(November):1–108, 2015.

[93] Efficiency Valuation Organization. *IPMVP Core Concepts 2016*. 2016.

[94] Helsingin kaupunki [City of Helsinki]. Ulkovalaistusta ja sisälämpötiloja säädetään – näin kaupunki vähentää energiankulutusta [Adjusting outdoor lighting and indoor temperatures – this way the city reduces energy consumption]. https://www.hel.fi/fi/uutiset/ulkovalaistusta-ja-sisalampotiloja-saadetaan-nain-kaupunki-vahentaa-energiankulutusta. Accessed: 2022-11-19.

[95] Helsingin kaupunki [City of Helsinki]. Näin varaudumme energiatilanteeseen [this way we prepare for the energy situation]. https://www.hel.fi/helsinki/fi/kaupunki-ja-hallinto/tietoa-helsingista/yleistietoa-helsingista/energia/. Accessed: 2022-11-19.

[96] Helsingin kaupunki [City of Helsinki]. Calendar application – sähköinen asiointi. https://asiointi.hel.fi/wps/portal/liikuntatilakalenteri. Accessed: 2022-10-28.

# A IDA ICE Model Calibration Index Calculation Scripts

```
/*  Code to compute: Calibration Indices  */
/*  Developed by: SNK   */
/*  Contact: si.s.nguyen@aalto.fi   */
```

A R script to create a semi-synthetic weather file to feed in IDA ICE simulation, to interpolate the missing logged values of the 201TK AHU for the Sali 1, to calculate the CV(RMSE) and MBE indices, and finally to visualise the calibration results.

```
---
title: "Latokartanon Liikuntahalli calibration"
author: "Si Nguyen-Ky"
date: "2022-10-24"
output:
  pdf_document:
    keep_tex: yes
---

```{r setup, include=FALSE}
library(rmarkdown)
library(formatR)
options(knitr.duplicate.label = "allow", width = 40)
knitr::opts_chunk$set(echo = TRUE)
#knitr::opts_chunk$set(tidy.opts = list(width.cutoff = 40),
                      tidy = TRUE, size = "small")
```

```{r load libraries, warning=FALSE,message=FALSE}
library(dplyr)
library(readr)
library(stringr)
library(ggplot2)
library(lubridate)
library(padr)
library(SimDesign)
library(forecast)
library(imputeTS)
library(data.table)
library(tibble)
library(tidyr)

Sys.setlocale("LC_TIME", "English") #set locality
setwd("X:/")

```

```{r weather file, warning=FALSE,message=FALSE}
#create a semi-synthetic weather file
```
```

```
outdoor <- read_delim("Latokartano-outdoor.csv",
    delim = ";", escape_double = FALSE,
    col_types = cols(Time = col_time(format = "%H:%M")),
    na = "NA", trim_ws = TRUE)

colnames(outdoor) <- c('year','month','day','time','temp',
                       'rh','windir','winspd','dirrad','difrad')
outdoor$cdottamp <- str_c(outdoor$year, '-',outdoor$month,'-',
                          outdoor$day,' ',outdoor$time)
outdoor <- outdoor %>%
    mutate(cdottamp=ymd_hms(cdottamp)) %>% #change time to posixct
    mutate(hour = (yday(cdottamp)-1)*24+hour(cdottamp)-1+24)
#shift one day because of the leap year structure in the IDA ICE
    weather file
  outdoor <- select(outdoor, -year, -month, -day, -time, -cdottamp)
  outdoor <- outdoor[,c(7,1,2,3,4,5,6)]
  #View(outdoor)

outdoor$dirrad[outdoor$dirrad<0] <- 0 #remove negative radiation
    values
outdoor$difrad[outdoor$difrad<0] <- 0

hki2012 <- read.table("Hki-Vantaa_Ref_2012.prn",
    sep= "\t", dec = ".", header = F, col.names = c("hour",'temp','
    rh','windir','winspd','dirrad','difrad'))
hki2012plus <- hki2012
hki2012plus[match(outdoor$hour, hki2012plus$hour),] <- outdoor
#replace recorded weather to the ref file
#view(hki2012plus)
write.table(hki2012plus,file="Hki-Vantaa_Semisynthetic_2022.prn",
            quote = FALSE, sep = "\t", row.names = FALSE, col.names
    = FALSE)
```

```{r logged data, warning=FALSE,message=FALSE}

#prepare logged data

logged_data_01 <- read_delim("201TK-sept.csv",
    delim = ";", escape_double = FALSE,
    col_types = cols(...1 = col_datetime(format = "%d.%m.%Y %H:%M")
    ),
    na = "NA", trim_ws = TRUE, locale=locale(decimal_mark = ','),
    col_names = TRUE)
colnames(logged_data_01) <- c('cdottamp','LPtemp','poistoilma','
    tuloilma','tuloLTOjaelkeen','kasalit')
logged_data_01 <- logged_data_01 %>%
  select(-LPtemp) %>%
  mutate(cdottamp=round_date(cdottamp,"hour")) %>% #floor cdottamp
    to hour
  pad(interval = "hour") #%>% #fill missing cdottamp rows
#calculate % of missing data
na_count_01 <- colSums(is.na(logged_data_01))/nrow(logged_data_01)*
    100
```

```
87
88 #continue to prepare logged data
89 logged_data_01 <- logged_data_01 %>%
90   mutate(poistoilma=na_interpolation(poistoilma, "linear")) %>%
91   mutate(tuloilma=na_interpolation(tuloilma, "linear")) %>%
92   mutate(tuloLTOjaelkeen=na_interpolation(tuloLTOjaelkeen, "linear"
     )) %>%
93   mutate(kasalit=na_interpolation(kasalit, "linear")-1) %>%
94   #-1 COMPENSATE FOR THE TE3_1 SO HIGH (ALMOST 4K)
95   mutate(hour = (yday(cdottamp)-1)*24+hour(cdottamp)+1)
96   #compensate for flooring hour donw
97 logged_data_01 <- logged_data_01[,c(1,6,2,3,5)]
98 #View(logged_data_01)
99
100 logged_data_02 <- read_delim("201TK-sept-co2.csv",
101     delim = ";", escape_double = FALSE,
102     col_types = cols(time = col_datetime(format = "%d.%m.%Y %H:%M")
    ),
103     locale = locale(decimal_mark = ",", grouping_mark = ""),
104     trim_ws = TRUE, col_names = TRUE)
105 colnames(logged_data_02) <- c('cdottamp','co2')
106 logged_data_02 <- logged_data_02 %>%
107   mutate(cdottamp=round_date(cdottamp,"hour")) %>% #floor cdottamp
     to hour
108   pad(interval = "hour") #%>% #fill missing cdottamp rows
109
110 #calculate % of missing data
111 na_count_02 <- colSums(is.na(logged_data_02))/nrow(logged_data_02)*
    100
112 na_count <- append(na_count_01, na_count_02)
113
114 logged_data_02 <- logged_data_02 %>%
115   mutate(hour = (yday(cdottamp)-1)*24+hour(cdottamp)+1) #same as
     above
116 logged_data_02 <- logged_data_02[,c(3,1,2)]
117 logged_data_02$co2 <- na_interpolation(logged_data_02$co2,"linear")
118
119 logged_data <- merge.data.frame(logged_data_01, logged_data_02,
120                                 by = c("hour","cdottamp"))
121 logged_data <- logged_data %>% add_column(from = "logged", .after =
     "hour")
122 #use to spec source later in viz
123
124 ```
125
126 ```{r modelled data, warning=FALSE,message=FALSE}
127 #prepare simulated values for calibration
128 calib <- read_delim("simcalib.txt",
129     delim = "\t", escape_double = FALSE, na = "NA", trim_ws = TRUE,
130     locale=locale(decimal_mark = '.'), col_names = TRUE, show_col_
    types = FALSE)
131
132 colnames(calib) <- c('hour','tuloilma','kasalit',
133                      'poistoilma','tuloltojaelkeen','co2')
```

```
calib <- calib %>%
  select(hour, poistoilma, tuloilma, kasalit, co2) %>%
  mutate(from="ida",.after="hour") %>%
  filter(hour %in% logged_data$hour)
calib <- merge.data.frame(calib, logged_data[,c('hour','cdottamp')],
                          by = "hour")
calib <- calib[,c(1,2,7,3:6)]


outdoor.trimmed <- outdoor %>%
  mutate(hour=hour-24) %>%
  filter(hour %in% logged_data$hour)

```

```{r calc, warning=FALSE,message=FALSE}
# calculate cvrmse of cw tempeature, simmed vs measured and visualise
#number of hours
nhour <- nrow(calib)
CV <- c()
MBE <- c()
# cv rmse calc
for (i in 4:7) {
  x <- sqrt(sum(((logged_data[,i] - calib[,i])^2)/(nhour-1))/
              mean(logged_data[,i])*100)
  y <- (sum(logged_data[,i] - calib[,i])*100)/((nhour-1)*mean(logged_data[,i]))
  CV <- append(CV,x)
  MBE <- append(MBE,y)
  rm(x)
  rm(y)
}

calibres <- data.frame(CV,MBE)
rownames(calibres) <- colnames(calib)[c(3:6)]

viz_data <- rbind(calib,logged_data)
viz_data <- viz_data %>%
  gather(series, value, poistoilma:co2) #convert data into long data format

# visualisation
vizrun <- ggplot(data=viz_data,aes(x=cdottamp, y=value)) +
  geom_point(aes(color=from))+ geom_line(aes(color=from)) +
  labs(title="Modelled vs measured data",
       subtitle=paste("calibrated model, 9 - 16 September, 2022"),
       caption=paste("201TK-Latokartano sali 1 calibration"),
       x="Time",y="Temperature [C-deg]",
       color = element_blank()) + #labelling and series naming+
  theme_minimal() +
  facet_grid(series ~ ., scales = "free_y",
             switch = "y",
```

```
      # flip the facet labels along the y axis from the right side to the left
            labeller = as_labeller(
      # redefine the text that shows up for the facets
              c(co2 = "CO2, ppm", kasalit = "Tm,  C ", poistoilma = "Tret,  C ",
                tuloilma = "Tsup,  C "))) +
  ylab(NULL) + # remove the word "values"
  xlab(NULL) +
  scale_x_datetime(date_labels = "%d.%m %H:%M", breaks = "6 hours") +
  #format cdoteries
  theme(strip.background = element_blank(), # remove the background
        panel.spacing.y = unit(0.75, "lines"),
        strip.placement = "outside",
        axis.text.x = element_text(angle = 90, hjust = 1))
# put labels to the left of the axis text)
vizrun
```

```{r print, warning=FALSE,message=FALSE, include=FALSE}
#print
png(filename = "~/latokartano_calib.png",
     width = 1440, height = 960, units = "px", pointsize = 24,
     res = 200
     )
vizrun
dev.off()

#render("latokartano_script.Rmd", output_format = "word_document")
```

```
/*  Code to visualise: DTS from simulated cases  */
/*  Developed by: SNK   */
/*  Contact: si.s.nguyen@aalto.fi   */
```

A R script to gather and visualise the predicted DTS values calculated from each case. The DTS result bundles were from the JBODY Web app.

```
---
title: "DTS thermal comfort"
author: "Si Nguyen-Ky"
date: "2022-11-21"
output: pdf_document
---

```{r setup, include=FALSE}
library(rmarkdown)
library(formatR)
options(knitr.duplicate.label = "allow", width = 40)
knitr::opts_chunk$set(echo = TRUE)
#knitr::opts_chunk$set(tidy.opts = list(width.cutoff = 40),
 #                      tidy = TRUE, size = "small")
```

```{r load libraries, warning=FALSE,message=FALSE}
library(dplyr)
library(readr)
library(stringr)
library(ggplot2)
library(lubridate)
library(padr)
library(SimDesign)
library(forecast)
library(imputeTS)
library(data.table)
library(tibble)
library(tidyr)
library(tidyverse)

Sys.setlocale("LC_TIME", "English") #set locality
setwd("X:/")

```

```{r sort data, warning=FALSE,message=FALSE}

dir <- c("./base cold", "./offset 2deg cold", "./offset 3deg cold",
    "./cold ref")
files <- lapply(dir, list.files, pattern="CMF.csv", full.names =
   TRUE)
df1 <- files %>%
    set_names(c("base","offset2deg","offset3deg","extreme")) %>%
    map_dfr(read_csv, .id = "from", col_names = FALSE,
    comment = "#")  %>%
```
```

```
    select(from, X1, X10) %>%
    mutate(series="cold")

dir <- c("./base warm", "./offset 2deg warm", "./offset 3deg warm",
    "./warm ref")
files <- lapply(dir, list.files, pattern="CMF.csv", full.names =
   TRUE)
df2 <- files %>%
    set_names(c("base","offset2deg","offset3deg","extreme")) %>%
    map_dfr(read_csv, .id = "from", col_names = FALSE,
    comment = "#")  %>%
    select(from, X1, X10) %>%
    mutate(series="warm")
df <- rbind(df1, df2)

```

```{r graph}
viz <- ggplot(data=df,aes(x=X1, y=X10)) +
  geom_line(aes(color=from), size = 1) +
  scale_linetype_manual(values = c("base" = "solid", "offset2deg" =
    "solid", "offset3deg" = "solid", "extreme" = "dashed"))+
  labs(title="DTS by IESD_FIALA model",
       subtitle=paste("baseline case + two proposed cases + extreme
    cases"),
       caption=paste("Latokartano sports hall sali 1"),
       #x="Minute",y="DTS [-]",
       color = element_blank()) + #labelling and series naming+
  theme_minimal() +
  scale_y_continuous(breaks = seq(-3, 3, by = 1))+
  scale_x_continuous(breaks = seq(0, 90, by = 10))+
    ylab("DTS [-]") + # remove the word "values"
  xlab("Time [min]") +
  geom_segment(aes(x=15, y=2, xend = 90, yend = 2), linetype = "
   dashed", color = "orange")+
  geom_segment(aes(x=15, y=-2, xend = 90, yend = -2), linetype = "
   dashed", color = "orange")+
  geom_segment(aes(x=15, y=-2, xend = 15, yend = 2), linetype = "
   dashed", color = "orange") +
  geom_segment(aes(x=90, y=-2, xend = 90, yend = 2), linetype = "
   dashed", color = "orange") +
  #scale_x_datetime(date_labels = "%d.%m %H:%M", breaks = "6 hours
   ") +
  #format timeseries
  facet_grid(series ~ ., scales = "fixed",
      #       switch = "y",
      # flip the facet labels along the y axis from the right side
   to the left
             labeller = as_labeller(
      # redefine the text that shows up for the facets
               c(cold = "coldest conditions", warm = "warmest
   conditions"))) +
  theme(strip.background = element_blank(), # remove the background
        panel.spacing.y = unit(0.75, "lines"),
```

```
        strip.placement = "outside",
        axis.text.x = element_text(angle = 0, hjust = 1),
        legend.position = "right")
viz
```


```{r print, warning=FALSE,message=FALSE, include=FALSE}
#print
png(filename = "c4-dtsres.png",
     width = 1440, height = 1152, units = "px", pointsize = 24,
     res = 200
     )
viz
dev.off()

#render("latokartano_script.Rmd", output_format = "word_document")
```

# B Thermo-physiological Simulation of an Amateur Football Player during a 60-minute Training Session

## B.1 Calculation of the Metabolic Rate of the Amateur Football Player by the Level 3 (Analysis) of the ISO 8896:2021

| | |
|---|---|
| Name of the player | : undisclosed |
| Activity | : football |
| Duration | : 60 minutes |
| Age | : 24 |
| Height $H_b$ | : 175 cm |
| Weight $W_b$ | : 78 kg |
| Heart rate at rest $HR_0$ | : 64 bpm |
| Body fat percentage | : 25.5% |
| BMI | : 25.5 – slightly overweight |

The lean body mass $W_{bl}$ of the player is estimated according to ISO 8896:2021, Annex C as

$$W_{bl} = (1.08 - \frac{W_b}{80 \cdot H_b^2}) \cdot W_b = (1.08 - \frac{78}{80 \cdot 1.75^2}) \cdot 78 = 59.4 \quad \text{kg}$$

. The maximum work capacity $MWC$ is evaluated based on age and lean body mass as

$$MWC = (19.45 - 0.133 \cdot Age) \cdot W_{bl} = (19.45 - 0.133 \cdot 24) \cdot 78 = 966 \quad \text{W}.$$

The DuBois area of the player is

$$A_{Du} = 0.007184 \cdot W_b^{0.425} \cdot H_b^{0.725} = 0.007184 \cdot 78^{0.425} \cdot 1.75^{0.725} = 1.94 \quad \text{m}^2.$$

The maximum heart rate $HR_{max}$ is

$$HR_{max} = 208 - 0.7 \cdot Age = 208 - 0.7 \cdot 24 = 191 \quad \text{bmp}.$$

The heart rate at rest $HR_0$ is 64 bpm at the thermally neutral conditions. Assume the basal metabolic rate (the metabolic rate at rest) $M_0$ is 87 W, similar to the standard male in the FIALA-IESD model. The increase in heart rate per unit of metabolic rate is then evaluated as

$$RM = \frac{HR_{max} - HR_0}{MWC - M_0} = \frac{191 - 64}{966 - 87} = 0.1447 \quad \text{bpm} \cdot \text{W}^{-1}.$$

The metabolic rate in Watt at instance $i$ is

$$M_i = M_0 + \frac{HR_i - HR_0}{RM} \quad [\text{W}] \tag{B1}$$

and in met at instance $i$ is

$$M_i = \frac{M_0 + (HR_i - HR_0)/RM}{58.1 \cdot A_D u} \quad \text{[met]} \tag{B2}$$

With the recorded heart rate at a 5-minute interval during the training session and the estimated values above, the metabolic rate respective to the heart rate is calculated with Equation B1. The result is presented in Table B1 and visualised in Figure 13. The procedure is scalable to a data set with finer time intervals.

The average metabolic rate of this player during the 60-minute training session is **5.5 met**, which is slightly above the lower range for the metabolic rate of the sports discipline «football» given by [46].

Table B1. Estimated metabolic rate of an amateur football player according to Annex C of ISO 8896:2021.

| Minute | HR in bmp | Metabolic rate in Watt | Metabolic rate in met |
|---|---|---|---|
| 0 | 112 | 412 | 3.7 |
| 5 | 121 | 474 | 4.2 |
| 10 | 135 | 571 | 5.1 |
| 15 | 164 | 771 | 6.9 |
| 20 | 141 | 612 | 5.4 |
| 25 | 131 | 543 | 4.8 |
| 30 | 161 | 750 | 6.7 |
| 35 | 134 | 564 | 5.0 |
| 40 | 154 | 702 | 6.2 |
| 45 | 172 | 826 | 7.3 |
| 50 | 126 | 508 | 4.5 |
| 55 | 159 | 736 | 6.6 |
| 60 | 134 | 564 | 5.0 |
| mean | 142 | 618 | 5.5 |

## B.2 Application of JOS-3 Model in Predicting the Thermo-physiological Performances of the Amateur Football Player

Applying the JOS-3 thermo-physiological model from [33], the skin mean temperature, rectal temperature, mean skin wettedness, and metabolic rate were simulated using the indoor conditions of the Latokartano hall 1. The results are presented in Figure B1.

It can also be observed that the mean metabolic rate calculated by the JOS-3 model is slightly lower than that by the ISO standard in the previous calculation. Although these are just simulated values, the result partly reflects the conclusion discussed in [23], which stated that the estimation method of metabolic rate by ISO overestimates the actual values by using the indirect calorimetry method.

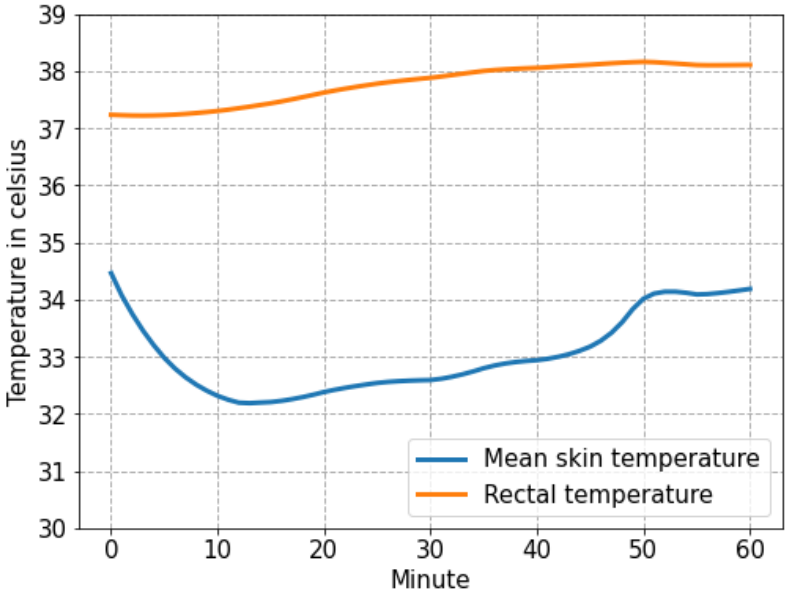


(a) Mean skin and rectal temperatures

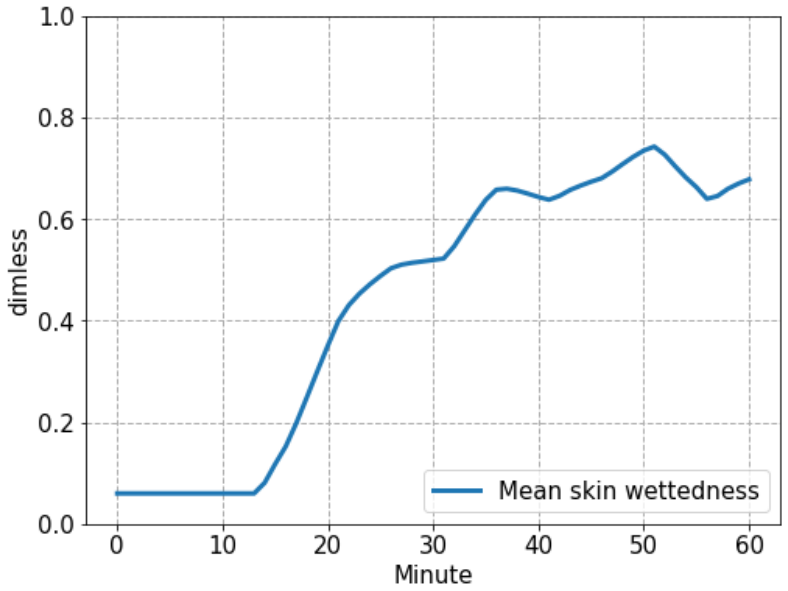


(b) Mean wettedness rate

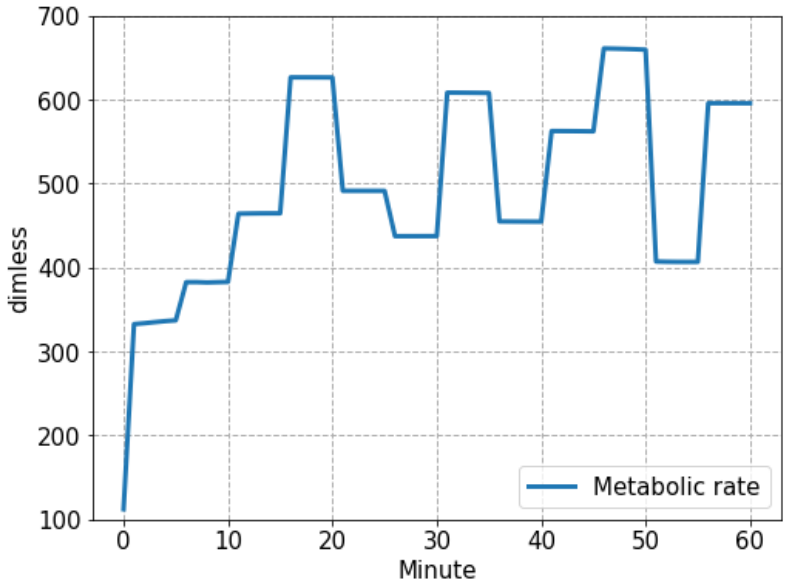


(c) Mean metabolic rate

Figure B1. Thermo-physiological simulation results of the amateur football player by JOS-3 model.

```
/*  Script: Application of JOS-3 model and visualise results */
/*  Written by: SNK   */
/*  Contact: si.s.nguyen@aalto.fi   */
```

A python script using JOS3 package.

```
#EXAMPLE: APPLICATION OF JOS-3 MODEL TO PREDICT THERMO-PHYSIOLOGICAL PERFORMANCES
----------------------------------------

import jos3
model = jos3.JOS3(height=1.75, weight=78, age=24,   )  # Builds a model

# Set the first condition
model.To = 19.7  # Operative temperature [oC]
model.RH = 58  # Relative humidity [%]
model.Va = 0.15  # Air velocity [m/s]
model.PAR = 3.7  # Physical activity ratio [-]
model.simulate(5)  # Exposure time = 5 [min]

# Set the next condition
model.PAR = 4.2  # Changes only Physical activity ratio
model.simulate(5)
# Set the next condition
model.PAR = 5.1  # Changes only Physical activity ratio
model.simulate(5)
# Set the next condition
model.PAR = 6.9  # Changes only Physical activity ratio
model.simulate(5)
# Set the next condition
model.PAR = 5.4  # Changes only Physical activity ratio
model.simulate(5)
# Set the next condition
model.PAR = 4.8  # Changes only Physical activity ratio
model.simulate(5)
# Set the next condition
model.PAR = 6.7  # Changes only Physical activity ratio
model.simulate(5)
# Set the next condition
model.PAR = 5.0  # Changes only Physical activity ratio
model.simulate(5)
# Set the next condition
model.PAR = 6.2  # Changes only Physical activity ratio
model.simulate(5)
# Set the next condition
model.PAR = 7.3  # Changes only Physical activity ratio
model.simulate(5)
# Set the next condition
model.PAR = 4.5  # Changes only Physical activity ratio
model.simulate(5)
# Set the next condition
model.PAR = 6.6  # Changes only Physical activity ratio
```

```
model.simulate(5)

# Show the results
import pandas as pd
import matplotlib.pyplot as plt
plt.rcParams.update({'font.size': 15})

f = plt.figure(1)
f.set_figwidth(8)
f.set_figheight(6)

df = pd.DataFrame(model.dict_results())  # Make pandas.DataFrame
viz1 = df.TskMean.plot(label = "Mean skin temperature", linewidth = 3)  # Show the graph of mean skin temp.
viz1 = df.TcrPelvis.plot(label = "Rectal temperature", linewidth = 3) #Show the graph of rectal temp. = pelvis core temp.
viz1.set(xlabel = "Minute", ylabel = "Temperature in celsius")
plt.legend(loc="lower right")
plt.ylim(30,39)
plt.grid(linestyle = '--', linewidth = 1)
plt.savefig("ac-jos3tmt1.png", bbox_inches='tight')

f = plt.figure(2)
f.set_figwidth(8)
f.set_figheight(6)

viz2 = df.WetMean.plot(label = "Mean skin wettedness", linewidth = 3)  # Show the graph of mean skin temp.
viz2.set(xlabel = "Minute", ylabel = "dimless")
plt.legend(loc="lower right")
plt.ylim(0,1)
plt.grid(linestyle = '--', linewidth = 1)
plt.savefig("ac-jos3tmt2.png", bbox_inches='tight')

f = plt.figure(3)
f.set_figwidth(8)
f.set_figheight(6)

viz2 = df.Met.plot(label = "Metabolic rate", linewidth = 3)  # Show the graph of mean skin temp.
viz2.set(xlabel = "Minute", ylabel = "dimless")
plt.legend(loc="lower right")
plt.ylim(100,700)
plt.grid(linestyle = '--', linewidth = 1)
plt.savefig("ac-jos3tmt3.png", bbox_inches='tight')

# Show the documentation of the output parameters
print(jos3.show_outparam_docs())
```

# C Technical Documentations of the Latokartano Hall 1


Figure C1. Latokartano sports hall site view from above. Photo by Aki Rask / Helsingin Kaupunki [87].

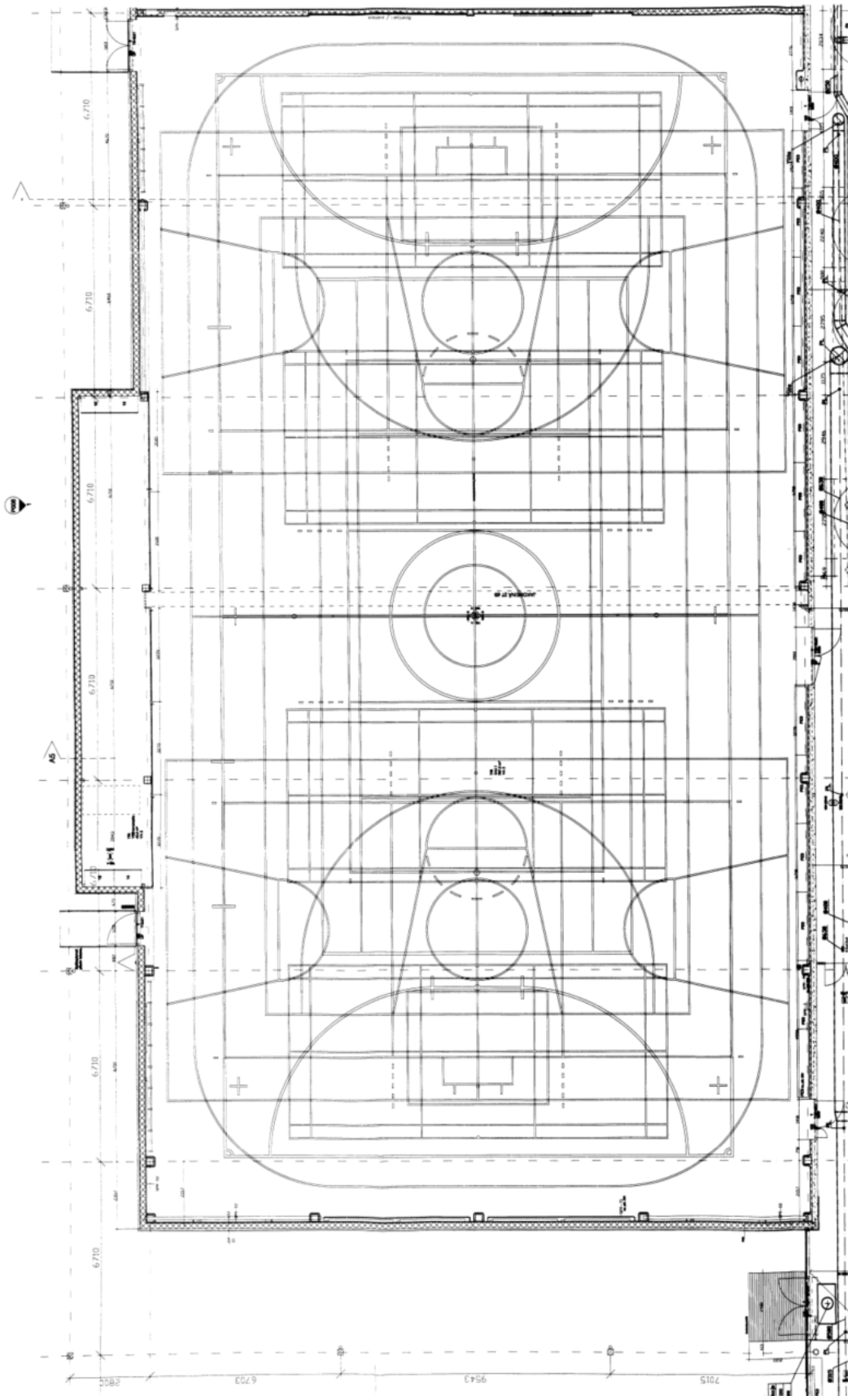

Figure C2. Floor plan of the Latokartano sport hall «sali 1».

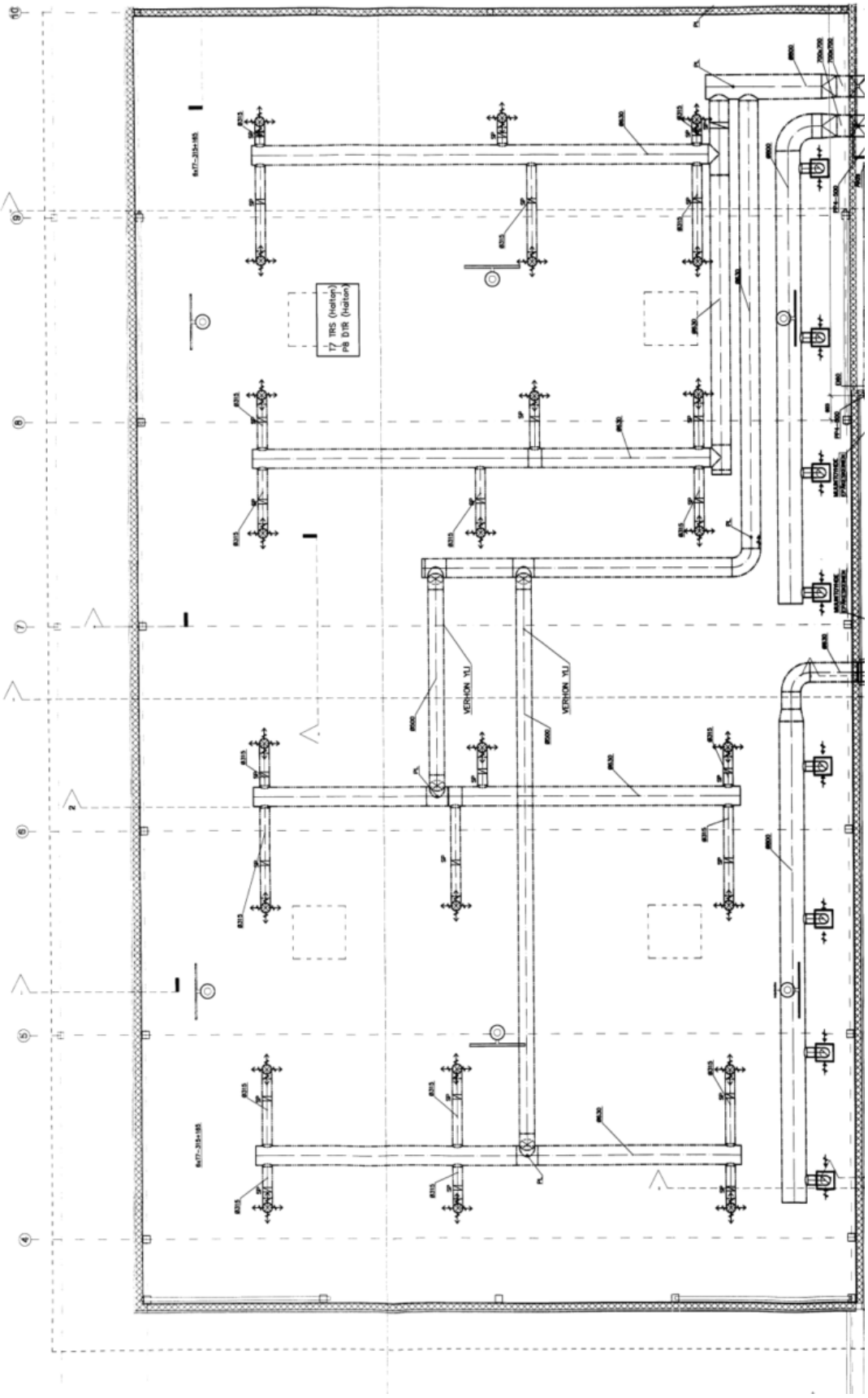


Figure C3. Ventilation drawing of the «sali 1» sports hall.

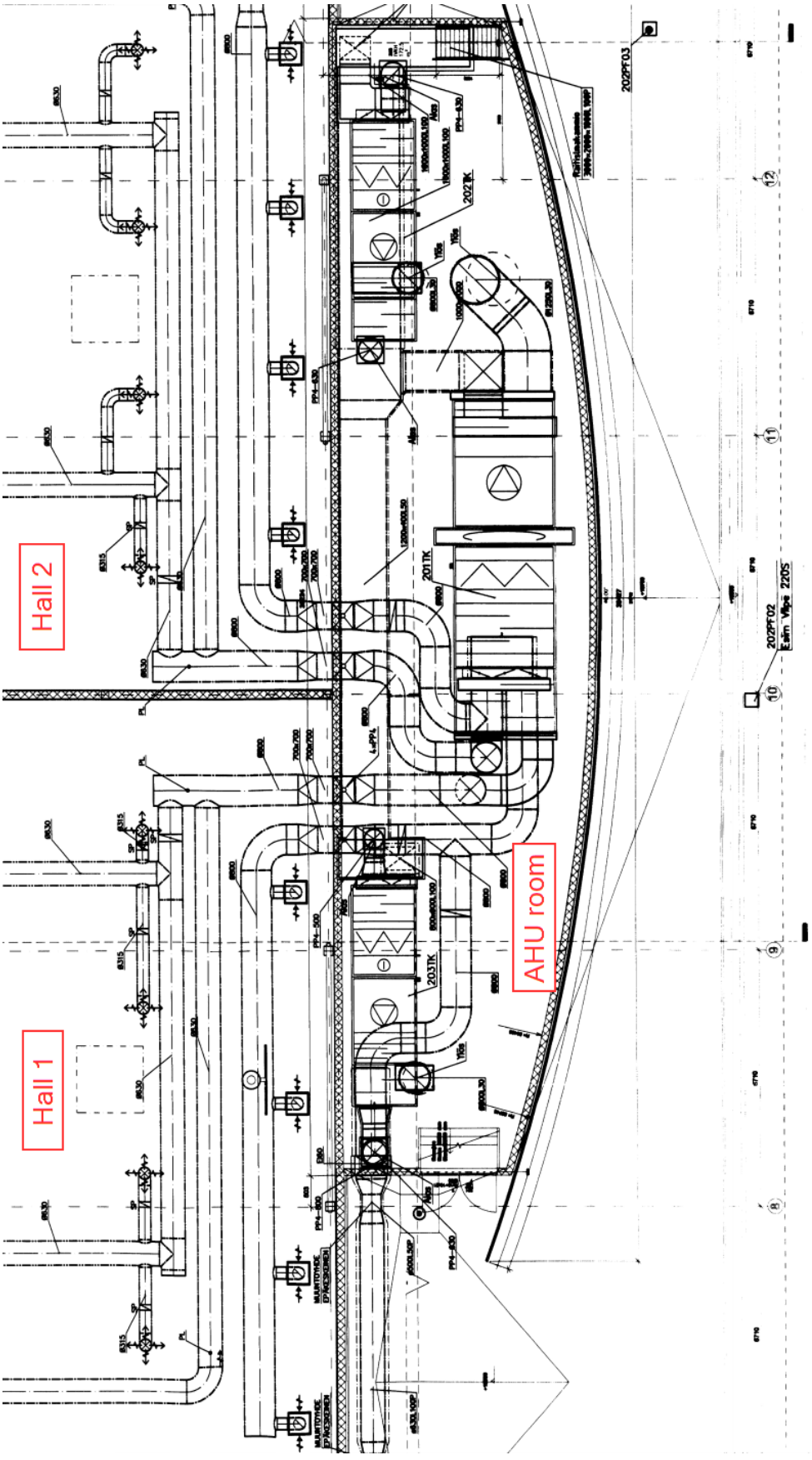


Figure C4. Air handling unit room layout and ductwork distribution.

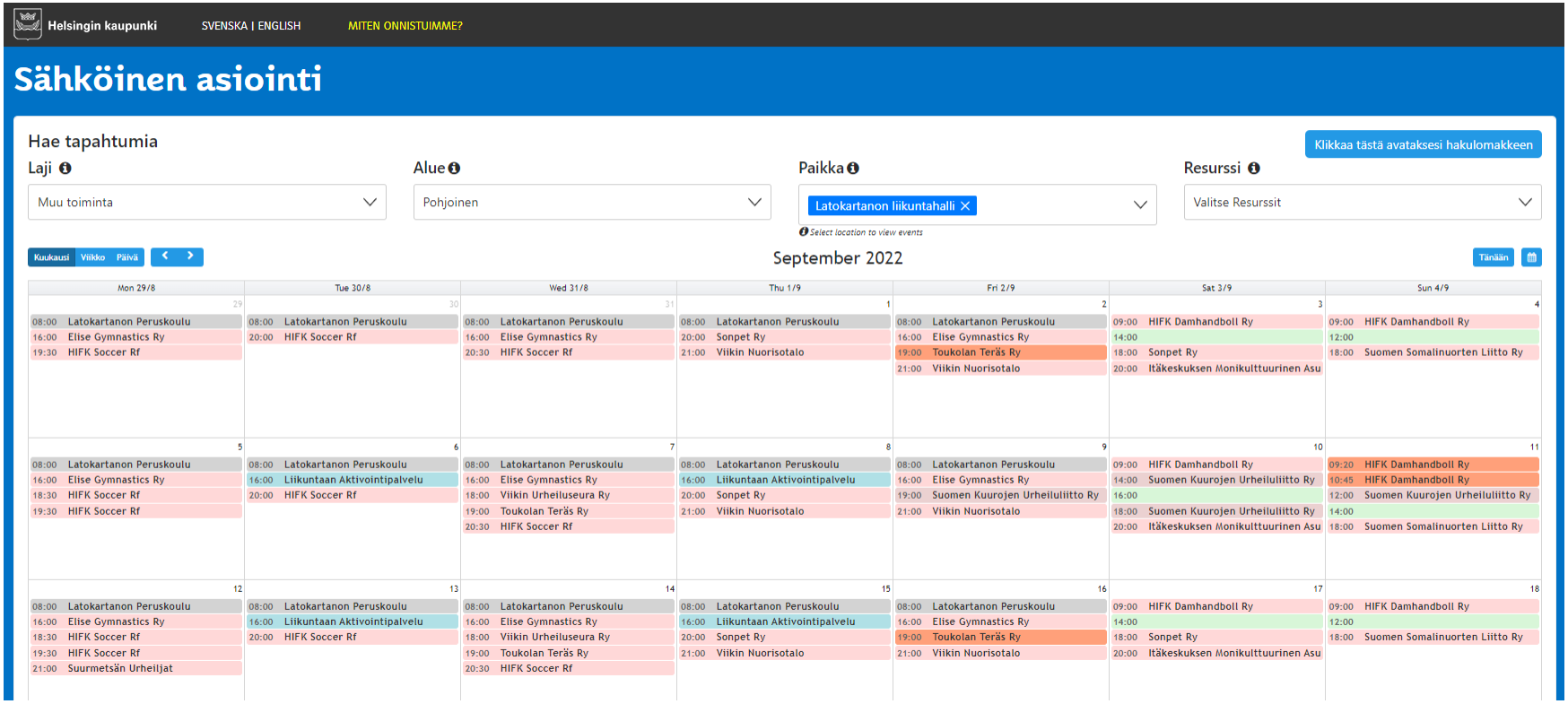


Figure C5. Reservation calendar of the Latokartano hall 1 during the calibration period. Source: [96].

# D Analysis on the Relative Humidity of the Indoor Air from the Simulated Cases

Indoor air relative humidity is recommended not to exceed 60–70% for mould and microbial risk control. The simulated indoor climate in the cases witnessed heightened relative humidity both diurnally and periodically. It is to be studied in future research whether and how influential the high relative humidity is to the structural, health, and mould risk perspectives.

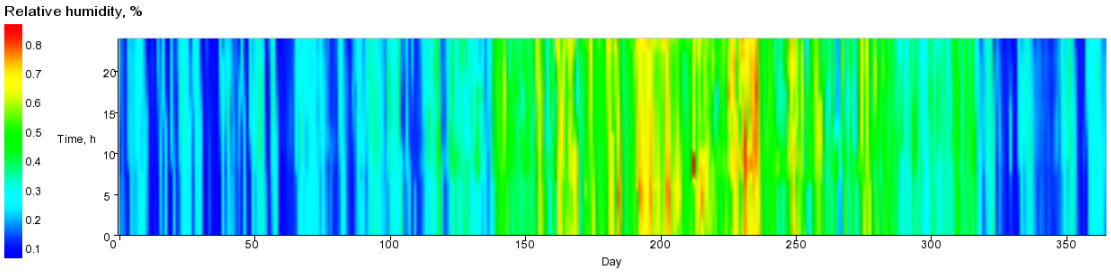


(a) Carpet plot of relative humidity in indoor air.

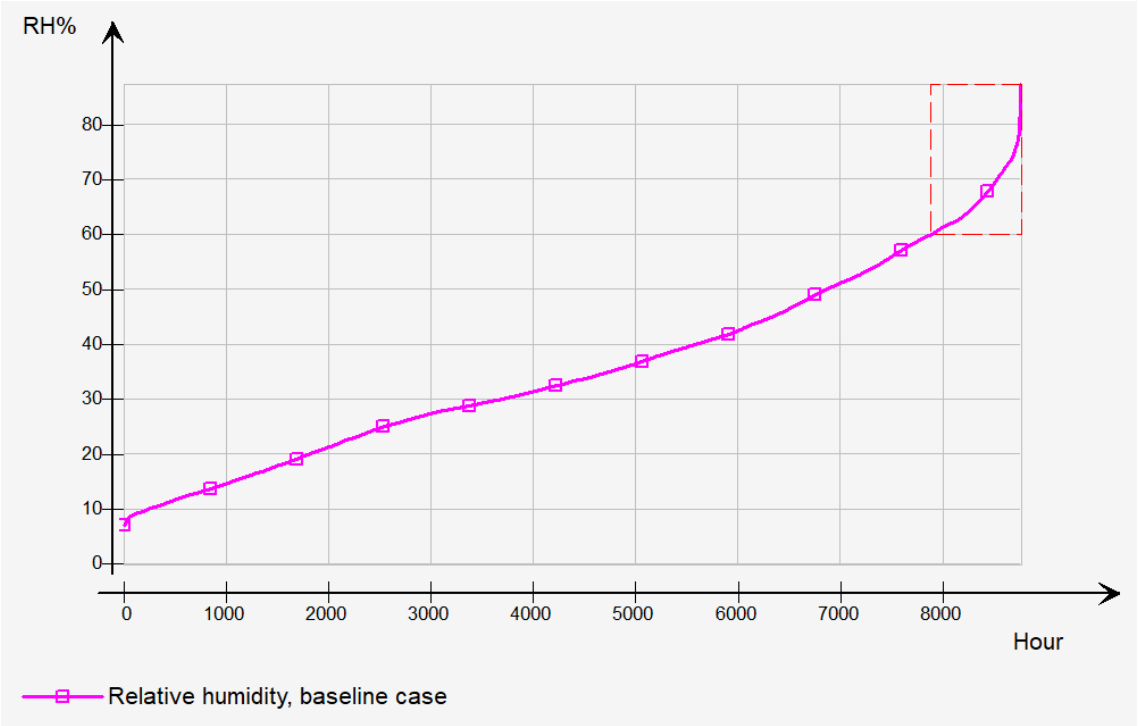


(b) Duration plot of relative humidity in indoor air.

Figure D1. Relative humidity in the indoor air of the baseline case.

It can be seen from Figures D1–D3 that from the baseline case to the case with offsetting 3℃ heating setpoint, the proportion of the duration of the year the indoor air relative humidity exceeding 60% increases, from approximately 10 to 16% (the segments within the dash red boxes). The heightened values happen the most

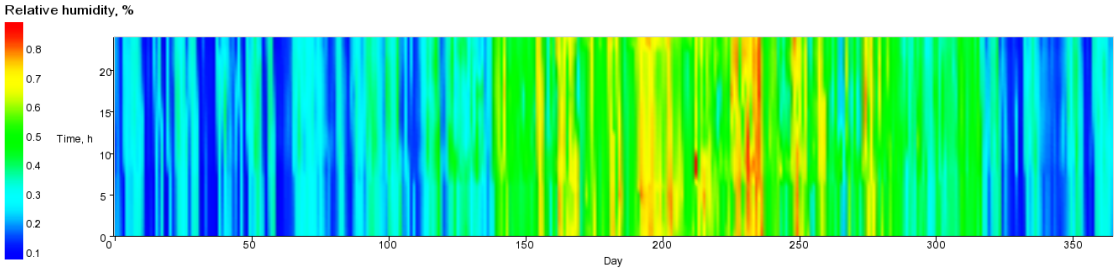


(a) Carpet plot of relative humidity in indoor air.

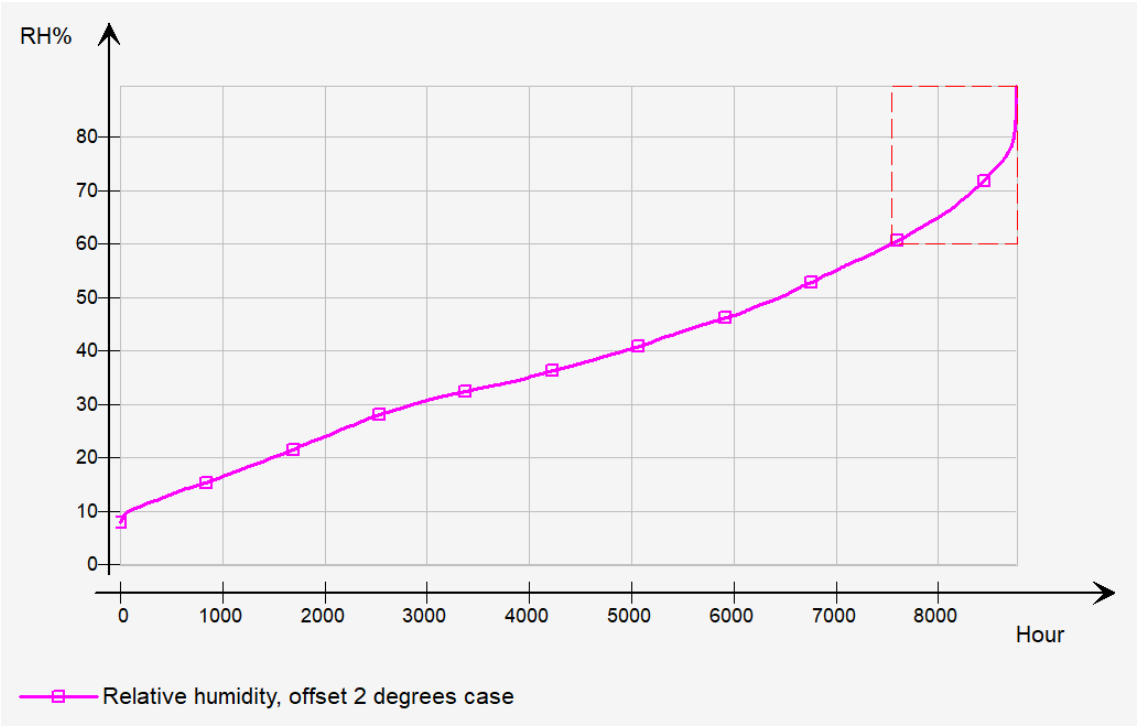


(b) Duration plot of relative humidity in indoor air.

Figure D2. Relative humidity in the indoor air of the offset 2 degrees case.

often during the summer months, from July to August.

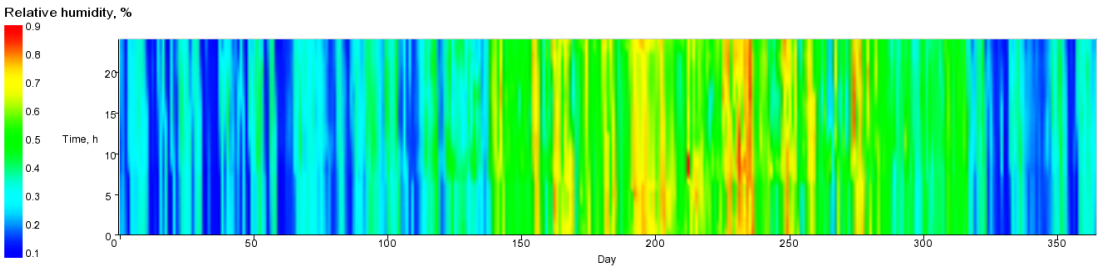


(a) Carpet plot of relative humidity in indoor air.

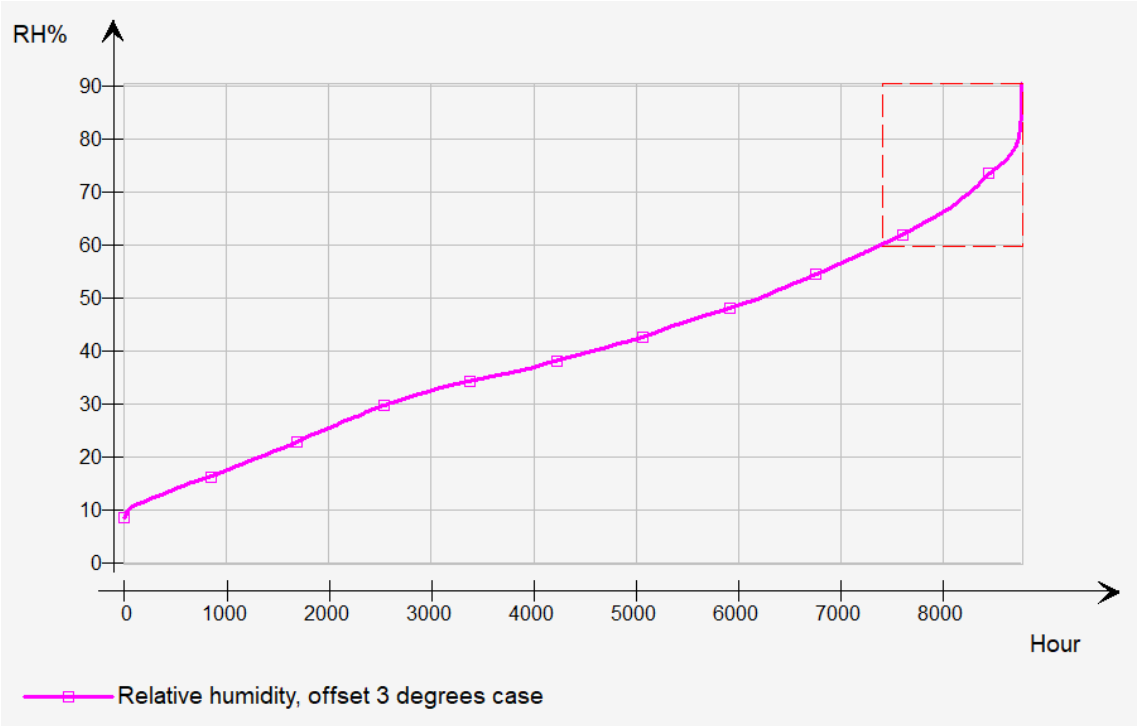


(b) Duration plot of relative humidity in indoor air.

Figure D3. Relative humidity in the indoor air of the offset 3 degrees case.